CELL-FREE DNA AND TUMOR EXOSOME CARGO AS DIAGNOSTIC AND PROGNOSTIC MARKER FOR PROSTATE CANCER

BY

DADA OLUWASEYI TEMILOLA

TMLDAD001

IN FULFILMENT OF THE REQUIREMENTS FOR THE DEGREE

DOCTOR OF PHILOSOPHY

IN THE DIVISION OF CHEMICAL AND SYSTEMS BIOLOGY, DEPARTMENT OF INTEGRATIVE BIOMEDICAL SCIENCES

SUPERVISOR: A/PROFESSOR LUIZ. F. ZERBINI

CANCER GENOMICS GROUP,
INTERNATIONAL CENTRE FOR GENETIC ENGINEERING AND BIOTECHNOLOGY

FACULTY OF HEALTH SCIENCES, UNIVERSITY OF CAPE TOWN.

DECEMBER 2022

i

DECLARATION

I Dada Oluwaseyi Temilola, hereby declare that the work described in this thesis is my own work done under the supervision of my supervisor. I declare that this whole work or part of has been submitted in the past is being or is to be submitted for another degree in this university or any other university.

I permit the university to reproduce in whole or partly the content of this thesis for research purposes.

Signature: .... Signed by candidate ....

DEDICATION

I dedicate this thesis to God, the giver of Life, the Author and Finisher of my Faith. Thank you,
Lord for the courage and ~~strength~~strength.

To my wife, Kelechi Temilola and my family thank you for the support. God bless you.

To Dr Luiz Zerbini, and all who guided me through this PhD journey.

ACKNOWLEDGEMENTS

TABLE OF CONTENTS

List of Abbreviations

ADT: Androgen deprivation therapy

AJCC: American Joint Committee on Cancer

AR: Androgen receptor

BPH: Benign prostatic hyperplasia

cfDNA: Cell free DNA

CSC: Cancer-stem-cell

CTCs: Circulating tumor cells.

ctDNA: Circulating tumor DNA.

DHT: Dihydrotestosterone

DNA: Deoxyribonucleic acid

DRE: Digital rectal examination

ESCRTs: Endosomal sorting complex required for transports.

FDA: Food and Drug Administration

GSH: Groote Schuur Hospital

GS: Gleason score

HDRB: High-dose rate brachytherapy

ICGEB: International Centre for Genetic Engineering and Biotechnology

ILVs: Intraluminal vesicles

KEGG: Kyoto encyclopedia of genes and genomes

mCSPC: Metastatic castration-sensitive prostate cancer

mCRPC: Metastatic castration-resistant prostate cancer

MIENTURNET: MicroRNA enrichment turned network.

miRNA: Micro-ribonucleic acid

mRNA: Messenger ribonucleic acid

MVB: Multivesicular body

NCCN: National Comprehensive Cancer Network

NGS: Next-generation sequencing

nsSNV: nonsynonymous single-nucleotide variant

PBS: Phosphate buffer saline

PCa: Prostate cancer

PSA: Prostate specific antigen

PSMA: Prostate specific membrane antigen

RIN: RNA Integrity Number

RNA: Ribonucleic acid

TCGA: The Cancer Genome Atlas

TEM: Transmission electron microscopy

TRUS: Transrectal ultrasound

WHO: World Health Organization

List of Figures

List of Tables

Chapter 1 Human Prostate Gland: Health and Disease

1.1 Human Cancer

Cancer is a major burden globally, with millions of cancer cases and deaths recorded annually. Prostate cancer (PCa) is the leading cause of male cancer death in Africa (1). Factors such as the aggressive nature of the disease and late diagnosis are responsible for the high PCa mortality among African men. (2). This thesis investigates the potential use of cell free DNA and tumor exosome cargo in diagnosing PCa in South African populations. This may contribute to developing new, less invasive biomarkers for PCa diagnosis in South Africa and Africa at large.

Worldwide, cancer is the second most non-communicable cause of death following cardiovascular diseases. Breast, prostate, lungs, colorectum, stomach, liver, oesophagus, and pancreas cancers are accountable for approximately 60% of all cancer deaths (3). In Africa, cancer is the fifth leading cause of all mortalities (4). Although cancer is a global disease, the incidence and death rates differ along geographical regions. For example, North and South America account for 20.9% of the global cancer cases with 14.2% of the mortalities, while Africa reports 5.7% of the global cancer cases but 7.2% of the mortalities (1). The regional variation in cancer incidence and death has been attributed to the unequal spread of cancer types and elevated case fatality rates in some regions such as Africa and Asia (1).

The population growth, in combination with an increase in risk factors related with economic change, such as obesity, smoking, and physical inactivity, is driving an increased cancer burden in Africa (5). Due to the increasing population growth and aging, it was projected that there will be a 70% increase in cancer incidence in Africa by 2030 (6).

Cancer mortality rates continue to increase in Africa due to absence of appropriate healthcare facilities (7). Despite the burden posed by cancer, the commitment towards fighting cancer in Africa remains largely insufficient. The majority of healthcare efforts in Africa are focused on investigating and management of communicable diseases, such as Malaria and AIDS, while little consideration is given to the burden posed by cancer and other non-communicable diseases (8).

There is also an increase in the financial burden of cancer. The increasing direct cost of cancer management is not only responsible for the economic impact of cancer, but other indirect cost such as impaired quality of life and productivity loss, contribute largely to economic impact of cancer (9). In United States, the estimated cost of cancer management in 2010 was $124 billion and increased to $157 billion in 2020 (10). The growing cost of cancer management has also been shown in African nations (11). Additionally, limited access to recent effective PCa therapies due to cost, low availability, and scarcity of well-trained specialists contribute to high morbidity and mortality PCa rate in Africa (12,13).

1.1.1 An overview of carcinogenesis.

The malignant transformation of normal cells to cancer cells is not fully understood. Several theories have been proposed to explain carcinogenesis, however, none of these theories can fully explain the development of all cancers. Some of the most acknowledged theories include somatic mutation theory, viral/microbial theory of cancer, cancer-stem-cell (CSC) concept, and tissue organization field theory (14,15).

Several regulatory genes usually control cell replication, keeping cell replication in functional homeostasis. These regulatory genes are referred to as tumor suppressor genes such as Deoxyribonucleic acid (DNA) repair genes, checkpoint genes, and apoptotic genes (16). Cancer develops when one or more regulatory genes are compromised or bypassed. Different explanations have been given to describe the multistep process of cancer development. Hanahan and Weinberg described six hallmarks: tissue invasion and metastasis, sustained angiogenesis, self-sufficiency in growth signals, evasion of programmed cell death (apoptosis), limitless replicative potential, and insensitivity to growth-inhibitory signals (17). In 2011, two provisional emerging hallmarks, avoiding immune destruction and deregulating cellular energetics, were added. Also added were two enabling characteristics, which are genome instability/mutation, and tumor-promoting inflammation (18). The cancer hallmarks were updated in 2022, and the two emerging hallmarks were validated as part of the core hallmarks (19). Additionally, the updated hallmark introduced two additional proposed emerging hallmarks and two enabling characteristics, which includes unlocking phenotypic plasticity, non-mutational epigenetic reprogramming, polymorphic microbiomes, and senescent cells (19).

Carcinogens are substances that cause cancer and can either be agents that initiate carcinogenesis or promote cell proliferation, also known as tumor promoters. Some examples of tumor initiating agents include radiation and chemical carcinogens such as arsenic, asbestos, beryllium, and benzene. These agents lead to damage DNA damage and thereby causing cancer development (20,21). Carcinogens such as oestrogen hormones and phorbol esters, known as tumor promoters, stimulate cell proliferation. Phorbol esters is known to activate protein kinase C, which eventually increases cell proliferation and promotes tumor development (22).

Viruses can also induce cancer development both in humans and animals. Cervical and liver cancer are typical examples of cancer caused by viruses.

Some types of cancers are known to have an autosomal dominant inheritance pattern, such as prostate cancer (PCa) (BRCA1 mutation), hereditary non-polyposis colon cancer (MSH2, MSH6, MLH1 mutations) with some of them occurring in syndromic form, for example, Li Fraumeni Syndrome (p53 mutation) (16). Cancer can be inherited in autosomal recessive patterns, for example, non-Hodgkin lymphoma (ATM mutation), and colon cancer (MUTYH mutation). Some of them also occur in syndromic form for instance, Fanconi anaemia (FANC mutation), MUTYH-associated polyposis (MUTYH mutation) (16).

1.2   Prostate cancer

1.2.1   The Prostate Gland

The human prostate gland develops from epithelial invaginations that arise from the posterior urogenital sinus during the first trimester (23). Prostate gland development occurs in the presence of 5α-dihydrotestosterone, a fetal testosterone enzyme (24). The enzyme 5α-dihydrotestosterone is usually localized in the external genitalia and urogenital sinus (24). The structural constitution of the prostate gland appears to remain the same from birth to the beginning of puberty. During puberty, the prostate gland undergoes morphological changes and grows up to about 20g (adult size) (25).

Anatomically, the prostate gland is cone-shaped with the apex towards the urogenital diaphragm and the base at the neck of bladder (26). Anteriorly, the prostate gland receives muscular fibres from the urogenital diaphragm and is separated posteriorly from the seminal vesicles by Denonvilliers' fascia (26). The prostate gland has long been classified into lobes.

However, in the adult prostate, the lobes are not well defined. Therefore, the McNeal zonal anatomic classification has become popular and is now widely accepted (27,28). The peripheral zone, representing 70% of the prostate gland, includes the tissues in close proximity to the capsule posteriorly and prostatic glandular tissue at the apex (Figure 1.1). The peripheral zone is most involved with prostatic diseases such as prostatitis, post-inflammatory atrophy, and PCa (27–29). Some studies have attributed the high predisposition of the peripheral zone to developing PCa to gene expression differences between the peripheral and other prostate zones (30,31). The central zone represents about 25% of the prostate gland (27–29). This zone is cone-shaped, with the apex directed towards the juncture between the prostatic urethra at the verumontanum and the ejaculatory ducts.
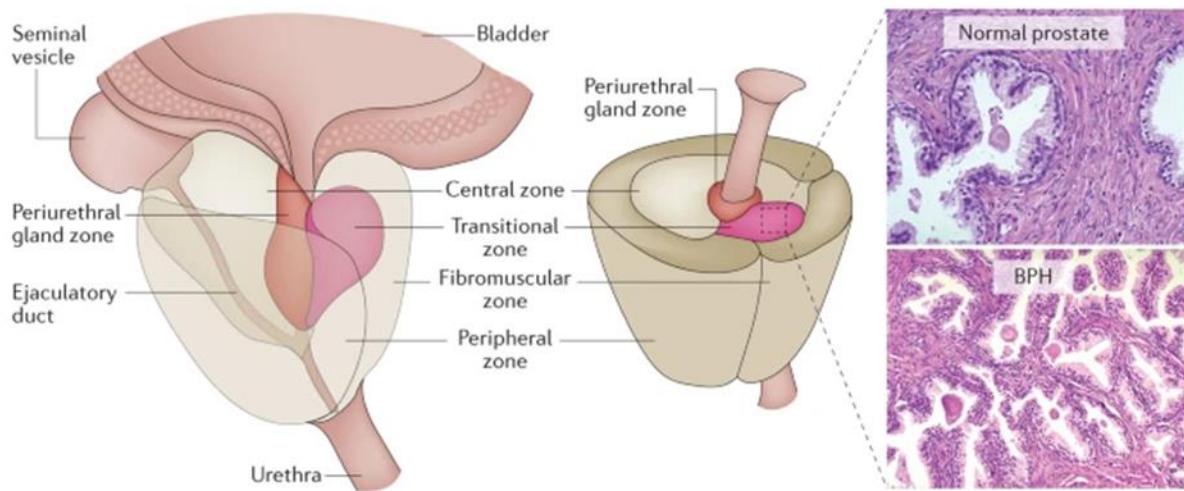
Figure 1.1: McNeal zonal anatomy of the prostate with hematoxylin & eosin stained specimen of normal prostate gland and benign prostatic hyperplasia (32)

The transition zone is the smallest zone representing about 5% of the prostate gland (27,29). This zone comprises of two equal parts of glandular tissue that surrounds the urethra (Figure 1.1). The transition zone harbours most of the age-related benign prostatic hyperplasia (BPH) (27,29).

Functionally, the prostate gland is a tubule-alveolar male accessory reproductive organ that produces and stores an alkaline fluid, which makes up approximately 70% of human semen

volume (~3mL) (33,34). This fluid helps in preserving the spermatozoa lifespan and semen liquefaction (33,34).

The most common prostatic diseases are prostatitis (chronic inflammation), BPH, and PCa. Usually, the size of prostate gland tends to increase with age, making the prostate tissue more susceptible to infection or injury (35–37).

Prostatitis refers to a group of inflammatory diseases such as chronic pelvic pain syndrome, and bacterial prostatitis (acute and chronic). Prostatitis is the third most common urinary tract disease among men of all ages. The 1998 National Institutes of Health classification of prostatitis is the most commonly used classification by the (38) (Table 1.1).

Table 1.1: Prostatitis syndromes classification (38).

Category	Name	Characteristics
I	Acute bacterial prostatitis	Acute bacterial infection Acute urinary tract infection
II	Chronic bacterial prostatitis	Persistent bacterial infection Recurrent urinary tract infections
III	Chronic prostatitis/chronic pelvic pain syndrome	Characteristic pelvic pains, urinary complaints, and sexual dysfunction Absence of other urological disorders
Subtype a	Inflammatory subtype	Leukocytes in the expressed prostatic fluid, post-prostate massage fluid or seminal fluid
Subtype b	Non-inflammatory subtype	No inflammation in the expressed prostatic fluid, post-prostate massage fluid or seminal fluid
IV	Asymptomatic inflammatory	Asymptomatic patients with inflammatory infiltrate in prostate tissue or seminal fluid specimens evaluated for other indications

BPH describes the non-malignant growth of the prostate gland usually caused by a proliferation of prostatic cells, thereby increasing the prostate size, thereby causing obstruction of urethral and other urinary tract symptoms (39,40). BPH is common among men of increasing age, with

approximately 50% of men diagnosed with BPH at age 50 years. BPH mostly affects the prostatic cells in the transitional zone. The hyperplastic growth of these prostatic cells is largely dependent on sex hormones and cytokine responses (39). The sex hormone, testosterone is transformed to dihydrotestosterone (DHT) by the 5α-reductase 2 enzyme. DHT, the major androgen in the prostate, is considered the mediator of prostatic hyperplasia. The role of DHT was shown when men with normal prostate size were shown to have significant lower DHT level compared with men having BPH (41). The risk factors of BPH include increase in age, functioning testicles, black race, family history of BPH, and obesity (39).

PCa is an abnormal, uncontrolled malignant growth of prostate gland tissue (42). PCa often develops as a small, slowly progressive growth limited to the prostate gland, referred to as localized. PCa could sometimes spread rapidly to invade the prostate gland and spread to distant sites, referred to as advanced PCa (43). It is generally accepted that PCa consists of indolent and aggressive varieties. Indolent PCa may be present in the patient for a long period without causing morbidity or mortality, while aggressive PCa often causes symptoms and may lead to cancer-specific mortality. Factors responsible for indolent PCa or aggressive phenotypes are not fully known.

1.2.2   Epidemiology of Prostate Cancer

Globally, PCa is the second most frequent cancer among men, according to the GLOBOCAN/ IARC 2020 databases. In 2020, there were 1 414 259 new cases of PCa (7.3% of all cancer incidence) and 375 304 deaths (3.8% of all cancer deaths) (3). The incidence and deaths from PCa globally correlate with increasing age. The mean age at the point of diagnosis PCa is 66 years. The database showed that PCa has the highest rate of new cases (93 173), death (47 249), and 5-year prevalence rate (17 8197) of all cancers among men in Africa (Figure 1.2) (3,44). Western Africa had the highest rate of new PCa cases (26 392) and the highest mortality rate (14 903), while Middle Africa had the lowest rate of new PCa cases (13 386) and Northern Africa had the lowest mortality rate (7 177) (3).

Estimated age-standardized incidence and mortality rates (World) in 2020, prostate, males, all ages

ASR (World) per 100 000
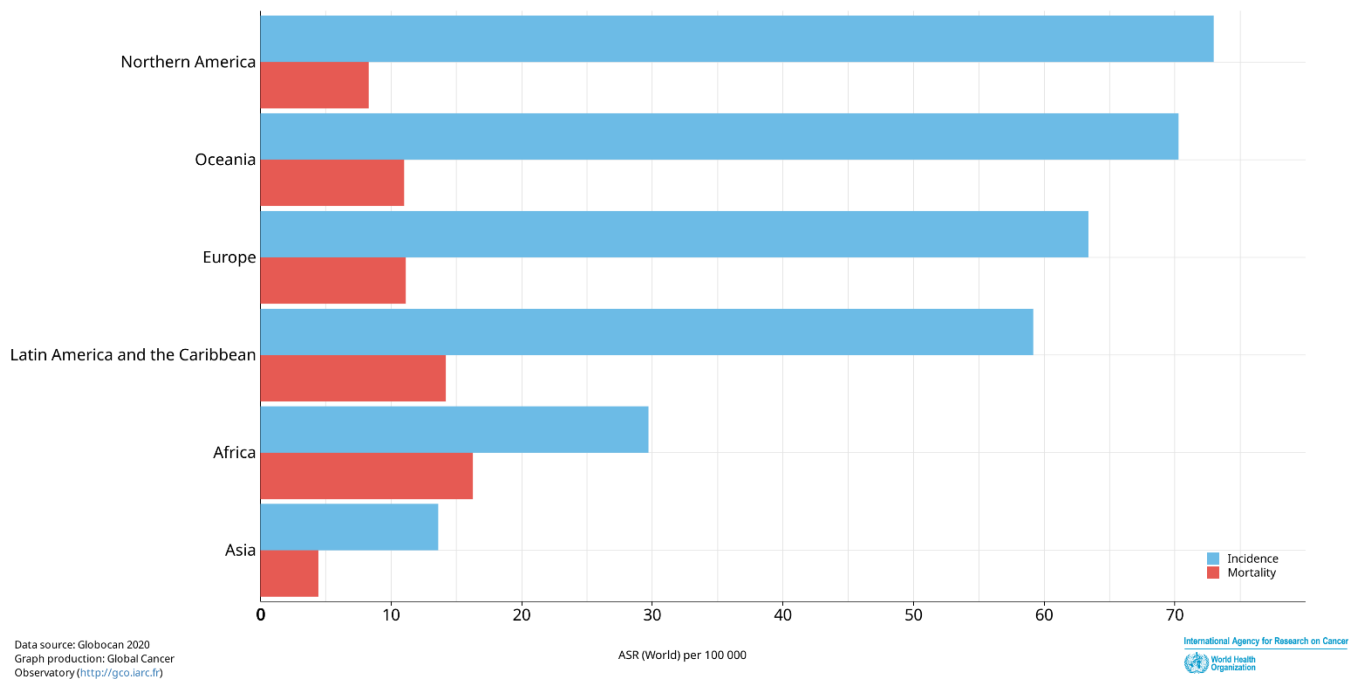
Figure 1.2: Global estimated age-standardized incidence & mortality rates (2020) of PCa. (GLOBOCAN 2020) (44)

Generally, Africa has high mortality and 5 years prevalence rate of PCa irrespective of the region in Africa (3). In the developed world, there is relatively lower mortality compared to the incidence rate of PCa when compared with the ratio of incidence to mortality rate in Africa (Figure 1.3 and 1.4) (44). This is partly due to the available health infrastructure and well-established health system that allow effective early diagnosis of patients compared to Africa, where there is a lack of proper health infrastructures (45).

Estimated age-standardized incidence rates (World) in 2020, prostate, males, all ages

ASR (World) per 100 000

- ≥ 68.5
- 45.0–68.5
- 32.3–45.0
- 14.5–32.3
- < 14.5

Not applicable
No data

Data source: GLOBOCAN 2020
Graph production: IARC
(http://gco.iarc.fr/today)
World Health Organization

World Health
Organization
© International Agency for
Research on Cancer 2022
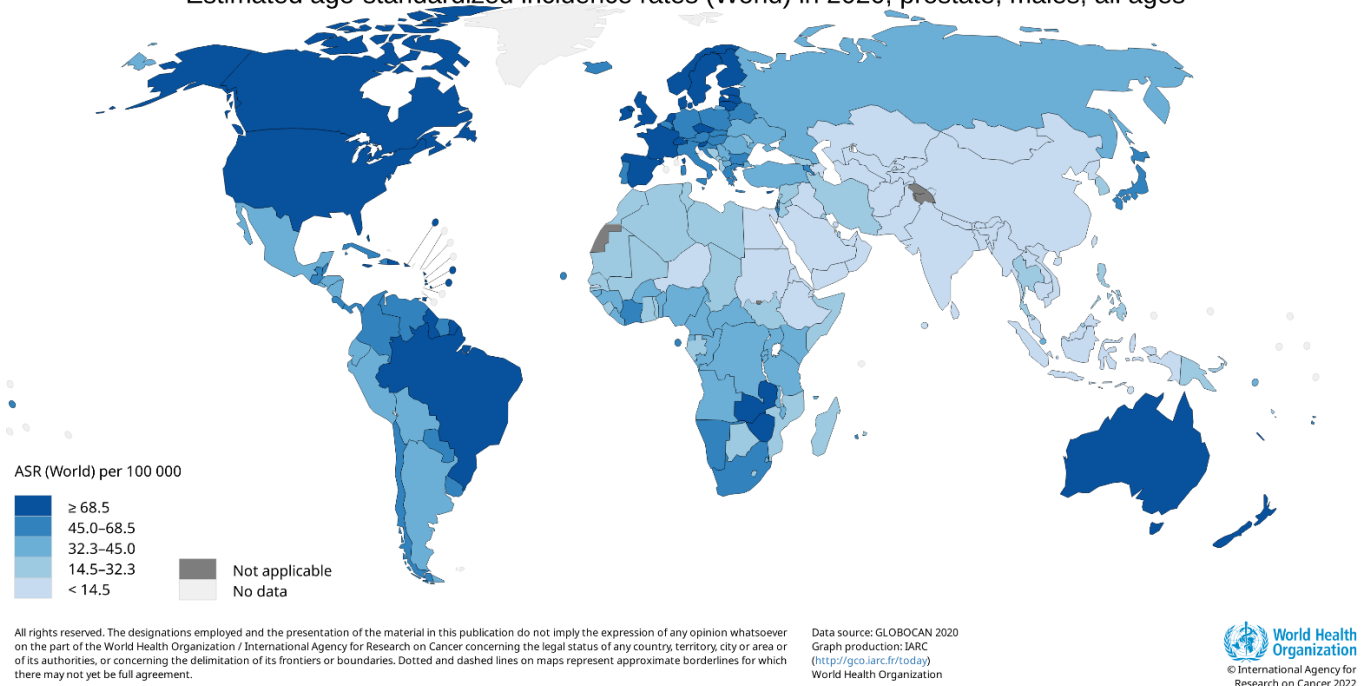
Figure 1.3: Global estimated age-standardized incidence rates (2020) of PCa. (GLOBOCAN 2020) (44).

8

Estimated age-standardized mortality rates (World) in 2020, prostate, males, all ages

ASR (World) per 100 000

≥ 20.8
14.3–20.8
10.6–14.3
6.0–10.6
< 6.0

Not applicable
No data

Data source: GLOBOCAN 2020
Graph production: IARC
(http://gco.iarc.fr/today)
World Health Organization

World Health Organization
© International Agency for Research on Cancer 2022
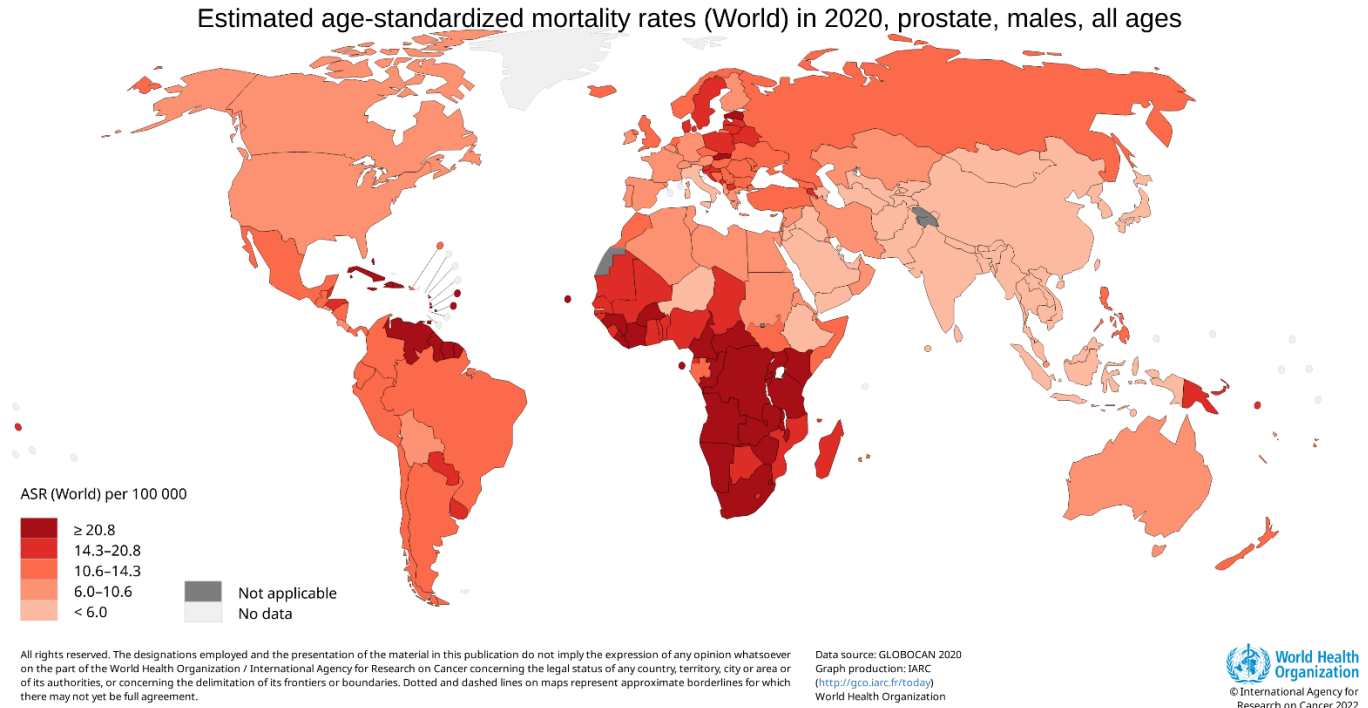
Figure 1.4: Global estimated age-standardized mortality rates (2020) of PCa. (GLOBOCAN 2020) (44).

1.2.3   Aetiology of prostate cancer.

The carcinogenesis of PCa, like many other human cancers, is not fully understood. However, some aetiological risk factors are associated with PCa development and progression (46). Some of these risk factors cannot be modified these include age, family history of PCa, and race. In contrast, others are modifiable, including smoking, alcohol use, obesity, diet, androgens, and diseases such as diabetes mellitus (46).

PCa is the most commonly diagnosed cancer among elderly males, making age an important factor in the development of PCa (3). The risk of developing PCa increases from 40 years of age among black men and 50 years in white men (47).

Previous studies have shown men of African origin to have a higher rate of developing PCa than other groups (48,49). Some studies have investigated this racial disparity in incidence, aggressiveness, and mortality rates (50,51). Variation in germline and genetic background, poor access to medical care and screening facilities, and socioeconomic status have been mentioned in different studies as the reasons for racial disparity (50–52). Blackburn et al. found

a lower frequency for TMPRSS2-ERG fusion in black South Africans than in those of European ancestry. There is inverse association between TMPRSS2-ERG fusion and aggressive PCa (53). Jaratlerdsiri et al. in their whole-genome sequencing study found an increase in small somatic variants when they compared paired tumor-normal tissues of African patients and European patients (54). They also found increased oncogenic driver mutations in tumors of African patients compared to the European patients (54).

Family history and other genetic factors are important risk factors in PCa development. The role of family history in PCa development depends on the degree of relationship and the age of the relative at diagnosis (55–58). About 15% of PCa patients of African origin have one or more relatives with PCa (48). A meta-analysis review of studies in European populations revealed an increased risk of about 2.5-fold of developing PCa among men with first-degree relatives diagnosed with PCa (56). Genetic predisposition of PCa has been widely researched. For example, the mutation in the RNaseL/hereditary prostate cancer 1 gene has been linked to PCa development below the age of 65 years, while HPC20 gene is associated with PCa diagnosis in older men (59). Other genes associated with PCa development include PTEN, BRCA2, RB1, MSR1 (8p22), NKX3.1, androgen receptor (AR), CYP17, and steroid-5-α-reductase type II (SRD5A2), CDKN1B, TMPRSS2, and ELAC2 (60).

The variation seen in PCa incidence globally agrees with variations in diet (61). The diet of people living in developed countries with a high incidence of PCa is known to be very rich in animal fat (61). In contrast, countries with a low incidence of PCa have a diet high in soy proteins and little animal fats (61). Studies have shown consuming food such as red meat and animal fat leads to a high risk of developing PCa, while diets rich in red tomatoes, cruciferous vegetables, and soy products have been linked with a low PCa risk (62–65).

Alcohol consumption and smoking have been well associated with many human cancers. A meta-analysis review on the relationship between smoking and PCa development showed a 14% increase in mortality risk of PCa (66). The association between PCa and alcohol consumption is somewhat contradictory as some studies have shown a positive relationship between alcohol consumption and PCa development, while other studies showed no relationship (67–69).

1.2.4 Clinicopathological Classification of Prostate Cancer

Diseases, including PCa, require an international standardized system of classification that will enhance easy communication between pathologists and clinicians, proper understanding of the disease aggressiveness and severity, and guide treatment decisions.

The three major criteria that must be considered in formulating a grading system are 1) reproducibility of the grading system among pathologists, 2) the prognostic ability of the grading system surpassing clinical parameters, and 3) the results of random biopsies sufficiently representative of the entire tumor (70).

1.2.5 Histological Classification of prostate cancer

The Gleason's grading system

Many grading systems have been used for grading PCa. However, the histopathological grading system for PCa has proven to be the strongest grading system for stratifying patients into different treatment options and determining the prognosis of disease recurrence and death. Among the grading systems developed over time for PCa, the Gleason grading system developed in 1966 by Donald Gleason has become widely accepted (71).

The grading system is based on research by Donald Gleason and his group at the Veteran's Hospital in Minnesota between 1959 and 1964 (71). The grading system was developed after considering the architectural pattern of hematoxylin and eosin slides of 270 PCa patients under a light microscope (71).

The Gleason grading was further tested in a larger cohort of 1032 patients, after which the grading system received global acceptance in grading PCa (72). Based on cell morphology, the Gleason grading system classifies prostatic carcinoma into five grading categories 1 to 5. As the grade increases from grade 1 to 5, histopathologic differentiation becomes poorer with increasing severity of malignancy (65,66,73) (Figure 1.5). Grade 1 is well-differentiated, while grade 5 is the worst differentiated morphology. Gleason score (GS) is usually calculated by adding the Gleason grade of the most predominant (primary) and the second most predominant (secondary) histologic patterns of the tumor (65,66,73). In cases with only one histologic pattern, the primary and secondary patterns will be regarded as similar and the GS of 3+3=6, 4+4=8, or 5+5 is obtained.

Although the Gleason grading system is widely accepted in the grading of PCa, some issues were not properly addressed. This includes that the Gleason study was on tissue morphology alone without immunohistochemistry, Gleason grading system did not offer any recommendations on reporting different grades of tumor nodules in radical prostatectomies, and new patterns of prostatic carcinoma have been defined and need to be integrated into the system (74–76).

Figure 1.5: Histologic grades of PCa (adapted from the original Gleason grading system) (77)

PROSTATIC ADENOCARCINOMA
(Histologic Grades)

D.F. Gleason, M.D.
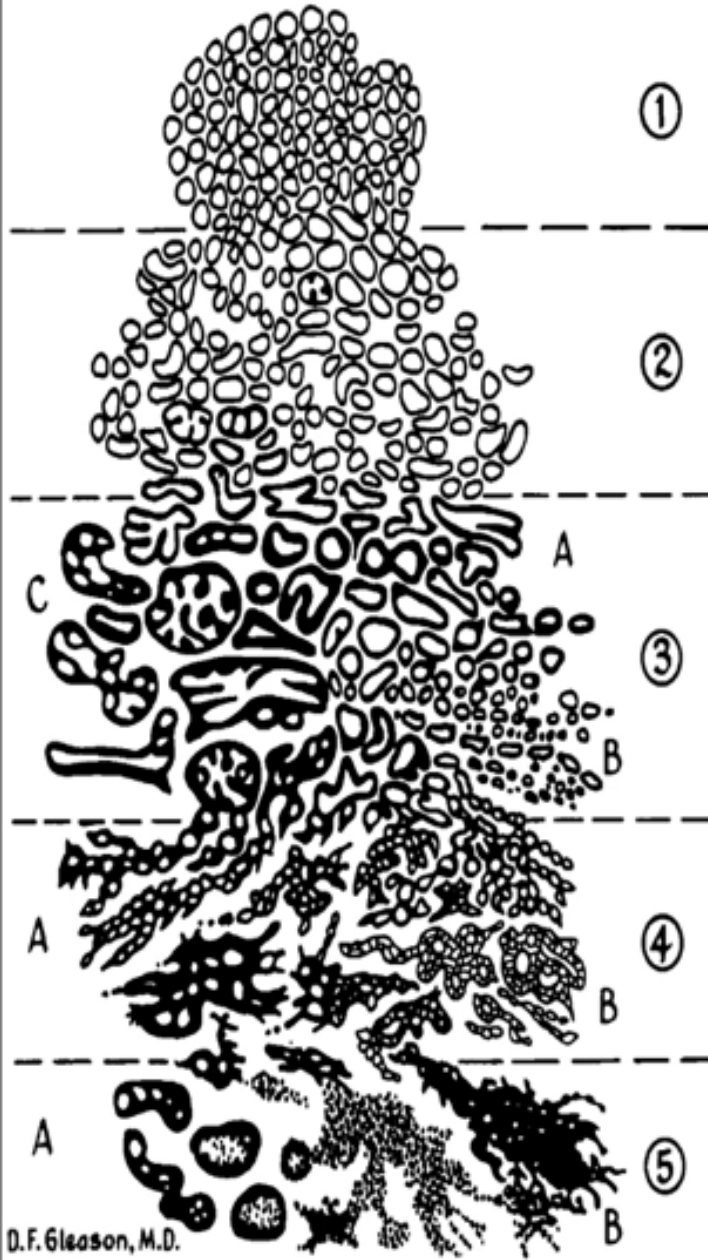
Grade	Description
1	1-Simple round glands, close-packed in rounded masses with well-defined edges
2	2-Simple rounded glands, loosely packed in vague, rounded masses with loosely packed defined edges
3	3A-Medium-sized single glands of irregular shape and irregular spacing with ill-defined infiltrating edges. 3B-Very similar to 3A, but small to very small glands, which must not form significant chains or cords. 3C-Papillary and cribriform epithelium in smooth, sharply circumscribed rounded cylinders and masses, no necrosis.
4	4A-Small, medium, or large glands fused into cords, chains or ragged, infiltrating masses. 4B-Very similar to 4A, but with many large clear cells, sometimes resembling 'hypernephroma'
5	5A-Papillary and cribriform epithelium in smooth, rounded masses, more solid than 3C and with central necrosis 5B-Anaplastic adenocarcinoma in ragged sheets

WHO histologic classification of prostate cancer.

In 2004, the World Health Organization (WHO) developed a detailed histological classification of prostate tumors (78). Due to better insight into the morphology of PCa immunohistochemistry and their associations with clinical features, the classification was updated in 2016 (79). The major differences between the 2004 and 2016 WHO classifications are: (1) inclusion of new immunohistochemical markers, which are important in making diagnosis, (2) modification of the Gleason grading system to accurately match the clinical outcomes, (3) an update of the variant of acinar adenocarcinoma and recognition of new subtypes of prostatic cancer (large cell neuroendocrine carcinoma and Intraductal carcinoma of the prostate) (80) (Table 1.2).

Table 1.2: WHO Classification of Prostate cancer in 2004 and 2016 (78,79)

2004 WHO classification	2016 WHO classification
Glandular neoplasms	Glandular neoplasms
Acinar adenocarcinoma	*Acinar adenocarcinoma*
	Intraductal carcinoma
Ductal adenocarcinoma	*Ductal adenocarcinoma*
Urothelial carcinoma	Urothelial carcinoma
Squamous neoplasms	Squamous neoplasms
Adenosquamous carcinoma	*Adenosquamous carcinoma*
Squamous cell carcinoma	*Squamous cell carcinoma*
Basal cell carcinoma	Basal cell carcinoma
Neuroendocrine tumors	Neuroendocrine tumors
Endocrine differentiation within adenocarcinoma	*Adenocarcinoma with neuroendocrine differentiation*
Small cell carcinoma	*Small cell neuroendocrine carcinoma*
	Large cell neuroendocrine carcinoma

1.2.6   Staging of Prostate Cancer

PCa staging is usually based on clinical examination, imaging, biomedical testing, and biopsy. The Whitmore-Jewett staging system has been used for a long time as a clinical staging method by clinicians (81,82). However, the new tumor, node, and metastasis (TNM) staging method developed by WHO is fast becoming the most common method by clinicians for staging PCa. The "T" in the TNM acronym represents tumor extent, while "N" represents lymph node invasion, and "M" represents the presence or absence of metastasis. The TNM classification described by WHO is shown in Tables 1.4 and 1.5.

Table 1.3: Definitions of clinical TNM classifications.

CATEGORY	CRITERIA
Clinical cT	
T Category	
TX	Primary tumor cannot be assessed
T0	No evidence of primary tumor
T1	Clinically inapparent tumor that is not palpable
T1a	Tumor incidental histologic finding in 5% or less of tissue resected.
T1b	Tumor incidental histologic finding in more than 5% of tissue resected.
T1c	Tumor identified by needle biopsy found in one or both sides, but not palpable
T2	Tumor is palpable and confined within prostate
T2a	Tumor involves one-half of one side or less
T2b	Tumor involves more than one-half of one side but not both sides
T2c	Tumor involves both sides
T3	Extraprostatic tumor that is not fixed or does not invade adjacent structures
T3a	Extraprostatic extension (unilateral or bilateral)
T3b	Tumor invades seminal vesicle(s)
T4	Tumor is fixed or invades adjacent structures other than seminal vesicles such as external sphincter, rectum, bladder, levator muscles, and/or pelvic wall

Table 1.4: Definitions of pathological TNM classifications.

CATEGORY	CRITERIA
Pathologic pT	
T Category	
T2	Organ confined
T3	Extraprostatic extension
T3a	Extraprostatic extension (unilateral or bilateral) or microscopic invasion of bladder neck
T3b	Tumor invades seminal vesicle(s)
T4	Tumor is fixed or invades adjacent structures other than seminal vesicles such as external sphincter, rectum, bladder, levator muscles, and/or pelvic wall
N Category	
NX	Regional lymph nodes were not assessed
N0	No positive regional lymph nodes
N1	Metastases in regional lymph node(s)
M Category	
M0	No distant metastasis
M1	Distant metastasis
M1a	Nonregional lymph nodes
M1b	Bone
M1c	Other site(s) with or without bone disease

The American Joint Committee on Cancer (AJCC) used TNM staging in combination with the GS and Prostate Specific Antigen (PSA) level to develop a more acceptable staging system for PCa. The first edition of the AJCC staging manual was published in 1977, and it has since been revised several times until the current 8th edition (83). In prostatic carcinoma staging, the TNM staging system was first introduced in the 4th edition of AJCC staging manual when the AJCC and the International Union Against Cancer approved a joint TNM staging system for PCa (Table 1.5) (84). The AJCC staging system has helped bring about a more multiparametric improvement to PCa staging and guides more appropriate treatment plans.

Table 1.5: AJCC Prognostic Stage Grouping.

T	N	M	PSA	GRADE GROUP	STAGE GROUP
cT2a pT2	N0	M0	<10 ng/mL	1	I
cT1a-c, cT2a	N0	M0	≥10, <20 ng/mL	1	IIA
pT2	N0	M0	≥10, <20 ng/mL	1	IIA
cT2b-c	N0	M0	<20 ng/mL	1	IIA
T1-2	N0	M0	<20 ng/mL	2	IIB
T1-2	N0	M0	<20 ng/mL	3	IIC
T1-2	N0	M0	<20 ng/mL	4	IIC
T1-2	N0	M0	≥20 ng/mL	1-4	IIIA
T3-4	N0	M0	Any	1-4	IIIB
Any T	N0	M0	Any	5	IIIC
Any T	N1	M0	Any	Any	IVA
Any T	Any	M1	Any	Any	IVB

Note that when either PSA or grade group is unavailable, grouping should be determined by T category and/or either PSA or grade group, as available.

1.2.7   Diagnosis of Prostate Cancer.

PCa diagnosis involves proper clinical history, digital rectal examination (DRE), testing for PSA in the blood. Transrectal ultrasound (TRUS) assisted biopsy is required in making final diagnosis when prostate irregularities are found during the DRE and/or elevated PSA levels.

The DRE is an examination where the healthcare practitioner palpates the prostate for any irregularities by inserting a lubricated glove finger into the rectum (Figure 1.6). The DRE is usually part of the complete general physical examination. Prostate gland irregularities such as enlargement, hard spot, tenderness is indication for prostate biopsy.
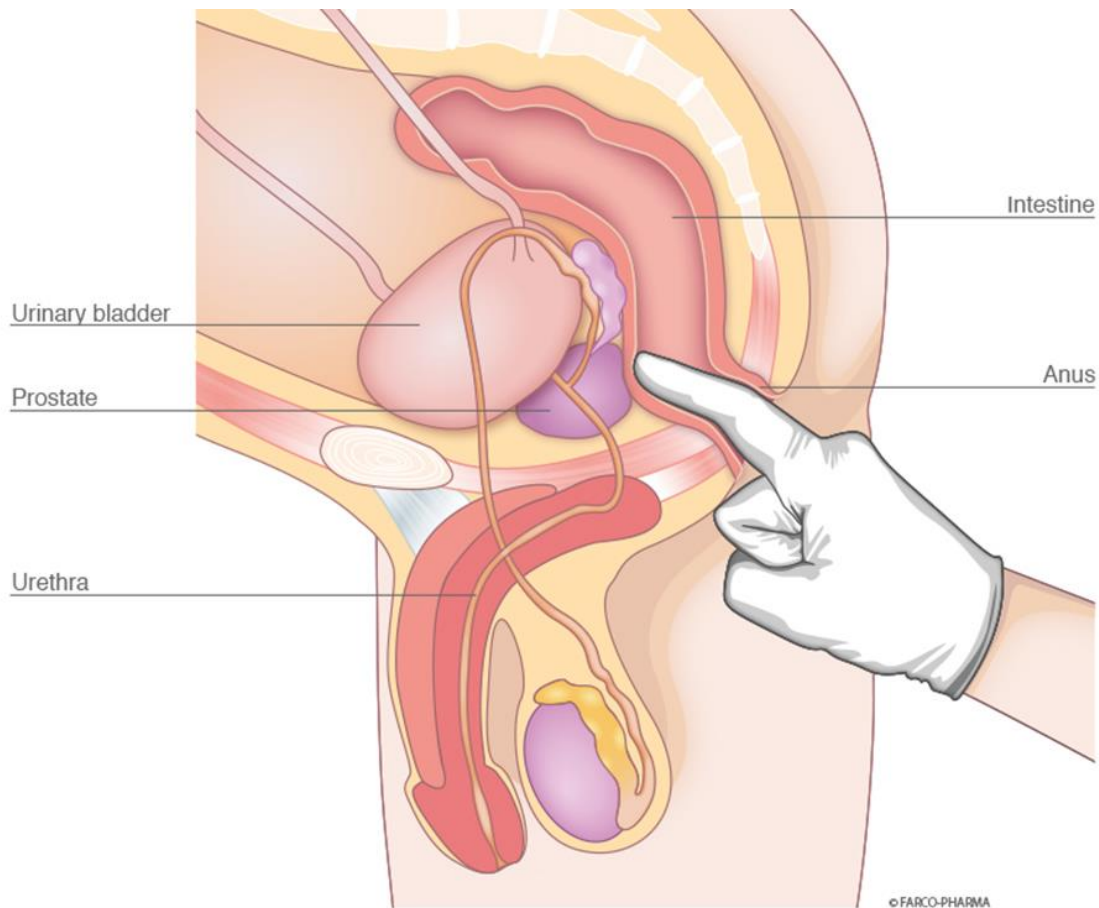
Figure 1.6: Digital rectal examination of the prostate (https://www.farco.de)

PSA level in the blood remains an important biochemical test in diagnosing PCa. Serum PSA level is specific to prostate gland and not PCa-specific, this explains high PSA levels reported in other prostate pathologies such as prostatitis and BPH (85,86). Generally, PSA levels above 4.0ng/mL may indicate a need to further investigation of PCa in men (87). However, PSA levels are age and population specific. Oesterling et al. developed an age-related reference range for serum PSA of white Americans in the United States (88). They showed that the recommended upper limit of normal serum PSA levels of white men is 2.5 ng/mL for 40-49 years, 3.5 ng/mL for 50-59 years, 4.5 ng/mL for 60-69 years, and 6.5 ng/mL for men aged 70-79 years (88). Black men generally have higher PSA levels when compared with white men (89). Ikuerowo et al. demonstrated that the upper limit of normal serum PSA levels of African men is 4.8 ng/mL for 40-49 years, 5.5 ng/mL for 50-59 years, 8.9 ng/mL for 60-70 years, and 6.5 ng/mL for men aged 70-79 years (90). Serum PSA level is specific to prostate gland and

not PCa-specific, this explains high PSA levels reported in other prostate pathologies such as prostatitis and BPH (85,86).

Hodge et al. 1989, showed that TRUS guided biopsies are superior to DRE guided biopsies (91). Since then, TRUS guided biopsy has been widely accepted as a standard technique for PCa diagnosis. The biopsy procedure involves the insertion of a hollow, thin needle into the prostate gland. This is usually either through the rectal wall (transrectal) or through the skin between the anus and scrotum (transperineal) (Figure 1.7) (91). The transrectal biopsy is the commonest form of the two types. As the thin needle is pulled out, a small portion of prostatic tissue is removed. This process is repeated about 8 to 10 times from different parts of the prostate to have an adequate prostatic sample for investigation. Other indications for using TRUS include measurement of prostate gland size, cryotherapy, or brachytherapy (92). The complications of TRUS guided biopsy include pain, prostate gland and epididymis infections, rectal bleeding, hematospermia, and hematuria (93).
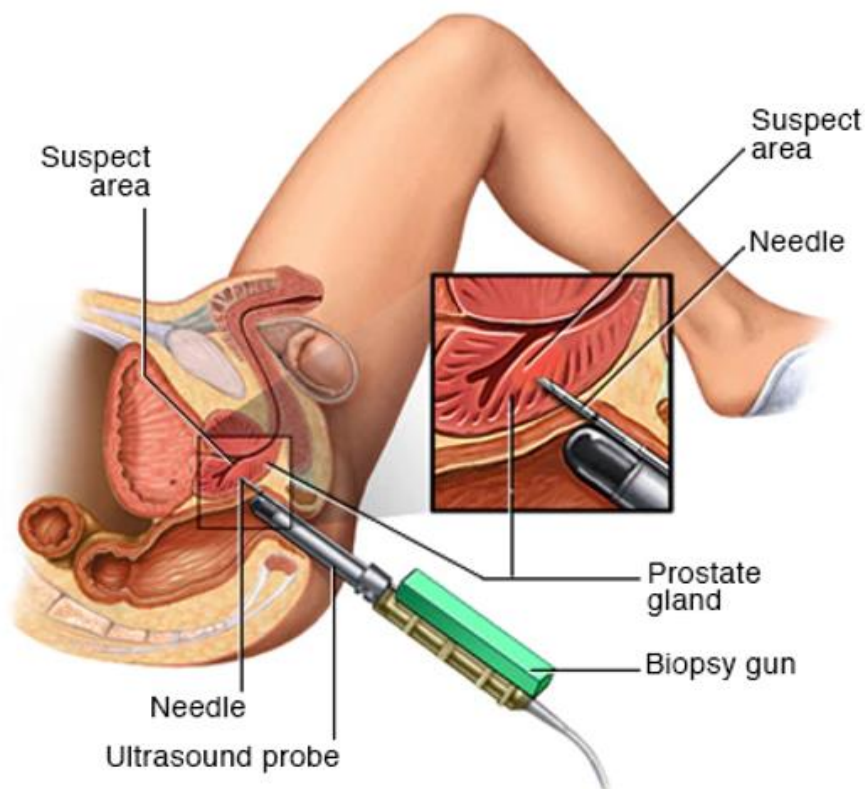
Figure 1.7: TRUS guided biopsy of the prostate (www.mayoclinic.org)

1.2.8 Management of Prostate Cancer

Factors such as history of prostate malignancy, the stage at presentation, the risk of progressing to more aggressive malignancy, age, and socioeconomic status of patients are important features to be considered in deciding the treatment plan for a newly diagnosed PCa (94).

The overall management of PCa is dependent on if the malignancy is diagnosed as a localized or metastatic disease. The treatment options for localized PCa are based on risk stratification of the clinical feature of the disease, such as the one developed by the National Comprehensive Cancer Network (NCCN) have been developed (94,95) (Table 1.6).

Table 1.6: NCCN Risk Stratification and Management of Localized Prostate Cancer (adapted from Kachuur 2018) (42). mm

NCCN Risk Stratification and Management of Localized Prostate Cancer	
Risk Group and Features	Initial Therapy
Very low Stage T1c, GS<6, PSA<10, <3 positive biopsy cores, cancer in 50% of each core, and PSA density <0.15	LE <10y: observation LE 10-19y: AS LE >20y: same as low risk with >10y expected survival
Low Stage T1-2a, GS<6, PSA<10	LE <10y: observation LE ≥10y: either: AS, EBRT, brachytherapy, RP±PLND
Favourable intermediate Stage T2b-2c or GS3+4=7 or PSA 10-20 and <50% positive biopsy cores	LE <10y: either: observation, EBRT, or brachytherapy LE ≥10y: same as low risk with >10y expected survival
Unfavourable intermediate Stage T2b-2c or GS3+4=7 or PSA 10-20	LE <10y: either: observation, EBRT + short-term ADT, or EBRT + brachytherapy + short-term ADT LE >10y: RP±PLND, EBRT + short-term ADT, or EBRT + brachytherapy + short-term ADT
High or Very High Stage T3a-T4, GS 8 to 10, primary Gleason pattern 5, PSA >20	LE >5y: either: EBRT + long-term ADT, EBRT + brachytherapy + long-term ADT, or RP±PLND
ADT: androgen deprivation therapy; AS: Active surveillance; EBRT: external beam radiation therapy; GS: Gleason score; LE: life expectancy; PLND: pelvic lymph node dissection; PSA: prostate-specific antigen; RP: radical prostatectomy.	

The treatment of PCa may range from expectant management (watchful waiting and active surveillance), surgery, hormone therapy, radiation, chemotherapy and other forms of palliative treatment. The treatment of choice is usually depending on factors such as stage of the disease at diagnosis, patient age, presence or absence of metastasis. Watchful waiting and active surveillance are two major components of expectant management (94,96). Watchful waiting

and active surveillance are sometimes used interchangeably, although they are two different entities. Watchful waiting involves less monitoring of patients with the goal of palliative treatment, while active surveillance involves more frequent monitoring with curative treatment in view (94,96).

Radical prostatectomy and pelvic lymphadenectomy are the two most common surgical procedures in treating PCa (97). Traditionally, radical prostatectomy has been discouraged in the management of localized PCa due to side effects such as urinary incontinence, erectile dysfunction, risk of lymph node metastasis and increase rates of positive surgical margins. However, studies have shown radical prostatectomy is more beneficial than watchful waiting (98,99). A clinical trial by Bill-Axelson et al. showed a reduction in local progression, metastasis and mortality rate among patients when radical prostatectomy was compared with watchful waiting (100).

PCa treatment by radiotherapy can either be with external-beam radiotherapy or brachytherapy (101). Brachytherapy can be administered as low-dose rate brachytherapy, which involves permanently placing into the prostate gland radioactive seeds of about sixty days half-life (102). High-dose rate brachytherapy (HDRB) involves the placement of applicators temporarily in the prostate in such a way to allow the exposure of high energy sources to different positions of the prostate and, at the same time, minimizing the exposure dose to the bladder and other surrounding tissues. HDRB is usually considered a good treatment option for patients with more locally advanced PCa (102).

Hormonal treatment in the management of PCa is based on the role of androgen in prostatic growth (103). Androgen hormone activates AR, a ligand-dependent transcription factor acting in the cell nucleus to promote prostatic growth. PCa develops when other surrogate pathways activate and amplify AR without androgen stimulation (104). Adrenal androgens have only minimal effect on the prostate at normal concentrations. However, when other surrogate pathways become involved in the activation of AR, androgens become fuel for the progressive growth of prostate tumor, making androgen deprivation therapy (ADT) an important therapy in the treating PCa (105). Bilateral orchidectomy is the original form of ADT that is still in use globally, although it is being replaced by medical options such as ADT drugs. Diethylstilbestrol was traditionally used as ADT and later replaced with luteinizing hormone-releasing hormone (106). The current medications used for ADT are agonists and antagonists of GnRH (Gonadotropin releasing hormone), these include estrogens and AR blockers (107). Orgovyx

(relugolix) is the first United State Food and Drug Administration (FDA) approved oral hormone therapy for the treatment of advanced PCa in adult patients (108). Some chemotherapeutic drugs have also been used in the treatments of advanced PCa. These include docetaxel, doxorubicin, carbazitaxel, and mitoxantrone.

The treatment of very low and low-risk localized PCa may include expectant management, radical prostatectomy, and radiation (94). The treatment of intermediate-risk PCa is concurrent radiation and ADT for a short period of 4-6 months (94). This treatment regimen is based on the results of some clinical trials that showed the addition of ADT to this category of patients led to an increase in overall survival among patients (109,110). For localized PCa patients with high- and very high-risk, the recommended treatment protocol is external beam radiation therapy and ADT for a long period of about 2-3 years or radical prostatectomy. Studies have shown that a combination of radiation therapy and ADT helped to improve the overall survival of patients (111,112).

In patients diagnosed with metastatic PCa, the first line of treatment is ADT, which can either be taken intermittently or continuously. Other new options for the treatment of metastatic PCa include the use of abiraterone in combination with prednisone or ADT and docetaxel (94). Metastatic PCa patients who initially respond to ADT may develop resistance to ADT, while in few cases, patients do not respond at all and continue to progress despite the patients been on ADT, this is referred to as castration resistant PCa (CRPC). The treatment options for CRPC patients depend on the disease symptoms and the presence or absence of metastases (94). For treatment of minimally symptomatic CRPC, ADT may be changed to abiraterone, or a complete change to second-line hormonal therapy such as progesterones, estrogens, or ketoconazole (94,113). Treatment of CRPC patients with metastases may include docetaxel with a corticosteroid, cabazitaxel with corticosteroid, or Sipuleucel-T (94,114).

So far, there is still no available approved biomarker for the screening of aggressive PCa in the management of PCa. A good biomarker for the screening of aggressive PCa will largely help in effective treatment of PCa and to avoid overtreatment of indolent, localized lesion. This makes it important for more studies to be done to investigate the role of liquid biopsy in the diagnosis of PCa.

1.3   Liquid Biopsy in Prostate Cancer

The microscopy analysis of tissue biopsy is considered the gold standard in the diagnosis and treatment monitoring of PCa (115). However, tissue biopsy is usually accompanied by varying complications, ranging from minor to more severe. Also, the accuracy of PSA in correctly diagnosing PCa is low, with a high false positive and negative rate (116). Studies explore liquid biopsy-based biomarkers in PCa diagnosis and prognosis in the quest for accurate, safe, and non-invasive diagnostic tool for PCa. Circulating tumor cells (CTCs) and other biological molecules such as cell-free nucleic acids (DNA and RNA), and extracellular vesicles are shed from tumor masses into the blood, urine, saliva, and other body fluids (Figure 1.8) (117). Generally, there is a growing focus on the discovery of liquid biopsy biomarkers in cancer diagnosis and treatment monitoring.
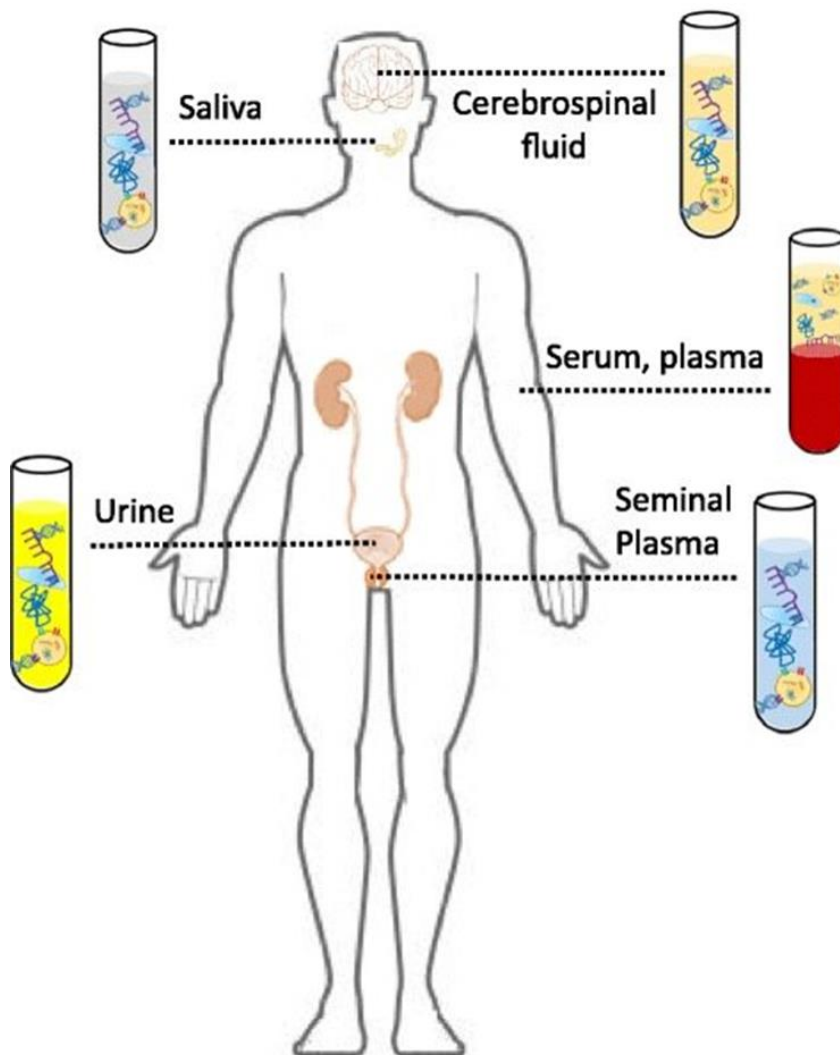
Figure 1.8: Body fluids used as liquid biopsy (117).

1.3.1 Cell free DNA

CfDNA was first identified in plasma by Mandel in 1948 (118). Some years after Mandel's discovery, Leon et al. showed an increased cfDNA concentration in cancer patients (119). The increased cfDNA levels distinguished healthy individuals from cancer patients and differentiated between patients with benign and malignant tumors (120). It has been shown that the increase in cfDNA levels in cancer patients is due to the release of DNA fragments from tumor cells. DNA fragments from tumors cells, known as circulating tumor DNA (ctDNA), have longer fragment size than the fragment size of DNA released from normal cells (121,122). The fragment size of cfDNA usually measures between 150 and 200 bp, with an average size of 167 bp (123,124).

CfDNA is found in body fluids such as blood, urine, and saliva (125–127). Although cfDNA fragments are free from cells, they are usually found in complexes with proteins (128,129). The mechanism of cfDNA released into circulation is not completely known, although cell lysis, necrosis, apoptosis and active release are considered major sources. The origin of cfDNA in a healthy person is mainly of hematopoietic origin, while the origin is both hematopoietic and tumor cells in cancer patients (130). CfDNA parameters used for diagnosis, monitoring of treatment response, and predicting the stage of cancer include cfDNA level and DNA integrity index (131). DNA integrity index is calculated using the ratio of long to short DNA fragments (132).

Tumor-specific abnormalities, such as copy number variation, oncogenes and tumor suppressor genes mutations, DNA methylation, and microsatellite instability, are present in cfDNA fragments (133–136). These genomic aberrations can be identified with techniques such as next-generation sequencing (NGS), real-time PCR, or droplet PCR, which can also aid in the cancer diagnosis and treatment response monitoring (137).

The role cfDNA play in metastatic PCa diagnosis have been described (138,139). Hennigan et al. found that ctDNA can be detected by low pass whole-genome and targeted deep sequencing in metastatic PCa patients but not in localized disease (139). Presently, the utility of cfDNA in the diagnosis of early PCa is limited. However, recent findings in some cfDNA studies show differences in healthy and tumor cells nucleosome footprints which may help in expanding the use of cfDNA to early detection (140,141).

Studies have described the potential use of cfDNA as prognostic biomarker for PCa (138,142,143). A study by Wyatt et al., compared cfDNA abnormalities with matched tissue in metastatic PCa and found many genetic alterations, such as AR amplifications, and inactivation of TP53, BRCA2, PTEN, APC, CDKN1B, RB1, and PIK3R1 genes (138). These findings revealed the possibility of using cfDNA as prognostic biomarker for PCa (138). So far, the FDA has approved five cfDNA based diagnostic tests for cancer. In 2021, FDA approved Guardant360 CDx to help in lung cancer diagnosis. In 2020, FDA approved FoundationOne Liquid CDx, a comprehensive genomic profiling assay, to aid in the diagnosis of PCa, lungs and other solid tumors. The Qiagen Therascreen EGFR Plasma kit got approval from FDA in 2019 to aid the breast cancer treatment. The Cobas EGFR Mutation Test v2 by Roche Molecular Diagnostics got approval from FDA in 2016, to assist in management of lung cancer (144). FDA approved The Epi proColon test, a PCR test was also approved in 2016 by FDA for the screening of colorectal cancer (145).

In Europe, three cfDNA-based tests have received approval to aid diagnosis of colorectal cancer. These are Idylla™ ctKRAS Mutation Test, Sysmex Inostics OncoBEAM RAS CRC Kit, and Idylla™ ctNRAS-BRAF mutation test (146). The Therascreen EGFR RGQ kit is also approved in Europe to aid the diagnosis of lung cancer (146). The Chinese FDA approved the Super-ARMS EGFR kit to aid lung cancer diagnosis and treatment.

1.3.2 Exosomes

Extracellular vesicles released by cells into body fluids have been explored as a biomarker source in the management of cancer (147). Extracellular vesicles are differentiated into three major subtypes, microvesicles, exosomes, and apoptotic bodies, based on their size, biogenesis, and function (148,149). Exosomes are the most studied of the major three forms (150). When exosomes were first discovered in the 1980s, they were initially considered cellular waste (151). They were later found to be a means of intercellular communication with key function in health and pathological state (152). Exosomes have a size ranging from 40–150 nm in diameter (153,154). Exosomes possess a lipid bilayer membrane of about 5 nm in width, which helps to preserve them from proteases and RNases activity. The lipid bilayer membrane contains various cargo, such as proteins, lipids, viral particles, DNA, messenger ribonucleic acid (mRNA), micro-ribonucleic acid (miRNA), and non-coding ribonucleic acid (RNA). Their

presence depend on the health status of the organism and the cells releasing the exosomes (155).

Exosomes are released by different cells, into the blood and other body fluids (156–158). Plasma and other body fluids from cancer patients contain more exosomes than healthy individuals (159,160). This proved that more exosomes are produced in cancer than normal cells (154). Exosomes serve as a vehicle for transmitting molecular messages between heterotypic and homotypic cells, thereby contributing to tumor progression, immune response, angiogenesis, and metastasis (161). This makes exosomes a potential biomarkers source for PCa and other cancer types.

Biogenesis of Exosomes

Exosomes originate from the late endosomes, which are produced by inward budding of the multivesicular body (MVB) membrane. Invagination of the late endosomal membranes leads to formation of intraluminal vesicles (ILVs) within the MVBs (162). This process involves the incorporation of some proteins into the late endosomal membranes and the engulfment of cytosolic components within the ILVs (163). Exosomes are formed either by fusion of ILVs with plasma membrane or by the trafficking of ILVs into lysosomes for degradation (163,164).

The MVBs and ILVs formation depend largely on endosomal sorting complex required for transports (ESCRTs) functional activities (165). The components of ESCRTs, which are made up of about 20 proteins consists of four complexes (ESCRT-0, -I, -II, and -III), with other proteins, such as VTA1 (Vesicle Trafficking 1, ALIX (Apoptosis-linked gene and TSG101 (Tumor susceptibility gene 101 protein) (166,167). The four complexes of ESCRT-0 functions at different stages of MVBs biogenesis for example, ubiquitinated cargo, which is the main pathway-specific signal in the biogenesis of MVBs to endosomal membrane uses ESCRT-0 (168,169). The formation of buds from endosomal membrane usually requires ESCRT-I and -II, while ESCRT-III complex helps in separating vesicles from cytoplasmic membrane (168,169). Evidence of other pathways, which affect exosomes but not dependent on ESCRTs have been shown in recent studies (170,171). Some of these pathways include neutral sphingomyelinase 2-dependent pathway, miRNA post-transcriptional 3′end modification and RNA induced silencing complex related pathway (171).

Exosomal microRNA

Exosomal RNAs include mRNAs and other non-coding RNAs such as miRNA, long non-coding RNAs, and circular RNAs (172–174). miRNA can the transported by exosomes to neighbouring cells, where they control gene expression and other biological functions (175–177). There are series of evidence to show that miRNAs are not randomly sorted into exosomes but are rather sorted into exosomes under well-controlled mechanisms (178,179). The small RNAs in exosomes are enriched with miRNAs, suggesting a selective loading of miRNAs into exosomes (180,181). Other studies have also shown that exosomal miRNA have different profiles from miRNA in cells supporting a well-organized sorting mechanism for miRNA into exosomes (182,183).

Presently, the specific mechanism for sorting miRNA into exosomes is not fully known. However, some mechanisms have been proposed to be responsible for the sorting of miRNA into exosomes, these include RNA-induced silencing complex; ceramide; sequence motifs and guide proteins; 3′ end non-template terminal nucleotide additions; and cellular levels of miRNAs and miRNA targets (175,178,184,185).

Growing evidence has shown tumor cell-derived exosomes, through their miRNAs cargo, play a major role in promoting proliferation of tumor cell, angiogenesis, and tumor metastasis (186). Studies have revealed that exosomal miRNA released from tumor cells including miRNA21, miRNA29, miRNA23, and miRNA210 promote tumor proliferation, angiogenesis, and migration (186–189). A study by Le et al., reported the transfer of exosomal miRNA most especially the miRNA200 family, could impact metastasis in cancer cells (190).

Exosomal miRNAs have been shown to be suitable potential diagnostic and prognostic biomarkers in PCa. Xu et al. found the potential use of exosomal miRNA145 as a biomarker for diagnosis of PCa (191). Foj et al. in their urinary exosomal study also found miRNA21, miRNA141, miRNA214, miRNA375, and let-7c as potential diagnostic biomarkers for PCa (192). Recent studies have also shown the role of miRNA424 as a potential biomarker for PCa (193–195). A study by Huang et al. showed the utility of exosomal miRNA as prognostic biomarker in PCa by identifying the prognostic role of miRNA1290 in CRPC (196).

Exosomal mRNA

Exosomal mRNAs have been shown to play major biological functions in various cancers (197). The composition of exosomal mRNA was found to be slightly different from that of the donor cells due to their selective uptake into exosomes (177,198). The mechanism regulating

the sorting of mRNA into exosomes is not well understood. However, few studies have shown that specific mRNAs, such as fragmented mRNAs with enriched UTRs and some full-length mRNAs, are transported into exosomes by the binding of multifunctional protein YB-1 and methyltransferase NSUN2 to specific motifs of mRNAs (ACCAGCCU, CAGUGAGC, and UAAUCCCA) (199,200).

Recent studies have proposed the potential use of exosomal mRNAs as biomarkers for different cancers (201–204). A study by Goldvaser et al. found in patients' blood of different cancer types an increased concentration of human telomerase reverse transcriptase (exo-hTERT) mRNA (204). The study further showed the role of exo-hTERT mRNA as a potential pan-cancer diagnostic marker (204). A study by Ji et al. identified six exosomal mRNA (CDC42, IL32, MAX, NCF2, PDGFA, and SRSF2) as diagnostic biomarkers for PCa (205). Some studies have also reported the diagnostic function of exosomal mRNA in other body fluids. Mckiernan et al., in their urine exosomes study, found the expression of erythroblast transformation-specific-related gene or PCa associated 3 (PCA3) mRNA to differentiate high-grade from low-grade PCa and BPH (206). Another urinary exosome study by Gan et al. found that the combination of PCA3 and prostate specific membrane antigen (PSMA) mRNAs to be a highly specific and sensitive diagnostic biomarker for PCa (207).

Exosomal protein

Since the discovery of exosomal miRNA in 2007, it has remained as the most explored of the exosomal cargoes with relatively less focus on the role of other exosomal cargoes potential liquid biopsy biomarkers in cancer diagnosis (177). Exosomal proteins are frequently overlooked even though they have great potential as cancer diagnostic biomarkers due to their unique advantages.

A major advantage of tumor-secreted protein enriched in exosomes is the ability to easily detect them when compared with circulating protein in blood. This is because proteins present in blood are diluted with other substances in circulation (208). Another advantage is that tumor-secreted proteins enriched within exosomes are well preserved within the exosomes as compared with protein in body fluid. The presence of protease in body fluids cause degradation of protein, thereby making tumor-secreted protein unstable (209). Also, exosomal proteins provide comprehensive information of the parent tumor because protein components from tumor-derived exosomes have similar profile as their parent tumor cells (210). Tumor-derived exosomes are well enriched for proteins including tetraspanins, heat-shock proteins, transport

proteins (TSG101), adhesion proteins, integrins, tumor specific proteins, lipid-anchored and glyco-proteins (211).

Studies have been done to elucidate the role of exosomal proteins as biomarkers for PCa (212–215). Nilsson et al. showed the expression of PCa gene-3 (PCA-3), β-catenin, transmembrane serine protease 2-ETS transcription factor family member-related gene fusion (TMPRSS2 - ERG) and other PCa-related markers in urinary exosomes of PCa patients (216). The study also showed the expression of PSA and PSMA in urinary exosomes of PCa patients demonstrating their potential use as biomarker for PCa diagnosis (216). A study by Sequeiros et al. found a panel of 5 proteins including PSA (CD63 SPHM, PAPP, GLPK5) able to differentiate between high and low grade PCa patients (217). Panigrahi et al., in their exosomal protein study, found distinct expression of Filamin A between African-American and Caucasian (213). They also observed lower expression of Filamin A protein among PCa patients compared to BPH and healthy individuals (213). Other studies have shown that African-American PCa patients have higher amount of Survivin, an inhibitors of apoptosis proteins, than European-American PCa patients (218,219).

1.4 Research Hypothesis and Aim

The factors that determine indolence or aggressive phenotype of PCa among the African population is not well known. Factors such as low educational levels, cultural beliefs, low socioeconomic status, and lack of sufficient healthcare facilities and manpower, have been attributed to the high mortality of PCa in this population (220). Since the introduction of PSA testing, most cases of PCa are diagnosed on TRUS-guided prostate biopsy triggered by an increased serum PSA level. PSA is inadequate in the diagnosis of PCa, especially in the lower reference ranges (2-10 ng/mL) where PSA is not able to differentiate benign from cancerous disease (221,222). There is a need for new accurate and cost-effective diagnostic approaches to enhance or replace the present techniques for PCa diagnosis.

The aim of this study is therefore to investigate the role of blood and urinary cfDNA and tumor exosome cargo as diagnostic biomarker for PCa in the South African population with the goal of discovery of reliable, non-invasive, and novel biomarkers of PCa.

Aim 1:

To investigate the role of serum exosomes cargoes as diagnostic and prognostic biomarker for PCa in South African populations.

> Objectives:

1. To isolate exosomes from the plasma of PCa and BPH patients.
2. To characterize exosomal microRNA cargo

Aim 2:

To investigate the role of blood and urinary cell-free DNA as diagnostic and prognostic biomarker for PCa in South African populations.

Objectives:

1. To determine the concentration of cell-free DNA in PCa and BPH patients in the South African population.
2. To determine the DNA integrity index in PCa and BPH patients in the South African population.
3. To determine genetic variation within the cfDNA fragments in PCa from South African populations.

CHAPTER 2: General Methodology

2.1 Background

The study was carried out at the Cancer Genomics laboratory of the International Centre for Genetic Engineering and Biotechnology (ICGEB), Cape Town. This study was done in collaboration with the Urology Departments of Groote Schuur Hospital (GSH). The staff of the Urology Clinics, which include specialists, registrars, intern doctors, and nurses, participated in successful recruitment of patients and sample collections.

2.1.1 Ethical Approval and Patient Recruitment.

Ethical approval for the project was received from the University of Cape Town, Faculty of Health Sciences, Human Research Ethics Committee (HREC 454/2012). The standard ethical guideline, as stipulated in the Helsinki declaration, was followed in carrying out the research (223–225).

The participants for this study were recruited from GSH and New Somerset Hospital. The two hospitals are part of the major referral hospital in Western Cape province. Patients scheduled for prostatectomy or Transurethral resection of the prostate were approached to recruit into the study. Information such as the study purpose, the roles of the study participants, the risk involved in participating in the study, participant's right to withdraw, and the sample collection process were fully explained to the patients. Patients that agreed to participate were given the consent form to sign, after which blood and urine samples were collected from patients.

Patients included in the study were South African men diagnosed with BPH, and PCa. Other inclusion criteria considered are:

(1) Patients who have not been previously treated for PCa.
(2) Patients who have not had hormonal treatment or surgical orchiectomy.
(3) Patients with no other comorbidities such as diabetes and arterial hypertension
(4) Patients with no previous history of cancer at any other site in the body.

2.1.2 Sample Collection and Laboratory Processing

Blood and urine samples were collected from every patient that accepted to be part of the study. Blood samples were collected intravenously into a 10 ml K2-EDTA tube. The EDTA tube was gently inverted a few times after and was transported on ice. Urine was collected by asking the patient to void urine into a 50 ml collection tube or drawn from a catheter bag in patients who

had a catheter bag in place. The urine sample was transported on ice to the ICGEB laboratory for further processing.

Blood and Urine Sample Processing: Separation of blood samples into plasma and other components was done by centrifuging at 1000×g for 10 min at 4ºC. The different separated layers were carefully removed from the EDTA tube after centrifugation into 2 ml microtubes and stored at -80ºC.

Urine samples were centrifuged at 1000×g for 10 min at 4ºC to remove particles and cellular debris. The supernatant was carefully removed into 5 ml tubes and stored and stored in -80ºC freezer.

2.2 Exosomes experimental framework

Exosomes are the smallest of the three extracellular vesicle subgroups ranging from 30-150 nm. Exosomes are intraluminal vesicles released from the exocytosis of MVB upon fusion with the plasma membrane (152). Exosomes are a snapshot of the cell content from which they are produced and contain cargo that modify the cell function of the recipient cell (149). Exosomal cargo such as proteins, lipids, metabolites, DNA, mRNA, and microRNA, may differ depending on the parent cell origin and cellular microenvironment (226).

An appropriate exosome isolation technique must consider the heterogeneous nature of exosome sizes and contents. Presently, no isolation technique can completely separate exosomes from lipoproteins and other extracellular vesicles with similar biophysical properties (227). There are four commonly used isolation methods, ultracentrifugation, size-based isolation, immunoaffinity capture, and polymer precipitation techniques. Various commercial kits based on these four isolation techniques are available. The advantages of these kits include time saving, ease to use and high yield while high cost and low purity are some of the setbacks. Presently, some of the most commonly used isolation kits include Total Exosome Isolation kit (Invitrogen), Eloquence (System Biosciences) (ExoQ), and Exo-spin (Cell guidance systems) (ExoS) (228). Major setbacks of the commercial kits include diverse purity and size distribution of isolated exosomes (229,230).

2.2.1 Exosome isolation from plasma and exosomal RNA isolation

Exosome isolation for this study was done using the Invitrogen™ Total Exosome Isolation Kit (from plasma) (catalog number: 4484450) according to the manufacturer's protocol. Exosomal RNA was extracted from exosomes isolated from plasma using Invitrogen™ Total Exosome

RNA & Protein Isolation Kit (catalog number: 4478545) after which miRNA sequencing was done. Below is the step-by-step protocol for exosome and exosomal miRNA isolation.

Steps in isolating exosomes from 1 ml of plasma (with proteinase K): Exosomes were isolated from 1 ml of plasma. The frozen plasma was thawed on ice until it was completely liquified. In order to remove cells and debris, the plasma sample was centrifuged at 2,000 × g for 20 min at room temperature and the supernatant was transferred to a new tube. The plasma was centrifuged again to further remove any available debris at 10,000 × g for 20 min at room temperature. The plasma supernatant was carefully transferred into a new tube and placed on ice.

This was followed by the addition of 500 μl of 1X phosphate buffer saline (PBS) (pH 7.4) and 50 μl of Proteinase K (50 μg/ml) into the tube. The mixture was mixed thoroughly by vortexing and incubated at 37°C for ten min. After incubation, 300 μl of the Exosome Precipitation Reagent (from plasma) was added and mixed thoroughly until a homogenous solution was observed. The tube containing the solution was incubated for 30 min at 4°C and the solution was centrifuged for 5 min 10,000 × g at room temperature. The supernatant was carefully removed and discarded. The exosomes contained as pellet in the tube. Then, 100 μl of 1X PBS was added to the tube containing the exosomes pellet and was vortexed until the pellet was completely suspended. The suspended exosomes were stored in -80°C freezer.

Steps in isolating total RNA from 50 μl of suspended exosomes: Total RNA was isolated from 50 μl of suspended exosomes. The isolation steps involved adding 150 μl 1X PBS and 200 μl 2X Denaturing Solution to the exosome sample in an RNase-free tube. The mixture was thoroughly vortexed and incubated on ice for five min. This was followed by addition of 400 μl of Acid-Phenol: Chloroform (125:24) and the mixture was thoroughly mixed by vortexing for 60 seconds. The mixture was centrifuged at 10,000 x g for 5 min at room temperature to separate the mixture into organic and aqueous phases. The upper aqueous phase was carefully removed and transferred into a new tube. A 1.25 volume of 100% ethanol was added to the recovered volume of the aqueous phase and thoroughly mixed. This was followed by placing filter cartridge in collection tubes. Then, 700 μl of the mixture was pipetted into the filter cartridge and was centrifuge at 10,000 x g. This was repeated until all mixture was completely centrifuged through the filter cartridge.

For the washing step, 700 µl miRNA Wash Solution 1 was pipetted into the filter cartridge and was centrifuge for 15 seconds at 10,000 x g. The flow-through was discarded and the filter cartridge was placed back into the same collection tube. This was followed by adding 500 µl Wash Solution 2/3 into the filter cartridge and centrifuged for 15 seconds at 10,000 x g. The washing done by Wash Solution 2/3 was repeated to completely remove the contaminants. The flow through was discarded and the filter cartridge was placed in the same collection tube and centrifuge at $10,000 \times g$ for one minute to remove from the filter possible residual fluid.

The filter cartridge was placed into a new collection tube and 50 µl of preheated (95°C) nuclease-free water was applied at the center of the filter. The filter cartridge was centrifuged for 30 seconds at 10 000 x g to recover the RNA and the eluate was stored in –80°C freezer.

2.2.2 Exosomes Transmission Electron Microscope Imaging

The transmission electron microscopy (TEM) was invented in 1931 by Ernst Ruska and Max Knoll (11). The invention of TEM has largely influenced the study of science. For example, TEM imaging was fundamental to discovering that the human nervous system is formed from separate cells interacting through neurotransmitters and not just a single structure (12, 13). TEM imaging also helped develop the field of virology by making possible the visibility of the complex structure of viruses (14, 15). With resolution of ~1 nm, TEM imaging contributed to detect and describe particles like extracellular vesicles (16). Electron microscopy is the standard imaging method for characterizing nanosized samples, including extracellular vesicles (17-19). Electron microscope such as TEM and cryo transmission electron microscopy (cryo-TEM) have been shown to be a standard imaging method for characterizing exosomes due to its highly effective ability to characterize single extracellular vesicles (20). In-vivo, exosomes appear rounded in shape but appear cup-shaped when characterized with TEM due to chemical fixing and uranyl acetate contrast (21, 22).

Steps in preparing exosomes sample for TEM imaging: Exosome samples was diluted 1:100 with double de-ionized water. The carbon-coated copper grid was first glow discharge before loading 5 µl diluted sample. After a one min incubation, the copper grid was blotted on a filter paper and wash twice with 5 µl of double de-ionized water. The exosomes loaded copper grid was then stained with 5 µl of 2% Uranyl acetate and blotted on filter paper after one minute. The grid was dried for 3 min and stored in grid cassette.

Capturing Exosomes Images on Transmission Electron Microscope

All the safety precautions for the use of TEM were properly followed. The copper grid was carefully loaded on the rod and inserted into the sample port of the electron microscope. After the rod had been properly placed, the column valve was opened, and the magnification turned down to 290 X. This was followed by taking out the aperture to select an appropriate field on the grid. After an appropriate field was selected the aperture was turned in and the magnification increased to 25500X. Exosomes images were captured after lifting up the field stage and focusing the image properly using the "Eucentric focus" on the control panel.

Figure 2.1: FEI TECNAI T20 TEM used in this thesis.

2.2.3 miRNA sequencing

Exosomal RNA quantity and quality were accessed using the ND100 Nanodrop (Thermo Fisher). The RNA integrity was determined using the Agilent 2200 TapeStation (Agilent Technologies, USA) with an RNA Integrity Number (RIN) value greater or equal to 7. A total amount of 10 ng of exosomal RNA is required for library construction for each sample.

SMARTer smRNA-Seq Kit for Illumina (New England Biolabs, U.S.A) was used in the construction of small RNA libraries. Libraries were generated according to the manufacturer's protocols.

Total RNA was subjected to sequential 3′ and 5′ adapter ligations (T4 RNA Ligase 2, Epicenter, LR2D1132K) followed by reverse transcription (SuperScript II Reverse Transcriptase, Invitrogen, 18064–014). The quality of library was determined using an Agilent Bioanalyzer 2100 system (Agilent). Library quantity was checked with qPCR according to the Illumina qPCR quantification manual. The cDNA libraries that passed the quality check were used to generate cluster and sequenced on the Illumina HiSeq. 2500 platform (Illumina) to achieve 125 bp pair-end reads.

Steps in the analysis of miRNA sequenced data

Data preparation: Two separate reads are usually produced from Illumina paired-end sequencing for each DNA fragment. Sequenced data for each sample have paired end singleton reads, which were concatenated in a single file per library and overlapping paired-end reads were merged with the BBmerge from BBMap package (2).

RNA identification step: RNA identification from the merged files was done using Oasis 2.0 (http://oasis.dzne.de/index.php). The merged files were uploaded on Oasis 2.0 website with information such as the email address, experiment name, reference genome and adapter sequence. The results were obtained from the website after a few hours. The stem-loop sequence code was obtained by using the miRBaseConverter, a broad and efficient tool used to convert and retrieve miRNAs information in different miRBase versions. R-Studio was used to analyse the miRNAs identified by Oasis 2.0 to determine differentially expressed miRNA in high and low Gleason's score PCa samples. R-studio was also used to determine differentially expressed miRNA in high and low Gleason's score PCa in the Cancer Genome Atlas (TCGA) PCa tissue miRNA. The differentially expressed exosomal miRNAs were compared with the differentially expressed miRNA in TCGA PCa tissue miRNAs. We selected the miRNAs common between the two cohorts, which are also expressed in the same direction.

TCGA Tissue miRNA: The results are based on data produced from TCGA Research Network. The cancer profiling data were produced by informed consent as part of studies published before and analysed according to each original study's data regulations. Primary samples from the prostate adenocarcinoma dataset were deduced using TCGA code "01A" (limiting the

analysis to a sample for each patient), which is the two-digit code according to TCGA usual sample name. The miRNA-sequencing data were acquired from The Broad Institute Firehose pipeline (http://gdac.broadinstitute.org).

2.2.4 miRNA validation experiments.

The selected miRNAs were further validated by accessing their expression in PCa and BPH exosomal miRNA samples. This involves the synthesis of complementary DNA (cDNA) from exosomal RNA, then followed by using a real time PCR. The Qiagen miRCURY LNA RT Kit (catalog no: 339340) was used for cDNA synthesis while miRCURY LNA SYBR® Green PCR Kit was used for real time PCR reactions.

Reagents and buffers in miRCURY LNA RT Kit: The reagents and buffers available in miRCURY LNA RT kit includes, 5x miRCURY RT SYBR® Green® Reaction Buffer, which consists of a universal reverse transcription primer for the SYBR® Green-based workflow, Mg2+, and dNTPs; 5x miRCURY RT Probe Reaction Buffer, which contains universal reverse transcription primer for the Probe-based workflow, Mg2+, Probe RT primer and dNTPs; 10x miRCURY RT Enzyme Mix, which is an enzyme for reverse transcription; UniSp6 RNA Spike-in Template for monitoring successful reverse transcription; and Nuclease-free water for elution.

Reagents and buffers in miRCURY LNA SYBR® Green PCR Kit: The reagents and buffer available in miRCURY LNA SYBR® Green PCR kit includes, 2x miRCURY SYBR® Green PCR Master Mix containing miRCURY SYBR® Green PCR Buffer, and dNTP mix (dATP, dCTP, dGTP, and dTTP). The kit also contains ROX™ Reference Dye, Nuclease-free water and QuantiNova® DNA Polymerase, which composed of Taq DNA Polymerase, QuantiNova Antibody, QuantiNova Guard.

Steps in synthesis of complementary DNA (cDNA) from exosomal RNA: For each cDNA reaction 2 μl of 5x miRCURY SYBR® Green RT Reaction Buffer was added to 1 μl of 10x miRCURY RT Enzyme Mix and 3 μl RNase-free water using 4 μl of exosomal RNA as template. The reverse transcription reaction was done at 42°C for 60 min and inactivation of reaction done at 95°C for 5 min. The was followed with cooling at 4°C and cDNA stored at − 20°C.

Steps in real time PCR protocol for miRNA expression: For validation of miRNA expression, a 1:30 dilution of the cDNA was made by adding 290 μl RNase-free water to the 10 μl reverse

transcription reaction product. Each 10 µl PCR reaction well contained1ul resuspended PCR primer, 1 µl RNase-free water, 5 µl 2x miRCURY SYBR® Green Master Mix, and 3 µl diluted cDNA template. PCR plate was centrifuged for 20 seconds at 1000 x g. Real time PCR was performed on LightCycler 480 system (Roche Diagnostics, Mannheim, Germany). Amplification was performed according to the following protocol: initial heat activation at 95°C for 2 min, denaturation at 95°C for 2 seconds followed by a combined annealing and extension at 56°C for 10 seconds for 45 cycles. Melting curve analysis was done at electrophoresis. The miRNA expression was normalized to the absolute copy number of all miRNAs.

2.3 CfDNA experimental framework

Due to the presence of different cell free molecules in plasma, urine, and other body fluids, it becomes important that cfDNA is properly and efficiently isolated from these body fluids. There are presently dozens of commercially available methods, including kits, to isolate cfDNA from plasma, urine, and other body fluids. These methods are either used manually or automated (4). The major differences between these methods are the mechanism by which they isolate cfDNA. Some of these kits isolate cfDNA by binding the cfDNA to silica gel membrane or magnetic particles or by precipitation with organic chemicals (231). Studies have compared the efficiency of these kits in terms of their ability to efficiently recover cfDNA, reproducibility, and size discrimination (232,233).

Many comparative studies of cfDNA commercial isolation kits have shown the QIAamp Circulating Nucleic Acid kit to be highly effective in the isolation of cfDNA from plasma and urine when compared with other manual commercial kits (234–236).

2.3.1 CfDNA Extraction

The QIAamp Circulating Nucleic Acid kit (Qiagen) was used in the extraction of cfDNA from plasma and urine in this study. The kit contains different reagents and buffers for the extraction process.

Reagents and buffers in the kit: The kit contains proteinase K solution and the following buffers ACL, ATL, ACB, ACW1, ACW2, and AVE. The proteinase K is usually added to samples prior to the addition of ACL buffer. It helps to digest protein and remove contamination from the sample. Proteinase K also inactivates nucleases that might cause degradation of nucleic acids. Buffer ACL is a lysis buffer used in combination with carrier RNA to ensure the

complete release of cfDNA from bound vesicles, protein, and lipids. The buffer also helps in inactivating DNases and RNases. Buffer ATL is an additional lysis buffer used to ensure complete release of cfDNA in urine samples. Buffer ACB is used just before the column binding step to adjust the binding conditions to allow maximum binding of nucleic acids to the silica membrane column. Buffer ACW1 and ACW2 were used as washing buffers to remove contaminants that bind to the membrane column. Buffer AVE is used as an elution buffer and to dissolve lyophilized carrier RNA.

Steps involved in cfDNA extraction from plasma and urine.

CfDNA extraction was done from 1 ml of plasma and 10 ml of urine. For plasma sample extraction, 100 µL Proteinase K was pipetted into a 50 ml centrifuge tube and 1 ml of plasma sample was added. For each urine sample extraction, 1.25 ml Proteinase K was pipetted into a 50 ml centrifuge tube and 10 ml of urine sample was added. Lysis was done by adding 0.8 ml of Buffer ACL (containing 1.0 µg carrier RNA) to the mixture of plasma and Proteinase K, after which thorough mixing was done by pulse-vortexing for 30 seconds. This was followed by incubation of the mixture at 60°C for 30 min. For urine samples, lysis was done by adding 10 ml of Buffer ACL (containing 1.0 µg carrier RNA) and 2.5 ml ATL buffer to ensure complete release of cfDNA. The solution was mixed thoroughly by pulse-vortexing for 30 seconds and the mixture incubated at 60°C for 30 min.

Then, 1.8 ml and 19.8m ml of ACB buffer was added to the plasma and urine mixture respectively, to ensure optimal binding of the circulating nucleic acids to the membrane. The lysate–buffer ACB mixture was incubated for 5 min on ice. This was followed by carefully applying the mixture into the mini column connected to a vacuum manifold to draw the lysates through the mini column. At this stage, the nucleic acids were bound to the column and the lysate was discarded.

Washing of the column containing the nucleic acids was done by applying 600 µl of buffer ACW1 into the mini column and drawn through the column using the vacuum pump. A second washing was done by applying 750 µl of buffer ACW2 into the mini column and drawn out with the vacuum pump. A final wash is done by applying 750 µl of 100% ethanol into the mini column and drawn out with the vacuum pump. The QIAamp Mini column was then placed in a 2 ml collection tube, and centrifuge for 3 min at full speed. Immediately after centrifugation, the mini column was placed in a new 2 ml tube and incubated at 56°C for ten min to dry the

40

membrane. The mini column was transferred into a new 1.5 ml tube. Elution of cfDNA was done by applying 50 µL of AVE buffer at the center of the membrane and incubated for 3 min at room temperature. The mini column in the 1.5 ml was centrifuged at full speed for one minute to elute the cfDNA through the membrane. The concentration and purity of cfDNA were measured using the NanoDrop ND-2000. CfDNA eluate was stored in -80°C freezer.

2.3.2 CfDNA Quantification

The quantification of cfDNA in this study was done using the quantitative real time polymerase chain reaction (qPCR). The qPCR is a polymerase chain reaction (PCR) technique that combines DNA amplification and detection into one step.

The PCR was invented in 1983 by Mullis [237]. PCR became widely used with the replacement of thermolabile Klenow fragment initially used for amplification with a thermostable polymerase from *Thermus aquaticus* [238]. In the early 1990s, real time detection of DNA amplification through fluorescence monitoring was introduced [239,240]. This was a major milestone because measuring fluorescence after each cycle allows quantification of target DNA. This is done using the calibration curve constructed with serially diluted standard samples with known concentrations or copy numbers.

The qPCR is one of the most used approach in the absolute quantification of cfDNA due to its reproducibility and accuracy [241]. Alu gene, human genome most abundant repeat, was used to quantify cfDNA concentration [242,243]. DNA integrity was calculated as the ratio of the longer DNA fragment (ALU 247) to that of shorter DNA fragment (ALU 115).

Steps in cfDNA qPCR reaction:

ALU primers master mix preparation: We made a 100 µM solution of Alu 115 forward and reverse primer sets and 100 µM solution of Alu 247 forward and reverse primer sets. A 2 µM solution of both ALU 115 and ALU 247 primers was prepared with nuclease-free water. The sequences of ALU 115 primers used were forward CCTGAGGTCAGGAGTTCGAG and reverse CCCGAGTAGCTGGGATTACA; ALU 247 primers sequence were forward GTGGCTCACGCCTGTTAATC and reverse CAGGCTGGAGTGCAGTGG.

We prepared a primer master mix in the ratio of 0.25 µl of 2 µM ALU primer and 5.75 µl of SYBR Green for each sample. We diluted 1 µl each cfDNA samples in nuclease free water in

the ratio of 1:400. For each qPCR reaction 6 µl primer master mix was added to 4 µl of diluted cfDNA into each well of the PCR plate

2.3.3 CfDNA exome sequencing

We performed whole exome sequence of cfDNA extracted from urine samples. The quantification of cfDNA samples for whole exome sequence was determined using Picogreen (Invitrogen, Catalog number: P7589). The quality of cfDNA fragment size was evaluated using High Sensitivity DNA Assay 2100 Bioanalyzer.

Whole exome sequencing was done on Illumina platform. Library preparation was done using SureSelect V6-Post(cfDNA) kit after samples quality control have been ascertained. The sequencing library was constructed by random fragmentation of DNA sample, after which 5' and 3' adapter ligation was done. Amplification and purification of adapter-ligated fragments was done using PCR and gel respectively. In order to generate clusters, the library was loaded into a flow cell where fragments were captured on a lawn of surface-bound oligos complementary to the library adapters. Bridge amplification was done to amplify each fragment into distinct, clonal clusters. The templates were ready to be sequenced after the cluster generation was completed. Sequencing was performed with Illumina SBS technology which make use of proprietary reversible terminator-based method.

The terminator-based method has four reversible, terminator-bound dNTPs available at every sequencing cycle, reduces incorporation bias, and raw error rates in comparison with other technologies. This produces very accurate base-by-base sequencing that practically removes sequence-context-specific errors. The data produced from the sequencing process was transformed into raw data that is ready for analysis.

2.3.4 Bioinformatics analysis of cfDNA experimental data

Data generated from cfDNA qPCR reactions and whole exome sequencing were analyzed using R. R is very helpful when analyzing large statistical data analysis, including graphical computing data (244). R-Studio (www.rstudio.com) is an easy-to-use tool based on the R interface and is accessible as an application on computer. The R (version 3.6.1) and R-studio (version 1.1.456) software were used for statistical analysis and graphical illustration of data generated from cfDNA experiments using in-house developed scripts.

CHAPTER 3: Exosome cargo as a source of biomarker for prostate cancer

3.1 Background

The most common approach for PCa diagnosis remains needle biopsy despite its invasiveness and other known associated complications. PSA has long been used as a biomarker for PCa

screening. However, factors such as low sensitivity of PSA, over detection leading to overtreatment, and the resultant side effects and complications limit the use of PSA (245). New and better biomarkers are, therefore, needed in the diagnosis, treatment monitoring and prognosis of PCa.

Exosomes are extracellular vesicles released by virtually all normal or pathological cells (246–248). Exosomes function in intercellular communication due to their ability to transmit protein, DNA, mRNA, miRNA, and lipid molecules from one cell to another (249,250). Exosomes can modulate physiological and disease state processes, elimination of toxic substances, including delivery of drug and therapeutic antibody (246,247,251). Also, tumor exosomes are a more comprehensive landscape of tumor heterogeneity that cannot be appreciated with tissue biopsy (252). These qualities made exosomes a promising biomarker for cancer diagnosis, prognosis, and treatment monitoring. Studies have explored exosome cargo as diagnostic and prognostic biomarkers for many cancer types, including PCa (216,226,253,254). Studies have shown blood and urinary exosomes from PCa patients possess PCa-specific components, which can serve as biomarkers for PCa metastasis (255,256). Huang et al. found that exosomal miRNA1290 and miRNA375 are possible biomarkers for prognosis of castration resistance prostate cancer (CRPC) (173,257). However, most of these studies are within European populations and studies in African populations are sparse, making this present study imperative.

Together with the Oncology Institute of Southern Switzerland and the Portuguese Oncology Institute of Porto, we investigated the oncogenic role of exosomal miRNA424 prostate tumor self-sustenance, disease recurrence and progression (195). The study and its findings are discussed briefly next.

We investigated the presence of miRNA424-loaded exosomes in blood circulation by measuring the expression level of miRNA424 in exosomes isolated from plasma of BPH and PCa samples. The expression of miRNA424 was shown to increase from primary PCa to metastatic castration-sensitive prostate cancer (mCSPC) and metastatic castration-resistant prostate cancer (mCRPC). There was no detection of miRNA424 expression in BPH samples ($Ct \geq 40$).

The role of miRNA424 in driving tumorigenic traits in recipients' cells was investigated by assessing the effect of prostate donor cells conditioned medium engineered to express

44

miRNA424 in miRNA424-negative recipient cells. We found an increased miRNA424 level in recipient cells after being supplemented with conditioned medium from prostate donor cells. Also, the transfer miRNA424 to recipient cells significantly increased clonogenic capability, tumor-sphere formation, and cell migration in recipient cells.

The study also assessed the association between miRNA424 secretion and transition from indolent to aggressive phenotype using PCa experimental models. We found significantly higher expression of miRNA424 in LNCaP[abl] cells, a CRPC cell model derived from LNCaP cells, compared to parental cells. LNCaP[abl] cells were found to secrete miRNA424 enriched exosomes compared to parental LNCaP cells. Furthermore, RWPE-1 recipient cells were supplemented with exosomes from parental and LNCaP[abl] cells. A similar uptake of exosomes in recipient cells using parental and LNCaP[abl]-derived exosomes was found. However, there was increased miRNA424 level, increased cell migration and enhanced tumor-sphere formation in recipient cells exosomes derived from LNCaP[abl]-cells compared to exosomes from parental LNCaP cells.

The release of miRNA424 into exosomes from prostate tumors was examined using a mouse model. This was done by subcutaneously establishing xenografts of control and miRNA424-positive LNCaP cells in mice. Tumors of miRNA424 expressing LNCaP cells grew bigger than control tumors. We also showed that exosomes from miRNA424-positive tumors have higher miRNA424 expression compared to control xenografts. Exosomes from miRNA424-positive tumors were found to be fully functional, promote tumor-sphere formation, and cell migration when supplemented with miRNA424-negative recipient cells. This confirmed that tumor xenografts in mice secrete functional exosomes that can transfer miRNA424 and induce malignant phenotypes in recipient cells.

We further hypothesized that tumors exosomes could cause low tumorigenic cells to acquire stem-like and tumorigenic traits distal metastatic sites. In order to test this, mice were injected with subcutaneous implants of RWPE-1 cells (≥100 mm3) with exosomes control and exosomes loaded with miRNA424 derived from LNCaP cells. We detected using DiD-labeling and in vivo imaging, fluorescently labeled exosomes in the tumor area at 24 h after injection, confirming that both exosomes' preparations reached the tumors. The supplementation of exosomes loaded with miRNA424 was found to enhance tumor growth compared to exosomes control. Also, miRNA424 level was significantly higher in mice receiving exosomes loaded with miRNA424 compared to exosomes control.

The findings from the mouse model were further verified in human circulating exosomes by supplementing RWPE-1 cells with exosomes isolated from plasma of BPH, primary PCa, mCSPC and mCRPC patients. We found, using confocal microscopy, similar intake of fluorescently labeled exosomes. Our findings showed that exosomes from mCSPC and mCRPC patients enhanced tumor-sphere formation significantly more than those from BPH and primary PCa patients. Furthermore, high miRNA424 content in exosomes was significantly associated with increased induction of tumor-sphere formation across all samples. These findings showed that exosomes containing miRNA424 could travel through the blood circulation and activate the oncogenic cascade associated with miRNA424 in recipient cells at distal sites.

In this collaboration, we showed that exosomes-mediated release of miRNA424 can serve as an efficient means for transferring oncogenic signals across cells in the surrounding microenvironment and at distal metastatic sites promoting disease recurrence and progression.

In the current chapter, we investigate exosomes and its miRNA cargo in PCa patients from a South African cohort. PCa exosome was characterized in terms of exosomal concentration and size using a transmission electron microscope (TEM). The miRNA cargo was identified and quantified with small RNA sequencing.

3.2. **Methodology**

3.2.1 Exosome and exosomal RNA extraction.

Exosome was isolated from 1ml of plasma samples of 32 PCa and 26 BPH patients using the Invitrogen Total Exosome Isolation Kit (from plasma) [Catalog number: 4484450], resuspended in 100 μl 1x PBS and stored in a -80ºC freezer (Figure 3.1).

RNA extraction: Total RNA extraction was done from 50 μl each of isolated exosomes using the Invitrogen Total Exosome RNA & Protein Isolation Kit (Catalog number: 4478545). Extracted RNA was eluted in 50 μl nuclease free water and stored at -80ºC.
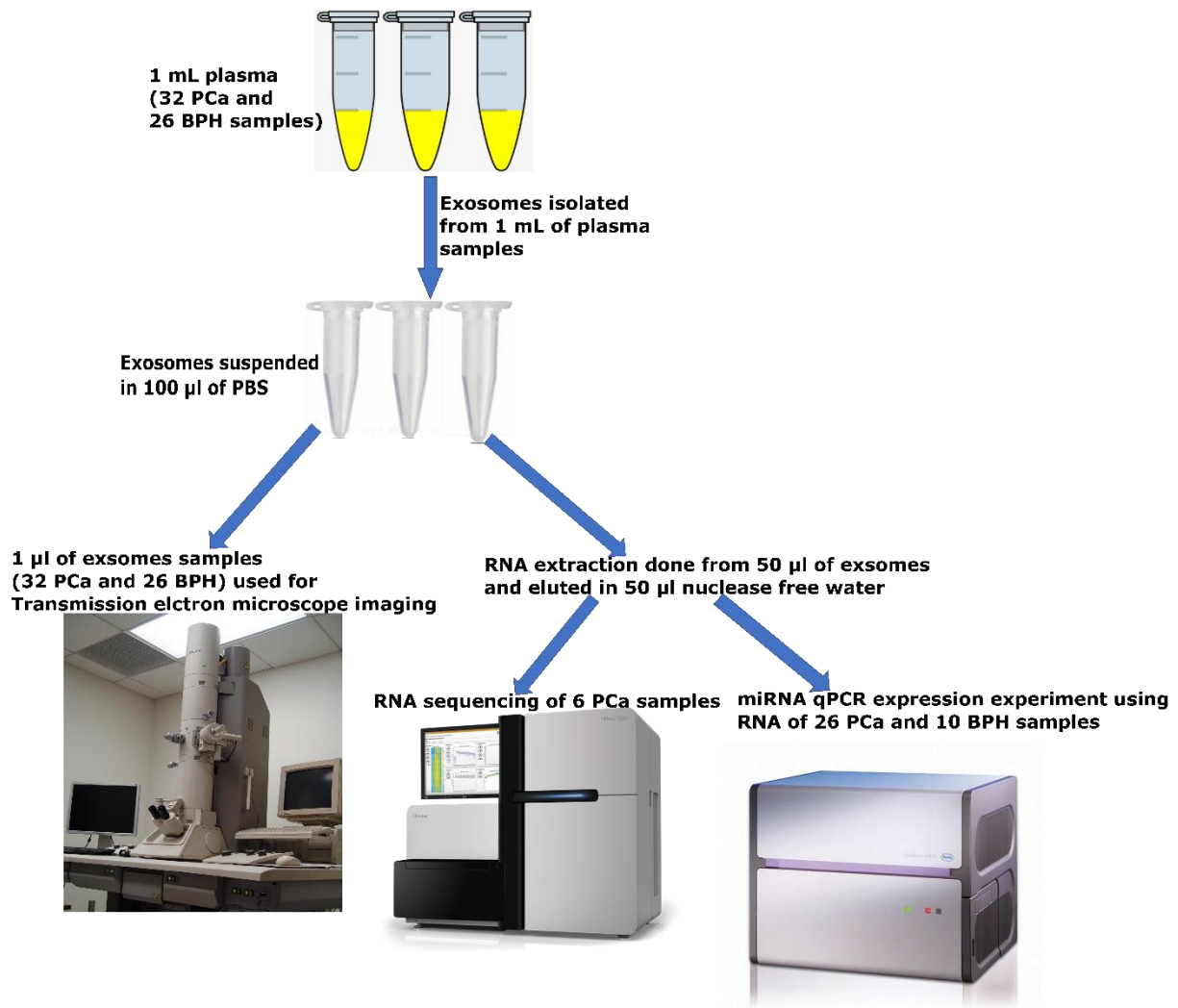
Figure 3.1: Workflow of exosomes experimental design

3.2.2 Transmission Electron Microscope imaging

In order to confirm the isolated exosomes and also to compare the size and number of exosomes present in PCa patients with BPH patients, we did an electron microscopy imaging of the exosomes from 32 PCa and 26 BPH patients.

For each exosome sample, a 1:100 dilution was made. We then prepared a glow discharged carbon coated copper grid by applying 5 μl diluted exosome sample on the discharged copper grid for one minute. The carbon coated copper grid was blotted on a filter paper and wash twice with 5 μl of double deionized water. The carbon coated copper grid was then stained with 5 μl of 2% Uranyl acetate and blot on filter paper after one minute. The copper grid was viewed on Transmission Electron Microscope (TEM) and ten photos were taken randomly in all quadrants of the grid.

Data and bioinformatic analysis:

Exosomal size profiling: The number of exosomes grouped by diameter range of 2 nm was calculated for each patient. The exosomal (diameter) size profile was smoothed using a loess function. The profile was deconvoluted using 8 Gaussian curves centered at 16, 19, 22, 25, 28, 31, 34, and 37 nm and with standard deviation of 3 nm. The quantification and the morphological features analysis of exosomes in clusters was done by manually calculating the number of exosomes in each cluster. Cluster with less than 10 exosomes were categorized as small cluster while clusters with more than 10 exosomes were categorized as big clusters. The number of exosomes and clusters were normalized based on the size and the number of the photos of each patient.

Data analysis: The analysis of the TEM images was done using ImageJ according to the following steps: (i) raw tiff image was imported into FIJI with the image type changed to 8 bit; (ii) the spatial scale of the image was define using a known distance (100 nm) on the image in other to calibrate the image in nanometer; The size of the area captured was of 4380x4380 nm or 5240x5240 nm, respectively; (iii) low-pass Gaussian filter (with sigma=10) was applied; (iv) the local median intensity was subtracted from the image to remove intensity gradient in the image; (v) the low intensity belonging to the first quintile were removed from the following analysis; (vi) the grayscale image is converted to a binary image using a threshold value calculated using the Otsu's method (258); (vii) holes in the identified exosomes were filled; (viii) morphological features of identified exosomes were computed and exosome with ratio between standard deviation and mean of radius larger than 0.4 were excluded; (ix) watershed transformation was applied and morphological features of identified exosomes were computed again; (x) exosome with ratio between standard deviation and mean of radius larger than 0.15 and exosome with a calculated area smaller than 150 nm^2 were excluded.

Bioinformatic analysis: Wilcoxon rank-sum test was used to compare differences in concentration of exosomes and exosomal clusters between BPH and PCa, and low and high GS. P values were adjusted for multiple testing with the Benjamini–Hochberg correction and a false discovery rate (FDR) cutoff of 0.01 was used. Statistical analysis and graphical images of the data were produced with the R (version 3.6.1) and R studio (version 1.1.456) software using in-house developed scripts.

3.2.3 Exosomal RNA sequencing

We performed small RNA sequencing of total RNA isolated from 3 high GS (total score ≥8) and 3 low GS (total score ≤7) PCa patients. Small RNA sequencing was done on Illumina platform. Quality control of small RNA was done using Agilent 2100 Bioanalyzer with a total amount of 10 ng of exosomal RNA required for each sample. The SMARTer smRNA-Seq Kit was used in preparing the library. Sequencing was done using the Illumina HiSeq. 2500 platform (Illumina) to obtain 151 bp pair-end reads. *Data preparation and miRNA identification:* The paired end reads of each sample sequenced were merged with the BBmerge from BBMap package (2). Identification miRNA from merged files was done using Oasis 2.0 (http://oasis.dzne.de/index.php). R-Studio was used to analyze the miRNAs identified by Oasis 2.0 to determine miRNAs that are differentially expressed in high and low GS PCa samples. R-studio was also used to determine miRNAs differentially expressed in TCGA high and low GS PCa tissue miRNA. The differentially expressed exosomal miRNAs were compared with the differentially expressed miRNA in TCGA PCa tissue miRNAs. We selected the miRNAs common between the two cohorts, which are also expressed in the same direction.

MicroRNA enrichment: To investigate the genes targeted by our selected miRNAs, a miRNA-target enrichment analysis was done using the MIENTURNET (MicroRNA ENrichment TURned NETwork) web tool (259). We made a regulatory network of genes that are related to PCa and their target miRNAs using the web tool. We also did functional enrichment analysis of selected miRNAs targets by querying the Kyoto Encyclopedia of Genes and Genomes (KEGG) (260) pathway through the MIENTURNET web tool (259).

Data and bioinformatic analysis:

Data analysis: The stem-loop sequence code of identified miRNA was obtained using the Bioconductor package miRBaseConverter. From 903 miRNA identified, 294 miRNAs with an average read counts above 10 were considered for the following analysis.

Bioinformatic analysis: We used the Trimmed Mean of M-values (TMM) scaling employed in the Bioconductor package to normalize miRNA read counts for the library size. This was followed by conversion into log2 counts per million. We used R to identify differentially expressed genes (DEGs) by applying the negative binomial differential expression method edgeR (261). Statistical analysis and graphical illustrations of the data were generated in the R (version 3.6.1) and R studio (version 1.1.456) software using scripts made in-house.

3.2.4 miRNA qPCR expression experiment

For validation of our selected miRNA qPCR expression experiment was done. We made complementary DNA (cDNA) from 26 PCa and 10 BPH exosomal RNA samples using Qiagen miRCURY LNA RT Kit (catalog no: 339340) following the protocol designed by the manufacturer.

This was followed by a real time PCR expression analysis of the miRNAs identified at the initial experimental phase. We included miRNA424 to broaden the analysis in our previous study (195). The qPCR expression analysis was done as described earlier in Chapter 2.

To determine the expression level of the 8 miRNAs, real time PCR reaction was done in duplicate for each cDNA sample of the 7 miRNAs. Real time PCR was performed on LightCycler480 system (Roche Diagnostics, Mannheim, Germany).

In order to determine the absolute copy number of the qPCR products for each of the 8 miRNAs, a 2% agarose gel of the qPCR products were made, the band size was determined after which the band excised. DNA was purified from the band using the QIAEX II Gel Extraction Kit (cat. no. 20021) and quantified using Nanodrop. The known band size (50bp) and concentration of cDNA was used to calculate the copy number of DNA present in 1 μl of cDNA using Avogadro's constant. The purified cDNA was serially diluted to construct standard curves on qPCR for each of the 8 miRNAs to determine the absolute copy number of miRNA present in each sample used for validation.

Data analysis: We used Wilcoxon rank-sum test to make comparison of logarithms of all miRNAs absolute copy number for the miRNA qPCR expression experiment. The absolute copy number for all the miRNA was used to normalize each of the miRNA. Statistical analysis and graphical illustrations of the data were generated in the R (version 3.6.1) and R studio (version 1.1.456) software using scripts developed in-house.

3.3 Results

3.3.1 Transmission Electron Microscope Image analysis

TEM image analysis of 32 PCa patients and 26 BPH were done (Table 3.1). Figure 3.2 showed some of the TEM images of PCa and BPH.

Table 3.1: Summary of clinical data of PCa and BPH patients used for exosomes transmission electron microscope imaging.

Patient ID	PCa	BPH	Total
Age, median [IQR] (years)	70 [63 74.25]	67 [65 71]	68.5 [63 73]
PSA, median [IQR] (ng/mL)	26 [14.125 76.15]	4.2 [1.245 13.175]	14.5 [5.075 35.25]
Number of patients	32	26	58
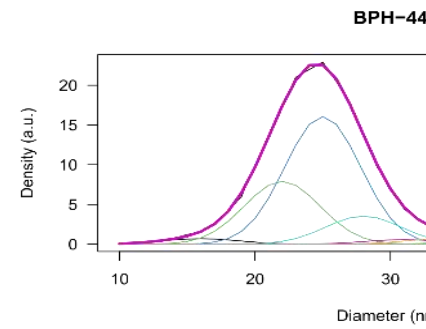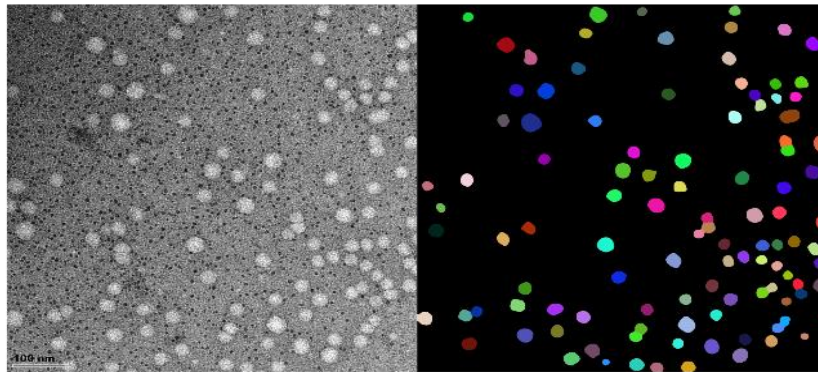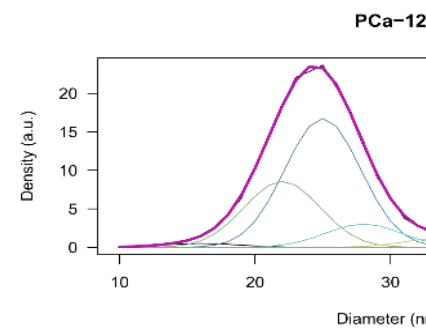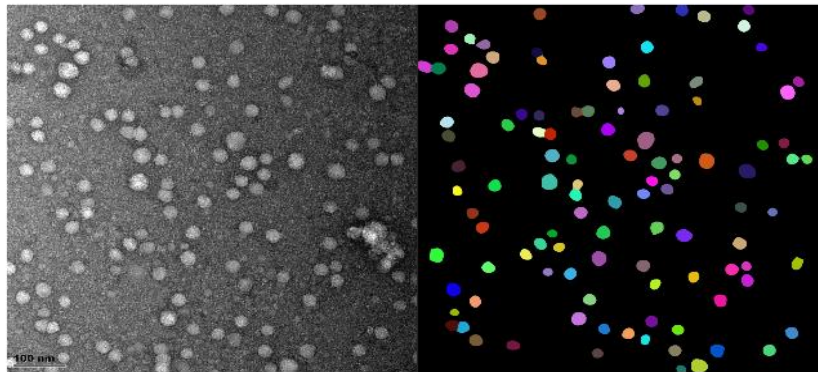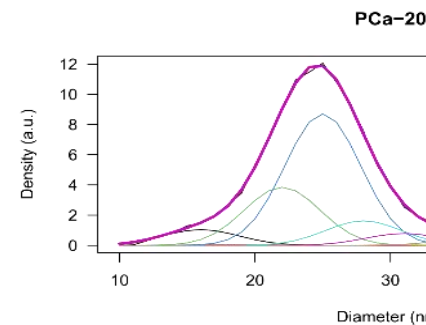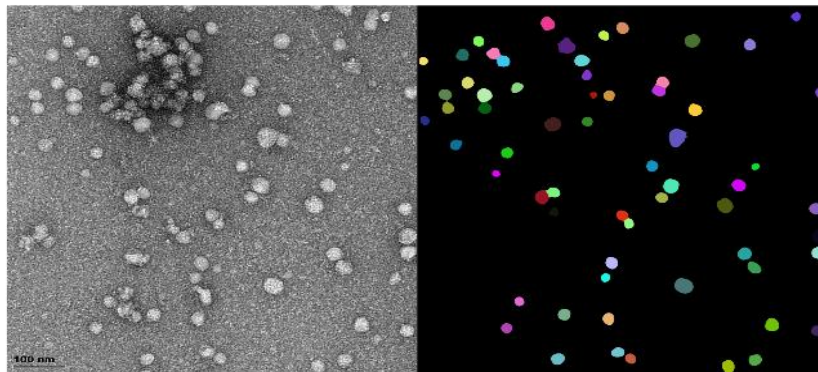
Figure 3.2: TEM imaging of exosomes isolated from patients with BPH, PCa with a low Gleason score, and PCa with a high GS. The first panel shows the TEM photo. In the second panel, exosomes were colored to indicate the different sizes. The third panel is the density graph of different size distributions. The color codes are 16 nm=gray, 19 nm=green, 22 nm=blue, 25 nm=purple, 28 nm=cyan, 31 nm=yellow, 34 nm=orange, 37 nm=red.

In order to understand the morphological differences in exosomes from PCa and BPH, exosomes size found both in PCa and BPH images were grouped into 8 groups of 16, 19, 22, 25, 28, 31, 34, and 37 nm. Table 3.2 showed the median sizes of exosomes for PCa and BPH

in each group. The PCa exosomes size was significantly higher than BPH in the 16 nm and 28 nm groups. Table 3.3 showed the median sizes of exosomes between low and high GS PCa patients. There was no significant difference in exosomes size between low and high GS PCa patients. We also analyzed the small and big exosomes clusters formed in BPH, low and high GS PCa samples. There was significantly higher number of small clusters formed in high and low GS than BPH (Figure 3.3).

Table 3.2: Size distribution of exosomes across 8 groups in BPH and PCa

Feature	BPH, median [IQR]	PCa, median [IQR]	Log change	p-value	FDR
16 nm diameter	3.82 [1.62 11.04]	12.09 [6.62 18.05]	0.98	9.78E-03	7.82E-02
19 nm diameter	3.79 [0 12.93]	8.70 [1.156 30.28]	0.52	2.94E-01	3.92E-01
22 nm diameter	49.98 [24.13 68.56]	25.73 [12.942 53.24]	-0.22	1.48E-01	2.66E-01
25 nm diameter	68.90 [46.64 106.79]	92.76 [67.292 128.33]	0.33	9.58E-02	2.55E-01
28 nm diameter	0 [0 10.33]	16.41 [0.24 45.08]	1.22	3.23E-02	1.29E-01
31 nm diameter	5.65 [0 13.06]	5.83 [0.48 13.31]	0.35	6.49E-01	7.42E-01
34 nm diameter	3.15 [1.22 5.45]	1.38 [0 4.44]	-0.39	1.66E-01	2.66E-01
37 nm diameter	3.34 [1.50 5.70]	2.69 [0.71 5.88]	0.31	8.55E-01	8.55E-01

Table 3.3: Size distribution of exosomes across 8 groups in low and high GS PCa

Feature	Low GS, median [IQR]	High GS, median [IQR]	Log change	p-value	FDR
16 nm diameter	12.11 [4.91 18.51]	8.78 [7.20 17.27]	-0.46	7.43E-01	9.32E-01
19 nm diameter	8.46 [3.05 46.55]	9.26 [0 11.03]	-1.25	4.21E-01	8.79E-01
22 nm diameter	35.45 [13.10 56.96]	25.73 [9.01 30.96]	-1.15	4.40E-01	8.79E-01

25 nm diameter	107.01 [77.83 139.04]	80.75 [62.79 89.08]	-0.5	1.06E-01	8.49E-01
28 nm diameter	10.65 [0.12 45.18]	17.68 [4.62 44.35]	-0.06	8.15E-01	9.32E-01
31 nm diameter	4.81 [0.24 13.54]	6.88 [1.56 9.05]	-0.16	9.38E-01	9.38E-01
34 nm diameter	2.469 [0 4.781]	0 [0 2.297]	-0.48	3.60E-01	8.79E-01
37 nm diameter	2.572 [0.81 5.525]	5.121 [0.688 5.736]	-0.01	5.89E-01	9.32E-01
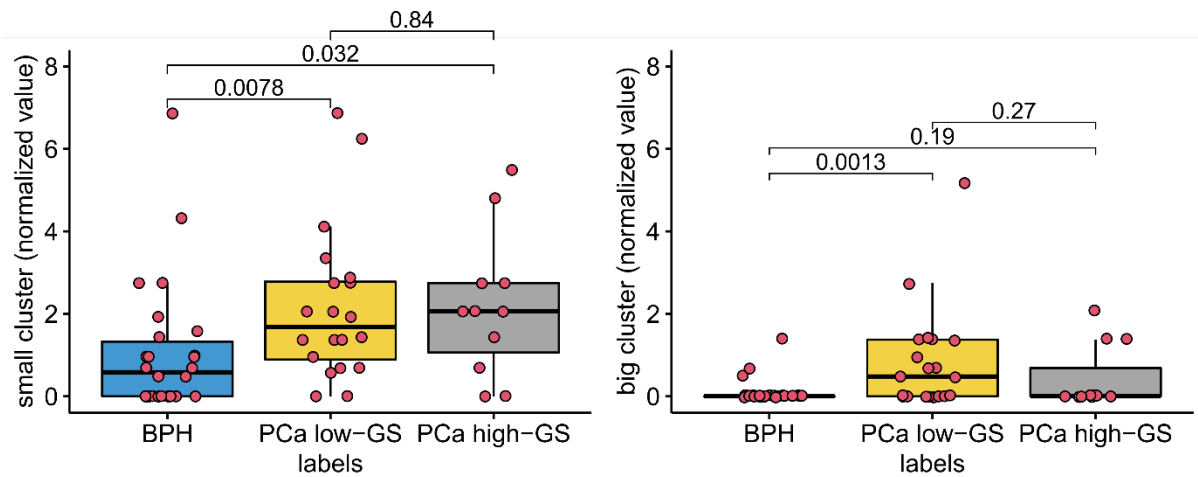
Figure 3.3: Boxplot of number of (A) small exosomes and (B) big exosomes in BPH, low GS and high GS

3.3.2 Exosomal miRNA Sequencing

Exosomal RNA isolated from six exosome samples (3 high GS and 3 low GS). The clinical information of all six samples is highlighted in Table 3.4.

Table 3.4: PCa patients' clinical data.

Samples	Age (years)	PSA	Race	GS	DRE	NCCN Classification
SAPC0164	74.2	2.5	Black	3+3	T1a	Very low
SAPC0180	58.1	5000	Black	5+5	T3/T4	Very high
SAPC0185	69	18	MA	4+5	T2c	High
SAPC0195	87.2	26.53	Black	4+5	T3	Very high
SAPC0203	66.8	18.56	MA	3+3	cT2a	Intermediate

SAPC0238	92.5	24.43	MA	3+3	T1a	High

DRE (Digital rectal examination), MA (Mixed ancestry).

Library construction for miRNA sequencing was done using SMARTer Small RNA library kit with library quality results shown in Table 3.5.

Table 3.5: Exosomal RNA library quality results

Samples	Conc. (ng/µl)	Conc. (nM)	Size (bp)
SAPC0164	0.35	2.72	200
SAPC0203	0.58	4.62	192
SAPC0238	0.86	7.15	186
SAPC0195	0.41	3.68	192
SAPC0203	0.23	1.72	209
SAPC0183	0.38	3.06	192

A total of 903 miRNAs were identified from the sequencing data, and which 294 miRNAs have an average read counts above 10. A total of 65 miRNAs were differentially expressed between high and low GS PCa (Figure 3.4). In order to compare our findings in plasma exosomal miRNA to tissue miRNA, a total of 1046 miRNA transcriptome data of TCGA prostate adenocarcinoma were obtained from GDC Data Portal. Differential expression of TCGA data identified 185 miRNAs. A comparison of the differential expressed TCGA miRNA and exosomal miRNA showed 13 miRNAs common between the two data (Figure 3.4). However, 7 of the 13 miRNAs are upregulated or downregulated in both TCGA miRNA and exosomal miRNA (Table 3.6).

Table 3.6: Significant miRNA commonly expressed in same direction between TCGA miRNA and exosomal miRNA.

miRNA	Exosome			TCGA		
	LogFC	Pvalue	FDR	LogFC	Pvalue	FDR

hsa-miR-10a-5p	9.21	2.78E-04	2.92E-03	0.3	9.52E-05	1.11E-03
hsa-miR-194-5p	3.45	5.11E-03	3.34E-02	0.25	3.41E-06	5.95E-05
hsa-miR-144-5p	2.3	5.72E-03	3.56E-02	0.27	7.70E-03	4.91E-02
hsa-miR-16-5p	1.89	1.67E-02	8.05E-02	0.19	4.42E-06	7.34E-05
hsa-miR-221-5p	-2.08	1.83E-02	8.51E-02	-0.55	1.55E-12	6.77E-11
hsa-miR-326	-2.15	1.84E-02	8.51E-02	-0.33	5.26E-04	4.83E-03
hsa-miR-93-5p	1.67	1.85E-02	8.51E-02	0.35	9.74E-09	2.55E-07
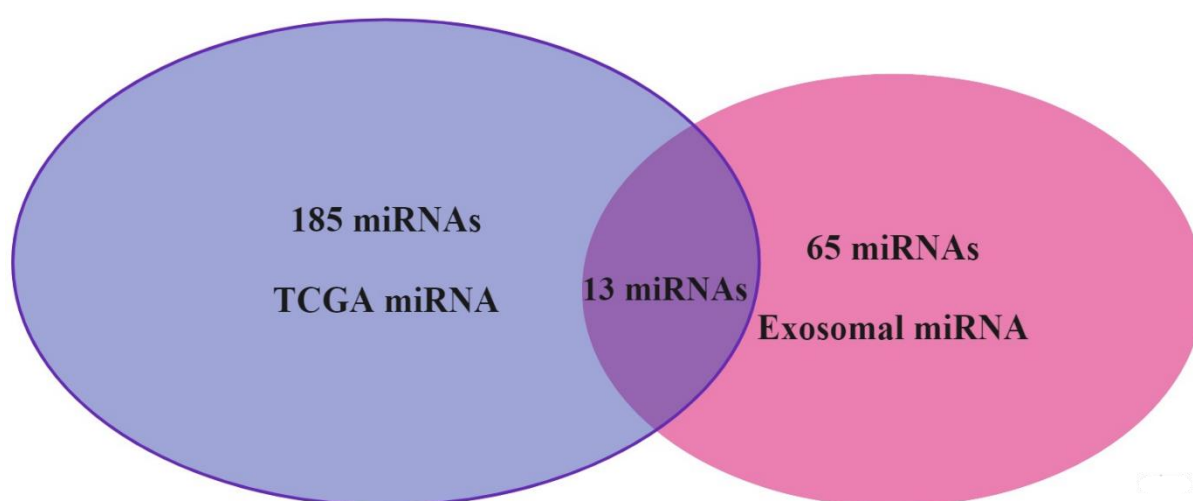
Figure 3.4: Venn diagram showing comparison between the differential expressed TCGA miRNA and exosomal miRNA.

Identification of exosomal miRNA Target Genes

To investigate the genes targeted by our selected microRNA, a miRNA-target enrichment analysis was done using the MIENTURNET web tool. The mRNAs potentially targeted by these miRNAs were predicted using miRTarbase database and a total of 450 genes were obtained. Some of the most significant genes are shown in Table 3.7 and Figure 3.5

Table 3.7: Mienturnet Enrichment results of top 20 most significant genes using miRTarBase.

Gene Symbol	p-value	FDR	Odd ratio	Number of interactions
NOB1	8.8086E-08	0,000277119	0,013466718	4
ERLIN2	2.3868E-07	0,000375451	0,005386687	3
FASN	2.8957E-06	0,003036679	0,030973451	4
AMPD1	6.2201E-06	0,003463858	0,002693344	2
AQP12B	6.2201E-06	0,003463858	0,002693344	2
POLR2A	6.6062E-06	0,003463858	0,014364499	3
AGER	1.8636E-05	0,005863083	0,004040015	2
CARD8	1.5012E-05	0,005863083	0,046460177	4
GARS	1.8636E-05	0,005863083	0,004040015	2
MRC2	1.8636E-05	0,005863083	0,004040015	2
CCT8	3.7225E-05	0,007319446	0,005386687	2
GTF3C2	3.7225E-05	0,007319446	0,005386687	2
NTHL1	3.7225E-05	0,007319446	0,005386687	2
PRPF8	3.0317E-05	0,007319446	0,023342311	3
PYGL	3.7225E-05	0,007319446	0,005386687	2
SOCS2	3.7225E-05	0,007319446	0,005386687	2
MIS12	6.1962E-05	0,010829702	0,006733359	2
TELO2	6.1962E-05	0,010829702	0,006733359	2
BTAF1	9.2824E-05	0,013906024	0,008080031	2
DDX54	9.2824E-05	0,013906024	0,008080031	2
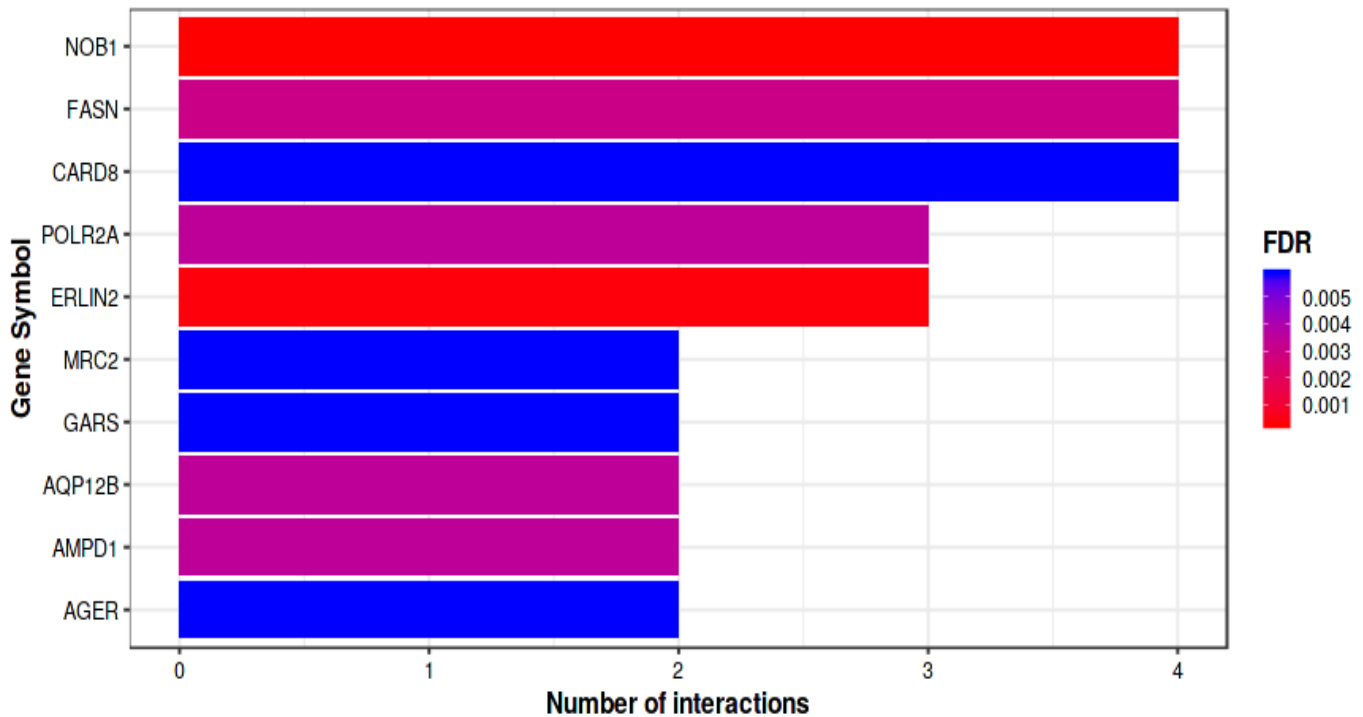
Figure 3.5: miRNA-target enrichment analysis, bar plot representing each target gene resulting from the enrichment along with the number of interactions (bottom). The color of the bars represents the adjusted p-values (FDR).

Regulatory network of the 7 Exo-miRNAs and their targets

In order to understand the interaction between our selected miRNA and their target gene, a target gene interaction networks were constructed with the miRNA-target gene pairs using MIENTURNET. In this network, hsa-miR-144-5p, hsa-miR-194-5p, hsa-miR-221-5p, hsa-miR-326, hsa-miR-93-5p, and hsa-miR-16-5p regulating 9, 38, 54, 57, 159, 294, and 344 target genes respectively (Figure 3.6). Among the targets, the nin one binding protein 1 (NOB1), fatty acid synthase (FASN), caspase activation and recruitment domain-containing protein 8 (CARD8), heterogeneous nuclear ribonucleoprotein A1 (HNRNPA1), and splicing factor 3b subunit 3 (SF3B3) were the genes with the highest connectivity.
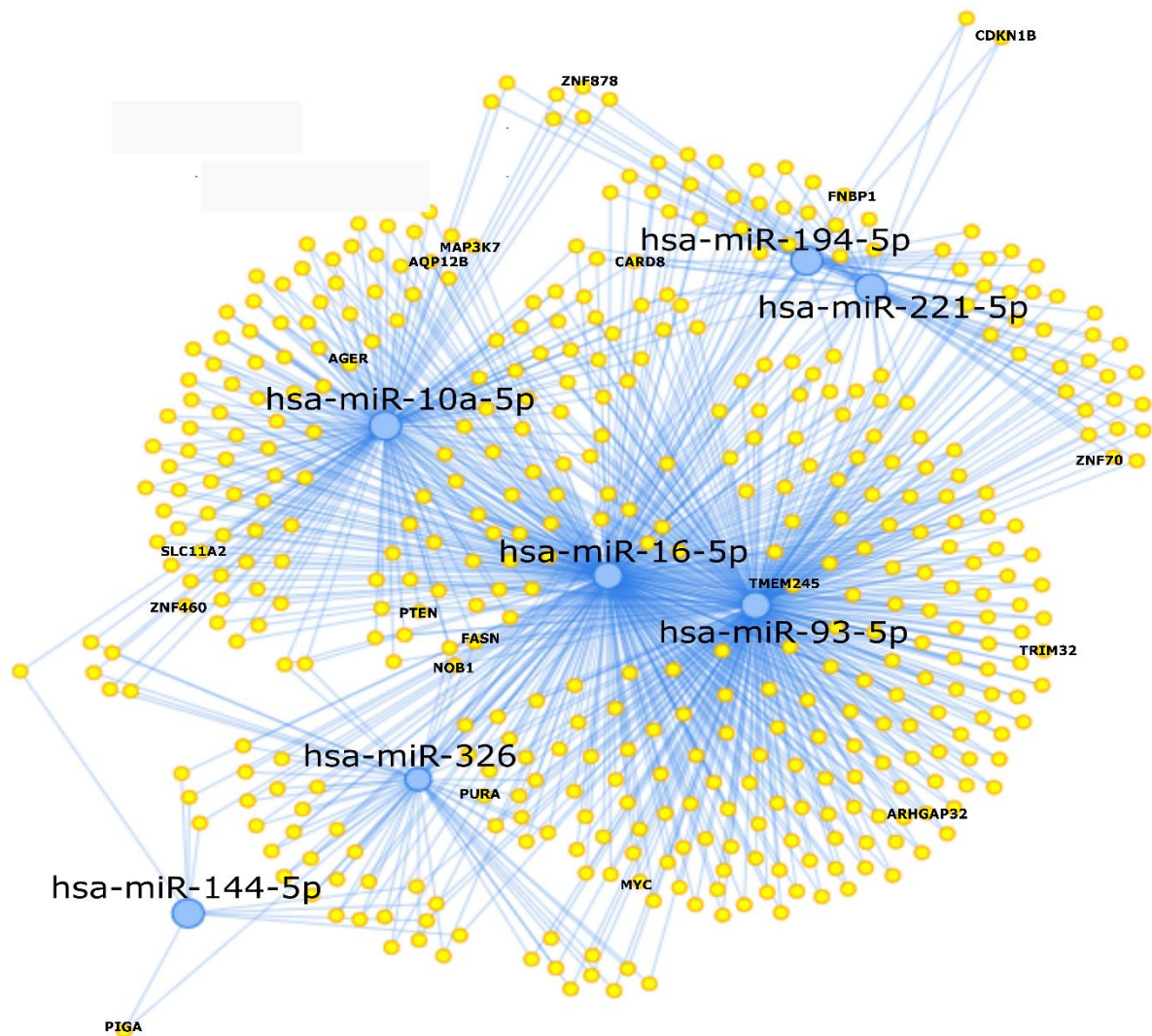
Figure 3.6: Regulatory network of PCa-associated genes and their target miRNAs. Blue nodes represent differentially expressed exosomal miRNAs. Yellow nodes represent miRNA associated genes. The genes with the highest numbers of interactions are also shown on their yellow nodes.

KEGG pathways analysis of target genes of 7 Exo-miRNAs

In order to understand the biological processes underlying the activity of the target gene we performed a functional enrichment analysis of the targets of our selected miRNAs by querying the KEGG (260) pathway through MIENTURNET web tool (259). KEGG analysis results revealed target genes enrichment in cancer such as PCa, small cell lung cancer, breast cancer, gastric cancer, pancreatic cancer, chronic myeloid leukemia, bladder cancer, melanoma, and glioma. The enrichment analysis also showed associated pathways such as IL-17 signaling pathway, PI3K-Akt signaling pathway, p53 signaling pathway, signaling pathways regulating

pluripotency of stem cells, and HIF-1 signaling pathway. The pathways are shown in Figure 3.7.
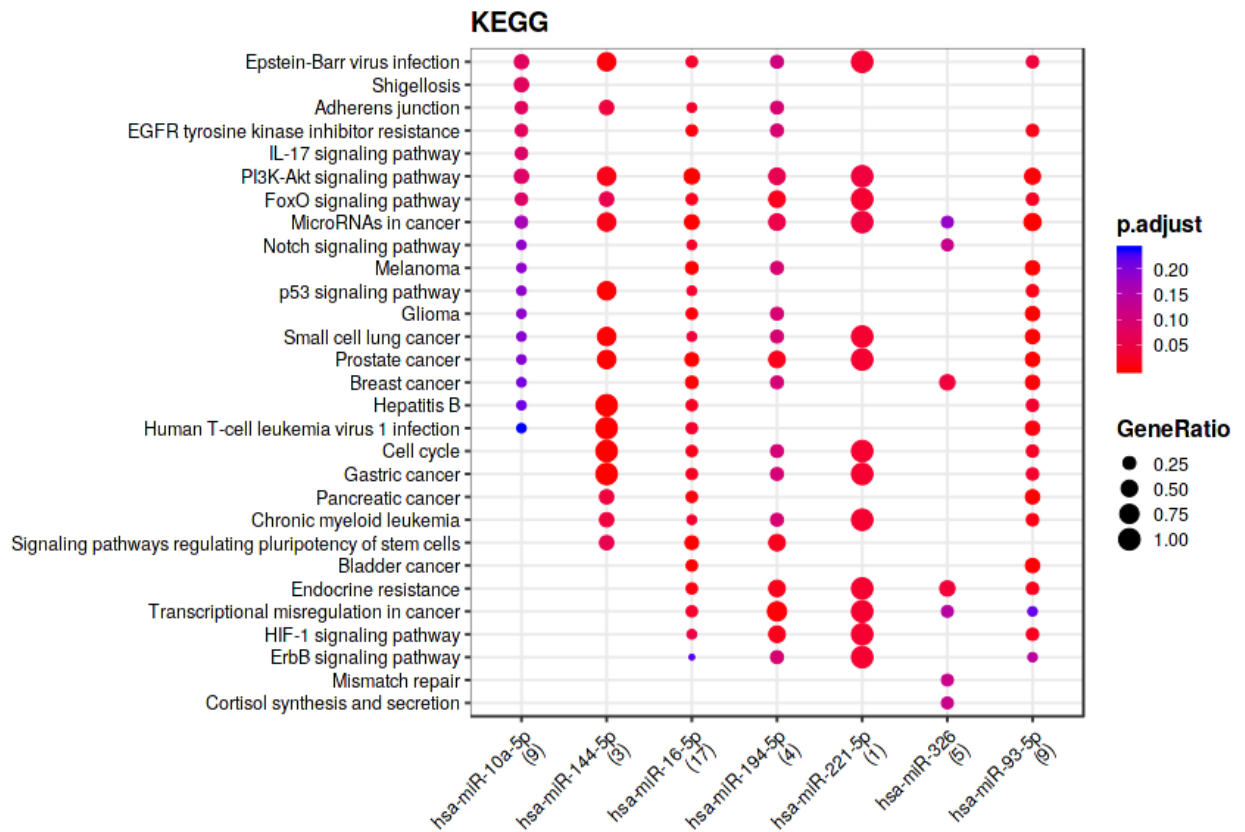
Figure 3.7: Dot plot of functional enrichment analysis for target genes of selected miRNAs resulting from the enrichment analysis. The Y-axis shows the KEGG pathways while the X-axis shows the selected miRNAs. The color of the dots denotes the adjusted p-values (FDR), while dots size signifies gene ratio (i.e., the number of miRNA targets found enriched in each category over the number of total genes associated to that category).

miRNA expression validation

For us to validate the selected miRNAs expressed, qPCR was done to determine the expression level in 26 PCa and 10 BPH patients. The absolute copy number of cDNA in each of the samples were calculated using the standard curve prepared with qPCR experiment.

To determine the miRNA that could best be used as biomarker for PCa, we calculated the expression ratio between each pair of miRNAs and correlated each ratio with the disease severity. A pairwise comparison may increase the accuracy and make the analysis independent

of the platform used. Initially we did correlate the single miRNA expression with the disease severity using Pearson coefficient, however we found the pairwise analysis improved the result significantly. The ratio between miRNA194 and miRNA16 was found to have the highest correlation coefficient (Fig 3.8). We also found significant correlation in the two miRNAs among BPH, low and high GS and metastatic PCa (Figure 3.9).
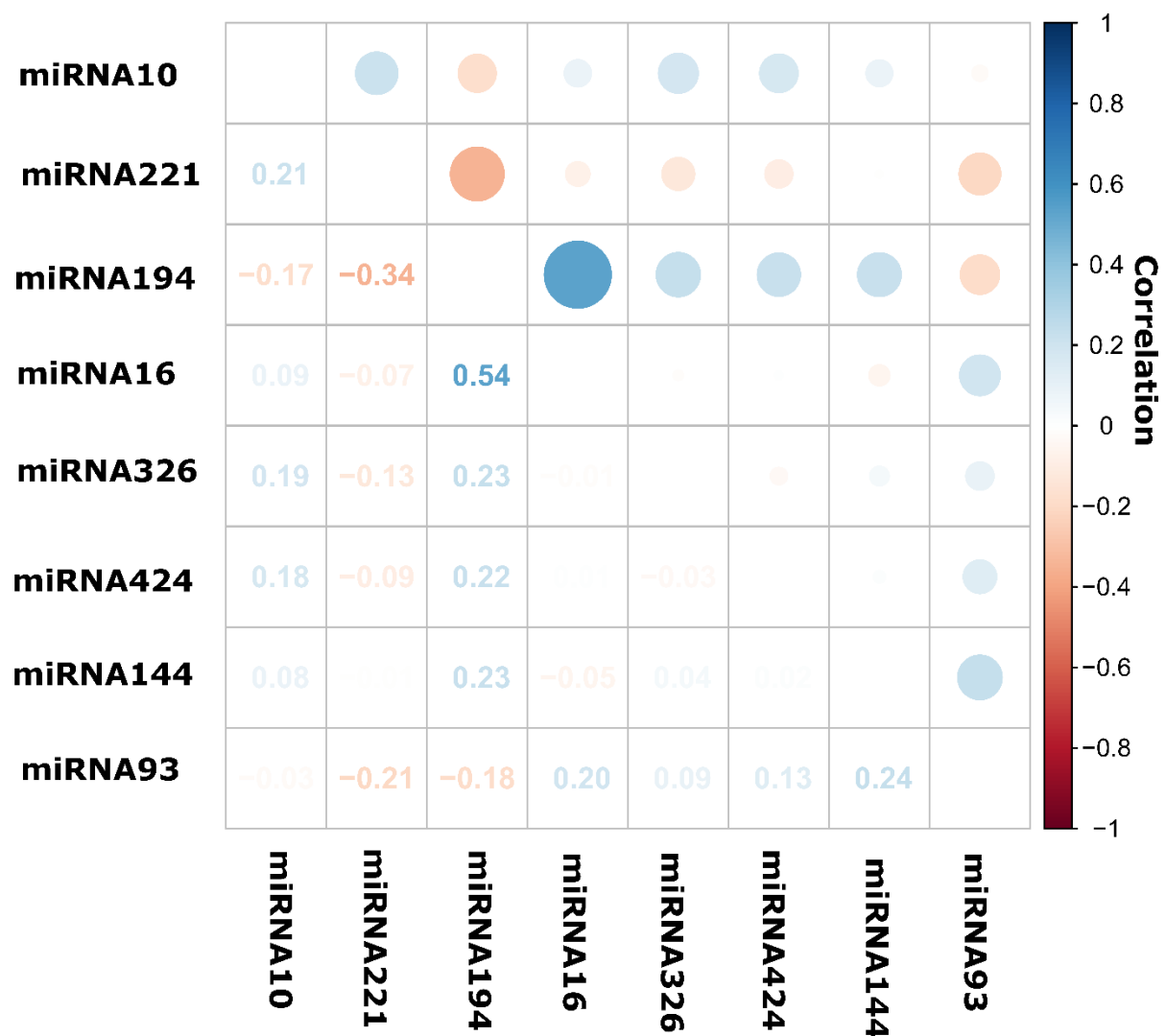
Figure 3.8: Heatmap showing Pearson correlation coefficient between each miRNA pairs and the disease severity. The blue color represents positive correlation and the red represent negative correlation.
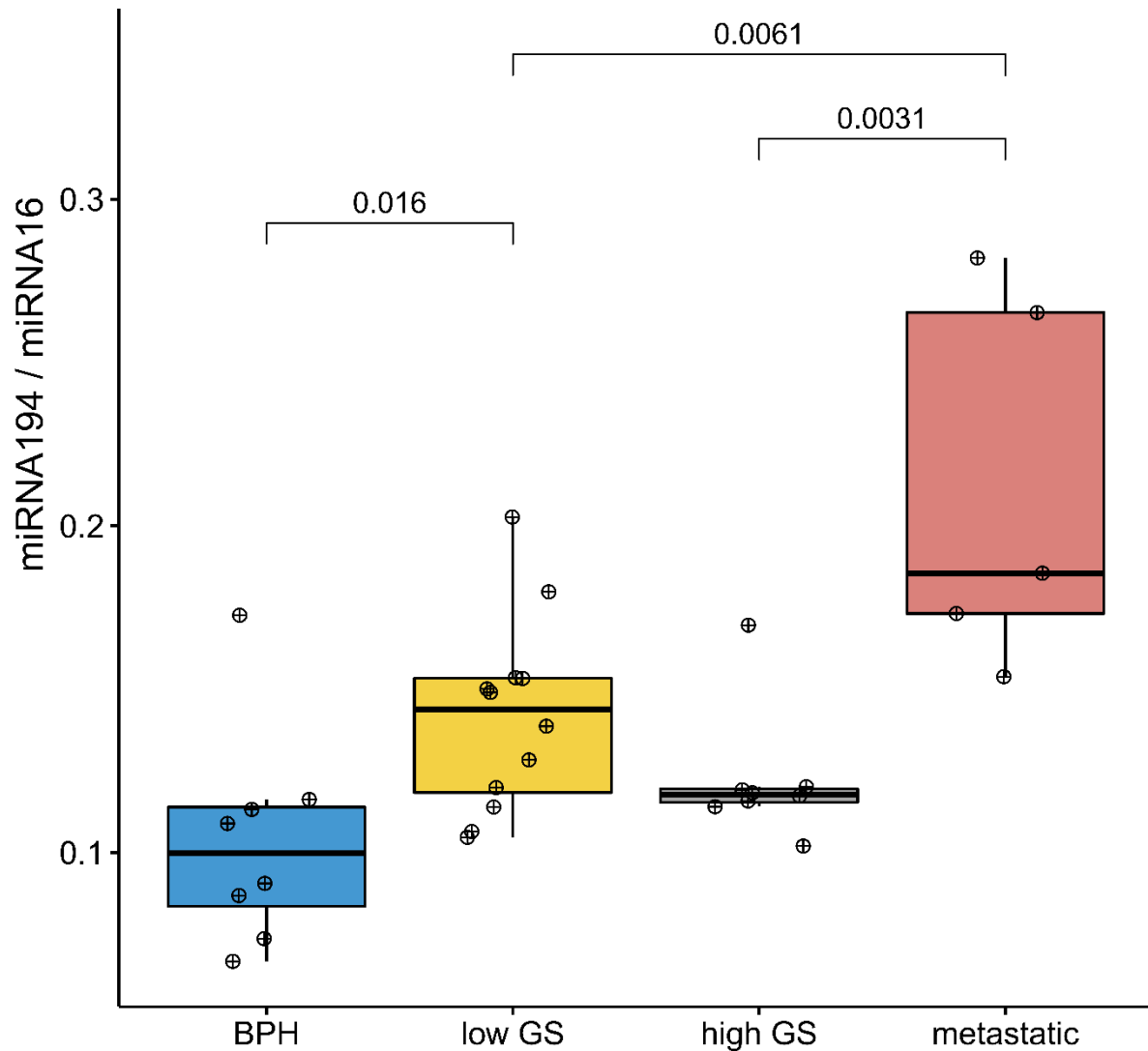
Figure 3.9: Boxplot of the correlation of miRNA194 and miRNA16 expression among BPH, low GS, high GS and metastatic PCa.

3.4 Discussion

Exosome cargoes are considered as key diagnostic and prognostic biomarkers of PCa (262). Exosomes in the blood and urine of PCa patients possess prostate-cancer-specific contents, which can serve as biomarkers for PCa (255,256). Previous studies have revealed the role of exosomal miRNA as biomarker in the diagnosis of PCa (192,196,263). A recent study by Li et

al. showed that a combination of exosomal miR-375 and miRNA451a can be used to distinguish PCa patients from BPH patients (264). However, studies evaluating exosomal miRNA as biomarker for diagnosis or prognosis of PCa in African populations are sparce. Our study was focused on finding potential exosomal miRNA among South African PCa patients. We investigated the role of exosomes number and size in the diagnosis of PCa. Our study showed no significant difference in size distributions of exosomes in both in PCa and BPH samples in the groups except for 16nm and 28nm groups where PCa exosomes size was significantly larger than BPH. Our finding is consistent with a previous study by Logozzi et al., which found higher exosomes concentration in PCa compared to BPH (265). Another study by Zlotogorski-Hurvitz et al. found significant difference in exosomes concentration and size distribution in oral cancer and normal individuals (266). However, the studies found significant larger exosomes size in cancer patients compared to their healthy control. The lack of difference in exosomes size in our PCa group and BPH group may be that increase in exosomes size is more tumor specific rather than cancer specific. We suggest that more studies to be done in a larger cohort to compare differences in exosomes size in BPH and PCa.

We also found that the exosomes formed clusters. The clusters were categorized into small (less than 10 exosomes) and big clusters (more than 10 exosomes) based on the number of exosomes forming the clusters. We found significant higher number of both small and big clusters in PCa than BPH. Our findings showed that exosomes cluster might be a good means of characterizing PCa and BPH.

It is important to mention that some of the exosome's size in our study were lower than usual exosomes diameter ranges between 30 to 100 nm. Studies have shown that the size of exosomes are usually underestimated by TEM due to the frequent collapse in the structure of exosomes resulting from chemical fixation and dehydration process involved in preparation (267,268). A study by Lyu et al. found a significant difference in size of exosomes measured by dynamic light scattering (DLS) and TEM (269). The study found that exosomes measured by DLS are 40nm larger than same exosome samples measured by TEM (269).

In our exosomal miRNA analysis, to determine if plasma level of exosomal miRNA identified are reflected in PCa tissues, we compared exosomal miRNA identified with PCa tissue miRNA of TCGA database. We found seven differentially expressed miRNA between plasma exosomal miRNA and tissue miRNA in TCGA.

We then investigated the genes targeted by the differentially expressed miRNA. The genes with the highest number of interactions are NOB1, FASN and CARD8 with each having interactions with four miRNAs. Notably, these genes have been shown to play major role in PCa development, progression, and metastasis (270–272).

NOB1, a subunit of the 26S proteasome play major role in the protein degradation pathway (273). In human, NOB1 is widely expressed in several organs, such as, spleen, prostate, lungs and liver (273). It functions as an oncogene for various human cancers (274,275). Previous studies have shown the role of NOB1 in PCa. Che et al. showed that NOB1 expression in the nucleus, correlate with lymph node metastasis in PCa patients (276). Also, another study showed that gene silencing of NOB1 inhibits the malignant transformation of PCa cells (277). NOB1 expression has been proposed as a potential marker of PCa prognosis (278,279).

FASN is an important enzyme used in synthesizing long-chain fatty acids from acetyl-coenzyme A (CoA) and malonyl-CoA using reduced nicotinamide adenine dinucleotide phosphate as a cofactor. The expression of FASN in human tissues is at a minimum level apart from adipose tissue and liver where it is highly expressed (280). However, in many human cancers the expression of FASN is largely increased and when it is overexpressed in tumors it is usually associated with poor prognosis (281–283). Studies have shown the role of FASN in PCa (270,282,284,285). FASN is found to be overexpressed in both early and late stages of PCa, suggesting its key role in PCa carcinogenesis, maintenance, and aggressiveness (282,285,286). Cao et al. found PCa patients with overexpression of FASN to have shorter biochemical recurrence free survival, signifying its role as a prognostic biomarker in PCa (270).

CARD8 belong to the caspase-associated recruitment domains (CARD) family, that are protein-protein interaction modules present in proteins. CARD8 is largely involved in apoptosis and serve as negative regulator of NF-κB and caspase-1 activation (287). Studies have revealed relationship between CARD8 mutation and increased in the risk of various human cancers (288). A study by Lavender showed that overexpression of CARD8 is linked with PCa aggressiveness, and poor prognosis (289).

We also performed an enrichment analysis querying KEGG pathways to investigate miRNAs-regulated pathways. We found p53 signaling pathway, PI3K-Akt signaling pathway, signaling pathways regulating pluripotency of stem cells, and HIF-1 signaling pathway to be related with the miRNAs.

The role of p53 pathways in cancers have been well studied (290–292). The tumor suppressor p53, serves as one of the major cellular barriers against carcinogenesis by regulating DNA damage responses and cell apoptosis (293,294). The expression of p53 have been shown to increase in response to cellular stresses including hypoxia, UV radiation, cytotoxic drugs. The role of p53 signalling pathway in PCa development, progression and proliferation have been largely described (295–298). Research have shown significant association between high expression levels of p53 and cell migration, proliferation, and adhesion capacities in PCa cells (299). Androgen-dependent genes in PCa have been found to be inhibited by overexpression of p53 (296). Also, advanced PCa cells that do not express a functional p53 protein have been found to be more resistance to chemotherapy and radiotherapy regimen (298).

The PI3K/Akt signalling pathway regulates cellular metabolism, tumor development, growth, proliferation, metastases, and cytoskeletal reorganization (300). PI3K/Akt pathway induce cancer development by activating the growth and survival pathways (300). In prostrate carcinogenesis, PI3K/Akt pathway has been found to play major role in the survival and proliferation of PCa stem cells (301). Akt and AR activation have been shown to synergize to increase the growth of PCa (302). Studies have demonstrated the reciprocal interactions between PI3K/Akt and AR pathways (303–305). An inhibition of the AR pathway leads to PHLPP-mediated Akt inactivation due to the decrease in androgen regulated FKBP5(303,306).

The hypoxia inducible factor (HIF) is a heterodimer, consisting of HIF1b and HIF1a subunits (307). HIF1a protein is ubiquitinated and rapidly broken down in oxygenated conditions. However, in conditions when there is lack of oxygen, HIF1a dimerizes with HIF1b subunits to produce an active HIF transcription complex (307). The HIF complex translocate to the nucleus and induces genes that promote cell survival, metabolism, angiogenesis, and invasion (308). In PCa, it has been found that hypoxia induced activation of HIF increase the expression AR (309,310). HIF signaling and AR pathways have been shown to play major role PCa progression (309). Also, the expression of HIF has been associated with poor PCa prognosis (311,312).

To further validate the miRNAs identified by sequencing, we performed qPCR miRNA expression on additional samples. We found that miRNA194 and miRNA16 expression ratio correlate with the disease severity to serve as potential biomarkers for PCa diagnosis. The miRNA194 and miRNA16 ratio significantly separate BPH samples from PCa samples. We also found the correlation of the expression ratio of miRNA194/ and miRNA16 expression

ratio ~~with the disease severity significantly~~ separate metastatic PCa from low and high ~~Gleason~~ GS PCa. Our findings showed that the ~~correlation~~ expression ratio of these two miRNAs could serve a potential diagnostic and prognostic biomarkers in PCa. Previous studies have reported the individual roles of miRNA194 and miRNA16 in PCa but none has described the potential role of combining miRNA194 and miRNA16 as biomarker for PCa most especially in African populations (313–315). A study by Das et al., found significantly higher levels of miRNA194 in serum of metastatic castrate-resistant prostate cancer than in those with localized PCa (314). Another study by Selth et al. showed that miRNA194 was elevated in metastatic PCa and related with poor prognosis among PCa patients (316). In prostate carcinogenesis, miRNA194 modulate cell survival and tumor growth by targeting cahedrin-2. miRNA194 play key role in PCa metastasis by increasing cell invasion in PCa through epithelial-mesenchymal transition induction. MiRNA16, which is located at chromosome 13q14 has been shown to be a tumor suppressor and is involved in the onset of PCa. A study by Alshalalfa et al showed that miRNA16 is an important master regulator of miRNA-mediated regulation in PCa (317).

In conclusion, our study for the first time revealed the potential uses of miRNA194 and miRNA16 in the diagnosis of PCa in South African populations. It further showed the potential role of exosome morphological features in the diagnosis of PCa. Studies in African populations with larger cohort are needed to further validate these findings.

CHAPTER 4: Cell free DNA as a source of biomarker for prostate cancer

4.1 Background

The sparsity of a less invasive, easy-to-use, PCa specific and cost-effective biomarker has made that PSA remains the gold standard biomarker in the diagnosis and prognosis of PCa. Circulating nucleic acids have been studied as biomarker for diagnosis, prognosis, and treatment monitoring of PCa (139,202,318–320). cfDNA are released by virtually all cells in the body and has been described in many body fluids (321–324). cfDNA released from tumor cells are known as ctDNA.

In a healthy state, individuals carry between 1 and 10 ng/mL cfDNA, while in cancer state, concentrations of cfDNA can rise to 50-1000 ng/mL of blood, with ctDNA comprising 3-90% of the total (125,325). The rise in cfDNA in cancer patients is due to a high turnover rate of tumor cells and an ineffective clearing of dead and dying cells (326). The presence of ctDNA in cancer patients has also been explored as a source of biomarker for early diagnosis of cancer because of the presence of tumor-specific variations corresponding to the patient's tumor, such as mutated tumor suppressor genes or oncogenes, microsatellite instability, and DNA methylation (135,327,328). A study by Chen et al. found in cfDNA of PCa patients somatic tissue alterations including nonsynonymous variants in FOXA1, ATM, PTEN, and MED12 (329).

Studies have shown the promising role of cfDNA as a biomarker for diagnosis, prognosis, and monitoring of PCa (330–334). A study by showed that AR gene alterations in cfDNA are associated with resistance to enzalutamide and abiraterone in mCRPC (333). The study concluded that genomic analysis of cfDNA is a less invasive way for investigating therapeutic resistance in mCRPC. Zimmerman et al. showed through genomic profiling of cfDNA the differences in genomic landscape between Caucasians and African American patients (335). The study found significantly higher frequency of AR gene alteration in African American patients than the Caucasians (335). It also reported a higher frequency of alterations in EGFR, MYC, FGFR1, and CTNNB1 in African American patients (335). This makes it imperative for studies to be done to explore the diagnostic role of cfDNA among African PCa patients, for

more precise management of PCa in the African population. This study is aimed at elucidating the role of cfDNA as a diagnostic biomarker for PCa in the South African population.

4.2. **Methodology**

4.2.1 Extraction and quantification of cfDNA in plasma and urine

cfDNA extraction: cfDNA was extracted from 1ml of plasma and 10ml of urine using QIAamp Circulating Nucleic Acid Kit (Catalog number: 55114). Extracted cfDNA was eluted in 50 µl nuclease-free water and kept in -80°C freezer.

qPCR cfDNA quantification: In this study, to accurately perform a qPCR quantification of our cfDNA samples, we used primers designed for ALU gene for real-time PCR reactions. We used ALU 115 set of primers to amplify the shorter fragments, while ALU 247 set of primers was used to amplify only the longer DNA fragments.

Gel electrophoresis: To determine the copy number of cell-free DNA samples, we performed gel electrophoresis analysis of qPCR DNA products and excised DNA bands of 115 bp. Excised DNA bands was purified with QIAEX®II Gel Extraction Kit (Catalog number: 20021). Purified DNA was eluted in 20 µl of nuclease-free water and concentration was checked with Nanodrop. Purified DNA was stored in -80°C freezer.

Real time PCR reaction set up: A 10 µl reaction of real time PCR was prepared for each cfDNA sample and for each of the primer set. For each 10 µl real time PCR reaction, we added 1 µl of 2 µM solution of either ALU 115 or ALU 247 forward and reverse primers to 5 µl Buffer SYBR Green with 1 µl cfDNA and 3 µl nuclease free water. All reactions were prepared in duplicates. The qPCR amplification was done with initial preincubation step at 95°C for 30 s, followed by 40 cycles of denaturation at 95°C for 5 s, annealing at 60°C for 34 s, and extension at 72°C for 30 s using Light Cycler 480 (Roche, Switzerland).

To do an absolute quantification of cfDNA using real time PCR, we did serial dilution of initially purified DNA with known concentration and copy number to construct a standard curve for cfDNA quantification. A 10 µl qPCR reaction was also prepared for each of the serial dilution made by adding 1 µl of 2 µM solution of both ALU 115 forward and reverse primers to 5 µl Buffer SYBR Green with 1 µl DNA and 3 µl nuclease-free water.

Real time PCR reaction steps include preliminary heat activation at 95°C for 2 minutes, denaturation at 95°C for 2 seconds, combination of annealing and extension at 56°C for 10

68

seconds (45 cycles) and melting curve analysis done at 60–95°C. Acquisition of the data for the real time PCR reaction was done during the annealing/extension step.

4.2.2 Data analysis:

The qPCR post-run data are semi-automated on all commercial qPCR systems. The absolute quantification data generated for each sample were exported into Excel file. The data analysis and graphical illustrations were produced in R (version 3.6.1) and R studio (version 1.1.456) software with the help of scripts made in-house. Wilcoxon Rank Sum test was used to compare differences in numerical covariates (e.g., age and PSA) between BPH and PCa. Spearman's test was used in calculating correlation coefficient (rho) between variables. Two-way ANOVA was used to estimate how their means change according to the PSA, GS, age, and their respective interactions.

4.2.3 Whole exome sequencing

Whole exome sequencing was done using cfDNA extracted from 12 urine samples. The concentration and fragment size of cfDNA were determined using Agilent 2100 Bioanalyzer and the Agilent High Sensitivity DNA chip. A concentration of 20 ng of cfDNA fragment size between 150-200 bp was required for whole exome sequencing.

Whole exome sequencing libraries were constructed with 20 ng of cfDNA using the SureSelect V6-Post (cfDNA) kit for the HiSeq2500 (Agilent Technologies, Inc., Santa Clara, CA). Library preparation was done by following the SureSelectXT Target Enrichment System for Illumina Paired-End Sequencing Library Protocol (version 1.5, November 2012) (Agilent). Whole exome sequencing was done on Illumina platform.

4.2.4 Data and Statistical Analysis

Data analysis: Data analysis for our cfDNA WES data was done using an in-house developed pipeline. The pipeline involves a preprocessing stage of de-multiplexing the raw data originally in BCL file using bcl2fastq tool into separate FASTQ files for each of the samples. The FASTQ files were then filtered using the AfterQC (336) tool optimized for cfDNA data to remove reads of low quality. The filtered FASTQ files was then aligned to reference genome with the help of BWA software (337). The SAM file generated after alignment was changed into BAM and then indexed using Samtools. Next, we removed duplicate reads using Samtools rmdup tool. After the BAM file processing was completed, we did variant calling for somatic mutation

using the VarScan2 (338). The VarScan2 caller have previously been used with good success in previous cfDNA analysis. The VCF file generated after the calling was annotated with the COSMIC database version 70 using ANNOVAR with build hg19 databases. Then, the false-positive mutations were marked using MySQL baseline technology, after which the VCF filtered and cleaned. The cleaned VCF file was used in reporting the final target mutations.

Statistical Analysis: A two-sample t-test was used to compare the mutation quantities between the BPH and PCa groups. The mutations with significant difference between PCa and BPH (p-value=0.05) were identified and plotted in a heatmap with two-way hierarchical clustering using the Jaccard distance measure and the Ward's linkage method.

4.3 Results

In order to quantify cfDNA using copy number, we performed gel electrophoresis analysis of real-time PCR DNA products and excised DNA bands of 115 bp. The purified DNA was used to prepare a standard curve for absolute quantification of cfDNA PCR reactions (Figure 4.1).
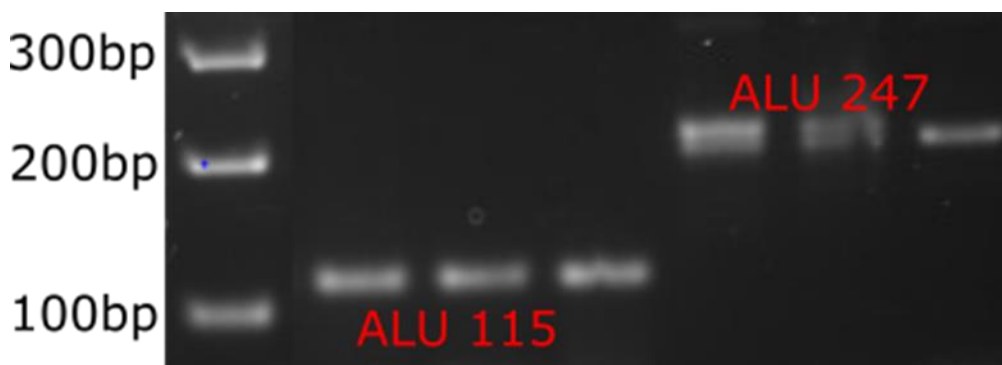
Figure 4.1: Electrophoresis gel mage of ALU 115 and ALU 247 DNA bands

4.3.1 Plasma cfDNA quantification

Quantification was done using cfDNA extracted from plasma samples of 59 (30 BPH and 29 PCa) patients. Thirteen of the PCa patients have high GS while 16 have low GS. The median age of all PCa patients was 71 [interquartile range (IQR) 63 74.8] years while the median age of all BPH patients was 72 [IQR 65.3 76.7] years. The median ALU 115 level in PCa patients [1.048 (IQR 0.25 2.285) ng/mL] was found to be higher than the median ALU 115 in BPH patients [0.865 (IQR 0.267 1.776) ng/mL]. The median ALU 247 level in PCa patients [0.049 (0.008 0.603) ng/mL] was also found to be higher than the median ALU 247 in BPH patients [0.035 (0.004 0.329) ng/mL] (Table 4.1).

Table 4.1: Plasma cfDNA quantification in BPH and PCa patients.

Feature	BPH	PCa	Total	p-value
No of patient (%)	30 (50.8)	29 (49.2)	59 (100)	
ALU 115, median [IQR] (ng/mL)	0.865 [0.267 1.776]	1.048 [0.25 2.285]	0.878 [0.246 2.247]	9.34E-01
ALU 247, median [IQR] (ng/mL)	0.035 [0.004 0.329]	0.049 [0.008 0.603]	0.037 [0.008 0.42]	6.55E-01
Integrity, median [IQR]	0.046 [0.013 0.239]	0.104 [0.014 0.347]	0.058 [0.013 0.279]	4.71E-01
Age, median [IQR] (years)	72 [65.3 76.7]	71 [63 74.8]	71.3 [63.1 76.2]	7.79E-01
PSA, median [IQR] (ng/mL)	5.33 [1.36 13.475]	24.61 [10.99 103.025]	12.9 [3.975 25.98]	1.13E-05

GS			

We performed secondary analyses to investigate the relationship between baseline cfDNA concentration and clinical characteristics among PCa and BPH patients. There was a significant positive correlation between patients' PSA level and DNA integrity in all patients. Among PCa patients, we found significant correlation between ALU 115 and ALU 247 cfDNA concentration and patient's age. Our study also showed a significant correlation between ALU 115 and ALU 247 cfDNA concentration and patient's age. There was also significant correlation between patient's PSA level and DNA integrity among PCa patients (Table 4.2).

Table 4.2: Correlation between cfDNA, age and PSA among BPH, PCa, and all patients

	Feature	rho	p-value
Correlation: cfDNA and age (all patients)			
1	ALU 115	0.11	4.05E-01
2	ALU 247	0.14	2.92E-01
3	Integrity	0.13	3.10E-01
Correlation: cfDNA and PSA (all patients)			
1	ALU 115	0.13	3.59E-01
2	ALU 247	0.25	6.61E-02
3	Integrity	0.26	5.27E-02
Correlation: cfDNA and age (PCa patients)			
1	ALU 115	0.37	4.68E-02
2	ALU 247	0.43	1.99E-02
3	Integrity	0.27	1.51E-01
Correlation: cfDNA and PSA (PCa patients)			
1	ALU 115	0.08	6.67E-01
2	ALU 247	0.41	3.25E-02
3	Integrity	0.43	2.23E-02
Correlation: cfDNA and age (BPH patients)			
1	ALU 115	-0.19	3.15E-01
2	ALU 247	-0.14	4.66E-01
3	Integrity	0.01	9.57E-01
Correlation: cfDNA and PSA (BPH patients)			
1	ALU 115	0.06	7.66E-01
2	ALU 247	0.05	7.90E-01
3	Integrity	0.07	7.43E-01

We also performed correlation tests to investigate the relationship between cfDNA concentration, DNA integrity, PSA, and age among PCa and BPH patients (Figure 4.2). We investigated the parameters between high (total score ≥8) and low (total score ≤7) GS PCa patients (Figure 4.3). There was significant correlation between DNA integrity and PSA among PCa patients. There was also significant correlation seen between ALU 247 cfDNA concentration and age among low GS PCa patients.
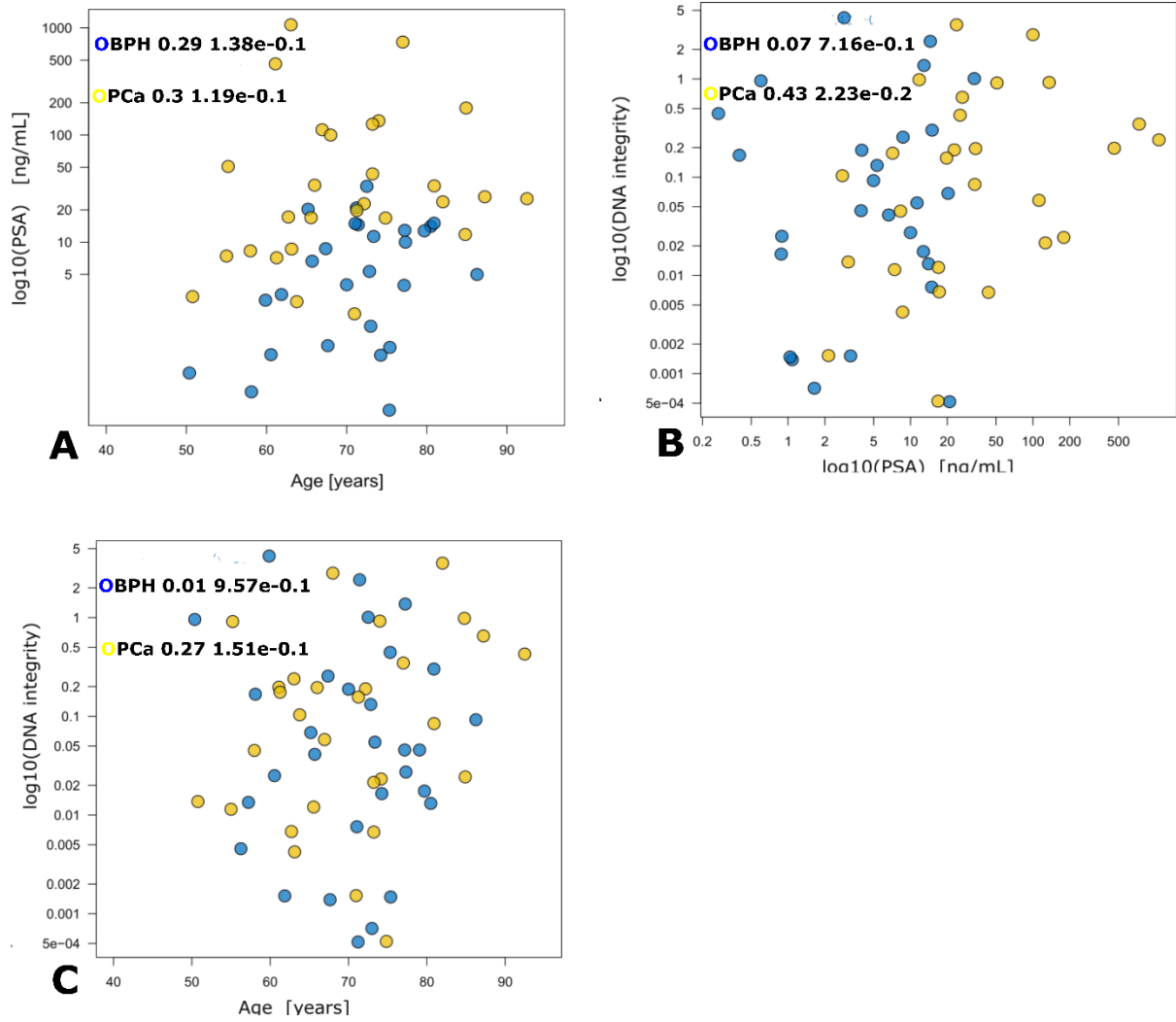
Figure 4.2: Correlation between A) PSA and age in BPH and PCa patients, B) DNA integrity and PSA in BPH and PCa patients, C) DNA integrity and age in BPH and PCa patients.
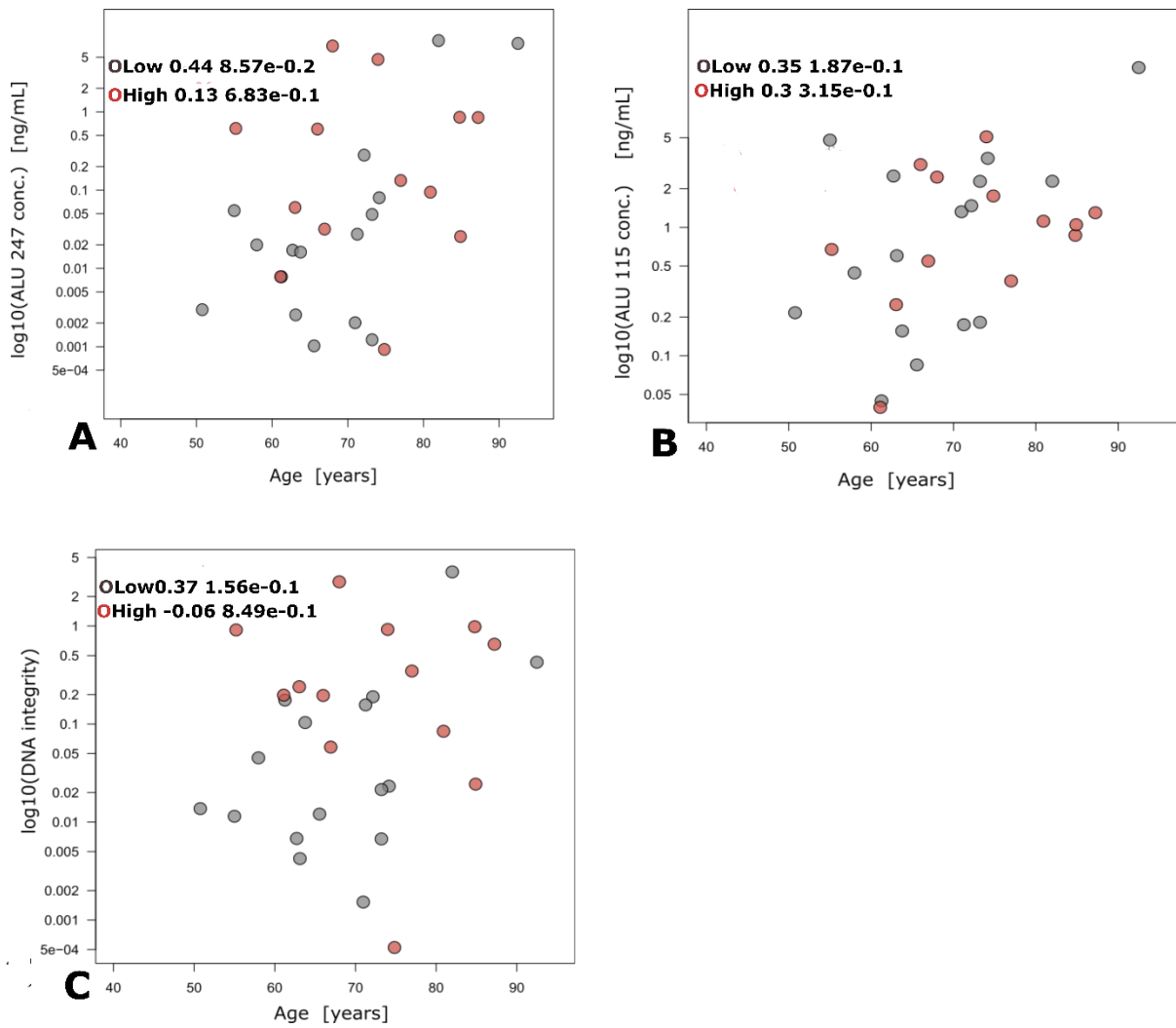
Figure 4.3: Correlation between A) plasma ALU 247 concentration and age in low and high GS PCa patients, B) plasma ALU 115 concentration and age in low and high GS PCa patients, C) plasma DNA integrity and age in low and high GS PCa patients.

To investigate the combined effects of the independent variables on variables such as cfDNA concentration and DNA integrity, we used a two-way ANOVA for secondary analysis of our data (Tables 4.3, 4.4 and 4.5). We found a significant relationship between ALU 115 and ALU 247 concentration and the combined effect of patient's age and Gleason's score. (Table 4.3 and 4.4).

Table 4.3: A two-way ANOVA between ALU 115 concentration and clinical data of all patients

	Df	Sum Sq	Mean Sq	F value	p-value
log10 (PSA)	1	0.107566	0.107566	0.014848	0.904231
Age	1	55.35293	55.35293	7.640819	0.011966

	Df	Sum Sq	Mean Sq	F value	p-value
GS	1	13.78501	13.78501	1.902857	0.182989
log10(PSA): Age	1	0.374996	0.374996	0.051764	0.822332
log10(PSA): GS	1	0.032546	0.032546	0.004493	0.947226
Age: GS	1	69.19189	69.19189	9.551123	0.005768
log10(PSA): Age: GS	1	18.90289	18.90289	2.609321	0.121903

Table 4.4: A two-way ANOVA between ALU 247 concentration and other clinical data of all patients

	Df	Sum Sq	Mean Sq	F value	p-value
log10(PSA)	1	1.703986	1.703986	0.401276	0.533609
Age	1	26.37594	26.37594	6.211338	0.021587
GS	1	2.493382	2.493382	0.587173	0.452464
log10(PSA): Age	1	1.376277	1.376277	0.324103	0.575491
log10(PSA): GS	1	0.521745	0.521745	0.122867	0.72961
Age: GS	1	37.19775	37.19775	8.759795	0.007747
log10(PSA): Age: GS	1	6.120957	6.120957	1.44144	0.243934

Table 4.5: A two-way ANOVA between DNA integrity and other clinical data of all patients

	Df	Sum Sq	Mean Sq	F value	p-value
log10 (PSA)	1	0.325227	0.325227	0.413553	0.527477
Age	1	0.999828	0.999828	1.271363	0.272857
GS	1	0.071068	0.071068	0.090369	0.766811
log10 (PSA): Age	1	0.402591	0.402591	0.511927	0.482576
log10 (PSA): GS	1	0.005389	0.005389	0.006852	0.934852
Age: GS	1	1.368478	1.368478	1.740133	0.202026
log10(PSA): Age: GS	1	0.121046	0.121046	0.15392	0.698966

4.3.2 Urine cfDNA quantification

Urine cfDNA quantification was done with a total of 26 samples. The median age of all PCa patients was 67.9 [IQR 62.7 73.5] while the median age of all BPH patients was 75 [IQR 69.4

77.3]. The median ALU 115 level in PCa patients [0.045 (0.011 0.1)] was found to be higher than the median ALU 115 in BPH patients [0.019 (0.013 0.028)]. The median ALU 247 level in PCa patients [0.037 (0.004 0.088)] was also found to be higher than the median ALU 247 in BPH patients [0.01 (0.004 0.042)] (Table 4.6).

Table 4.6: Urine cfDNA quantification in BPH and PCa patients

Feature	BPH	PCa	Total	p-value
ALU 115, median [IQR]	0.019 [0.013 0.028]	0.045 [0.011 0.1]	0.021 [0.012 0.097]	5.51E-01
ALU247, median [IQR]	0.01 [0.004 0.042]	0.037 [0.004 0.088]	0.024 [0.004 0.058]	4.75E-01
Integrity, median [IQR]	0.686 [0.504 0.88]	0.598 [0.375 1.266]	0.616 [0.381 1.069]	8.56E-01
Age, median [IQR]	75 [69.4 77.3]	67.9 [62.7 73.5]	70.3 [63.5 75.4]	6.57E-02
PSA, median [IQR]	9.345 [5.942 12.425]	46.275 [17.56 177.875]	16.56 [9.018 68.808]	9.10E-04
GS				
high, n (%)	-	8 (50.0)	8 (50.0)	
low, n (%)	-	8 (50.0)	8 (50.0)	

We also performed secondary analyses to investigate the relationship between baseline cfDNA concentration and clinical characteristics among PCa and BPH patients. There was no significant correlation found cfDNA and any of the clinical data (Table 4.7).

Table 4.7: Correlation between cfDNA, age and PSA among BPH, PCa, and all patients

	Feature	rho	p-value
Correlation: cfDNA and age (all patients)			
1	ALU 115	0.13	5.49E-01
2	ALU 247	0.11	5.88E-01
3	Integrity	0.14	5.15E-01
Correlation: cfDNA and PSA (all patients)			

1	ALU 115	0.1	6.09E-01
2	ALU 247	0.15	4.50E-01
3	Integrity	0.1	6.11E-01
Correlation: cfDNA and age (PCa patients)			
1	ALU 115	0.28	2.94E-01
2	ALU 247	0.3	2.57E-01
3	Integrity	0.17	5.19E-01
Correlation: cfDNA and PSA (PCa patients)			
1	ALU 115	0.17	5.19E-01
2	ALU 247	0.21	4.36E-01
3	Integrity	0.15	5.71E-01
Correlation: cfDNA and age (BPH patients)			
1	ALU 115	0.22	5.74E-01
2	ALU 247	0.04	9.15E-01
3	Integrity	0.46	2.13E-01
Correlation: cfDNA and PSA (BPH patients)			
1	ALU 115	-0.33	3.49E-01
2	ALU 247	-0.47	1.66E-01
3	Integrity	0.25	4.92E-01

4.3.3 CfDNA whole exome sequencing

We performed whole exome sequencing of cfDNA from 12 urine samples. Patients' clinical data are shown below in Table 4.8

Table 4.8: Clinical data of patient's samples used for whole exome sequencing.

SAMPLE ID	Sample type	Age (years)	Race	Pathology	GS	PSA
SAPC0108	Urine	56	Black	PCa	3+4	82.6
SAPC0164	Urine	74	Black	PCa	3+3	74
SAPC0195	Urine	87	Black	PCa	4+5	26
SAPC0249	Urine	63	MA	PCa	5+4	1070

SAPC0321	Urine	63	MA	PCa	3+3	8.62
SAPC0281	Urine	71	MA	PCa	3+3	19
SAPC0331	Urine	75	MA	PCa	4+5	53.23
SAPC0334	Urine	73.22	MA	PCa	3+4	126.8
SAPC0339	Urine	77	MA	BPH		12.9
SAPC0346	Urine	69.45	MA	BPH		1.05
SAPC0119	Urine	69	MA	BPH		5.49
SAPC0224	Urine	81	MA	BPH		14.05

MA (mixed ancestry)

To identify nonsynonymous single-nucleotide variant (nsSNV) in the absence of germline mutation, we analyzed the data using pipeline developed in-house to identify SNVs in PCa and the BPH samples used as control. We identified a total of 4095159 nsSNV in the coding region of all samples. We filtered the total mutations for nsSNV and found a total of 194112 nsSNV for all samples. Due to the absence of corresponding germline mutation in our samples, we compared the nsSNV found in our samples with that of PCa nsSNV in COSMIC database. A total of 9461 genes were found at COSMIC annotated sites. The mutated genes found were then analyzed according to the frequency of their occurrence in PCa and BPH samples.

In order to identify significantly mutated genes in PCa, we made a comparison of genes found in PCa samples and BPH. We found 31 (ZNF286A, MMAB, IMPG1, BRCA1, ERCC6, KCNMB3, CGB7, JMJD1C, CD109, ADGRV1, SLC13A2, NLRP5, SELP, ARHGAP21, HTR3E, CEP85L, TMEM106B, CLYBL, MGP, ZNF615, PLIN4, MADCAM1, MTHFR, CPLANE1, NTAQ1, NUSAP1, AOC1, CYFIP1, ADAMTSL3, GDF3, and MST1) genes that showed significant difference between PCa and BPH samples Figure 4.4.
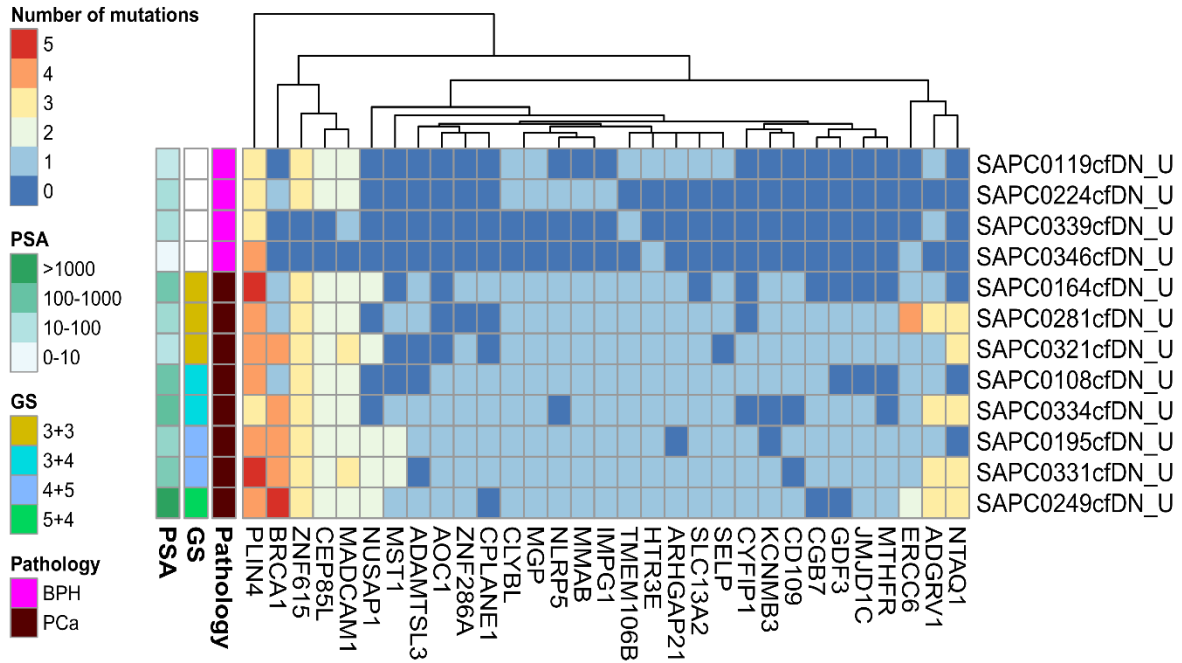
Figure 4.4: Heatmap of significant mutated gene between BPH and PCa patients colored according to the number of mutations found in each of the samples. [GS-Gleason score]

4.4 Discussion

Our study investigated the role of plasma and urinary cfDNA level and DNA integrity as diagnostic tools for PCa. CfDNA released from tumor cells is a mirror of the ongoing state of the tumor and measuring cfDNA level can serve as an ideal diagnostic and prognostic tool for tumors (339). We used Alu gene, the most abundant repeats in the genome sequence, to measure the level of cfDNA in plasma and urine (242,243). ALU 115 concentration represents the shorter DNA fragments and the total amount of plasma or urinary cfDNA, while ALU 247 represents the longer DNA fragments usually products of necrosis. DNA integrity, the ratio of longer to shorter cfDNA fragments, is higher in cancer patients and higher in metastatic cancers than in non-metastatic cases (340,341). DNA integrity also predict the progression of tumor and lymph node metastases in PCa patients (342,343).

In this study, we found significant association between plasma cfDNA concentration and age among PCa patients while no association between urinary cfDNA concentration and age. There have been conflicting reports from previous studies that explore the relationship between cfDNA concentration and age. Sozzi et al. reported a significant association between age and

plasma cfDNA concentration (344). On the contrary, other studies observed no association between the concentration of plasma cfDNA and age (345,346).

Our study also found significant association between plasma concentration of longer fragment cfDNA (ALU 247) and PSA in PCa patients and a significant positive correlation between DNA integrity and PSA among PCa patients. However, there was no association between urinary cfDNA concentration and PSA. This is consistent with Seyedolmohadessin et al. which found significant association between PSA and serum cfDNA concentration (319). The lack of association between PSA and urinary cfDNA may be due to small sample size of the urinary cohort in our study. Although, there is no logical direct relationship between PSA and cfDNA concentration, studies have explored the possibility of combining cfDNA concentration and PSA in the diagnosis and monitoring of PCa (319,347,348). Gordian et al. reported that combination of cfDNA concentration with PSA helped increase the specificity of PSA test for detection of PCa (348). Another study by Torquato et al. found a positive correlation between PSA and cfDNA and concluded that the combination of PSA and cfDNA might improve the early diagnosis of PCa (349).

In order to determine genetic variation within the cfDNA fragments in PCa from South African populations, we performed exome sequencing of urinary cfDNA. Our study is the first African based whole exome sequencing of urinary cfDNA in PCa. This is important because it help to give better understanding of the specific genetic alteration in PCa among African populations. In our study we sequenced urinary cfDNA of 8 PCa samples and 4 BPH samples and found 31 significantly somatic mutated genes.

Our finding of this novel panel of mutated genes in PCa of South African men largely contribute towards the effort of identifying genetic mutation specific to African populations. These mutated genes may potentially serve as PCa diagnostic biomarker particularly in African populations. Also, this finding is a great contribution towards the search of more specific liquid biopsy for African men considering that the presently available liquid biopsy for PCa diagnosis was based on studies done among Caucasians populations (350,351).

Interestingly, four of the 31 genes (BRCA1, ERCC6, ARHGAP21, and ADAMTSL3) have been described in previous studies to be frequently mutated in PCa of African men (352–354). The role of BRCA1 gene in the development of PCa has been extensively described (170,355–357). BRCA1 is a tumor suppressor gene inherited in an autosomal dominant fashion with

incomplete penetrance. The development of tumor in persons with germline mutations in BRCA1 genes requires somatic inactivation of the remaining wild-type allele (357). BRCA1 plays major role in cellular control systems, due to its role in different cellular processes such as transcriptional regulation, DNA damage response and repair, and chromatin modelling (358,359). BRCA1 has been shown as a coregulators of AR, which mediates a signalling pathway important in prostrate carcinogenesis and progression (360,361). Mutations in BRCA1 and BRCA2 genes are linked with poor prognosis of PCa (356,362,363). Studies have shown a higher BRCA1 mutation in PCa in men of African ancestry than the Caucasian populations (352,353,364,365). Yadav et al. found an increase in BRCA1 mutation in men of African ancestry than Caucasian men (352). A study by White et al. found about 2.16-fold increase of BRCA1 mutation in men of African ancestry compared to European men (353).

The excision repair cross-complementing group 6 (ERCC6) gene encodes a protein which, play key repairing of damage DNA (366,367). ERCC6 functions through transcription and nucleotide excision repair (NER), which works by removing bulky adducts and repairing of DNA damage produced by environmental agents, such as ultraviolet light, (368). ERCC6 gene mutation can reduce its activity, thereby leading to defects in NER repair of damage DNA. Yadav et al. found ERCC6 to be more frequently mutated in PCa of African-American populations (352).

ARHGAP21 belong to RhoGAP protein family which, play major role in conversion of Rho-GTPases from an active to inactive bound state (369,370). Rho family GTPases are involved in regulation of several cell functions, such as cell adhesion, migration, proliferation, and survival (371). ARHGAP21 play major function in cell-cell interaction, vesicular trafficking of Golgi membranes, and cardiac stress (369,372,373). Studies have reported ARHGAP21 has negative regulator of cancer cell growth, migration, and invasion (374–376). A low expression of ARHGAP21 have been shown to correspond with worse prognosis in prostate, lung, ovarian, and colon cancer (376–379). Xu et al. reported the diagnostic potential of ARHGAP21 gene in African American PCa patients (354). ADAMTSL3 is one of the superfamilies of cell surface associated glycoproteins comprising of nineteen ADAMTS proteases and seven ADAMTS-like (ADAMTSL) proteins (380). ADAMTS proteases play major function in biological processes including, procollagen maturation, connective tissue assembly, angiogenesis, and cancer (381–383). ADAMTSL proteins do not directly participate in proteolytic activity, they are majorly involved in regulation of ADAMTS activity and assembly of extracellular matrices

(380,384,385). The proliferative role of ADAMTSL3 has been described in different human cancers (386–388). Koo et al. described the expression of ADAMTSL3 in PCa (388). Xu et al. revealed the potential of ADAMTSL3 in the diagnosis of PCa in African populations (354).

PCa is the leading cause of cancer related death in Africa. Factors that contribute to high mortality of PCa in Africa include late diagnosis of the cancer among African men. Also, the aggressive nature of PCa among men in Africa make early diagnosis of the cancer imperative. PSA has long been the main biomarker for diagnosis and prognosis of PCa. However, PSA has low specificity and sensitivity for PCa has it been more organ specific than disease specific. Screening with PSA has led to early identification, overdiagnosis, and overtreatment of PCa (5–7) making a need for new biomarkers that is more sensitive and specific highly important. Previous studies including studies done among African populations have shown the potential role of cfDNA concentration and DNA integrity as diagnostic and prognostic biomarker for PCa, which are consistent with our findings. Our findings on the genetic profiling of cfDNA in South African patients help to contribute to the possibility of finding genetic mutation specific to African populations known for aggressive PCa disease. This will largely help in developing a population specific biomarker in the diagnosis PCa in South African populations. Our study also gave support to earlier postulation made that the combination of PSA and cfDNA will serve as more specific and sensitive biomarkers in the diagnosis of PCa.

In conclusion our study contributed to existing knowledge on the potential use of cfDNA as biomarker for diagnosis of PCa in South African populations.

Chapter 5: General Discussion and Conclusion

5.1 General Discussion

PCa is the most common cause of cancer death among African men (3). Factors such as poor healthcare, late presentation and the aggressive nature of PCa in black men are responsible for high mortality rate of PCa in Africa (389,390). Histopathological examination of tissue biopsy remains the gold standard for diagnosing PCa (391). However, tissue biopsy is known to be invasive and associated with surgical complications (392). This makes it imperative for studies to be done in search of a less invasive liquid biopsy in the diagnosis of PCa, especially in African men known to have more aggressive disease.

Our previous review paper highlighted the prospect and challenges facing the use of liquid biopsy in Africa (393). We discussed the lack of data verifying the efficacy of FDA approved PCa liquid biopsy assays in African populations (393). This is important due to the varying genetic landscape of different population groups (394). This makes it important for more research to be done in quest for more specific diagnostic biomarkers in the management of PCa in African populations.

Exosome cargoes and cfDNA are two major biological molecules that are largely explored as liquid biopsy markers for PCa. However, African based studies on exosomes and cfDNA in the diagnosis, prognosis, and treatment monitoring of PCa are limited, hence, the need for this study. This dissertation characterized cfDNA and exosomal miRNA in the South African population.

Our study investigated exosome morphology in South African populations using transmission electron microscope. PCa patients showed significantly higher levels of plasma exosomes than BPH in the 16nm and 28nm exosome size groups. This is consistent with an earlier study reporting higher concentration plasma exosomes in PCa than BPH (318). These findings will encourage more exosome-based studies on potential opportunities in maximizing exosome morphology as biomarkers for PCa diagnosis either alone or in combination with other biomarkers.

In the exosomal miRNA analysis, we found that the correlation of the expression ratio of miRNA16 and miRNA194 with disease severity was able to differentiate between high and low Gleason's score PCa. These findings from an African population known to have more aggressive PCa is very important. This may result in development of aggressive PCa diagnostic biomarkers, which will further help in prompt and better disease management.

One major limitation of our exosomal miRNA study is the small number of samples sequenced. Although, we tried to mitigate this limitation by validating the miRNAs found in more PCa and BPH samples using real-time PCR, a larger number of samples will be required to be sequenced to ascertain these findings.

PSA remains the most used biomarker in the diagnosis and treatment monitoring of PCa. However, it is limited due to its low specificity in the diagnosis of PCa leading to overdiagnosis. A combination of other biomarker with PSA that improves its specificity in PCa diagnosis will be of great help in the management of PCa. We characterized cfDNA in PCa patients from South Africa. We found a significant positive relationship between cfDNA concentration and PSA. The potential combination of cfDNA level and PSA in improving the specificity of diagnosis of PCa was earlier proposed by Gordian et al. (348). Our findings help to give credence to this assertion.

Our study is the first African study to perform a whole exome sequencing of urinary cfDNA. We found 31 significantly mutated genes between PCa and BPH samples. We reported for the first time an association between 27 of these genes and PCa in an African population. Four of the genes have earlier been described among PCa patients of African origin previously (352,354). These findings are important because it contribute to existing knowledge in the search of less invasive diagnostic and prognostic PCa biomarkers specific for African populations.

A major limitation of our cfDNA study is the small number of urinary cfDNA sequenced. It will also be valuable if we performed whole exome sequencing of plasma cfDNA samples from same patients to compare if there are possible differences in the mutated gene found. This will help to mitigate the lack of reference genome for African populations which is a major limitation in our study.

5.2 Conclusion

In conclusion, our study found the potential uses of cfDNA and exosomes in diagnosis and prognosis of PCa in South African populations. Our findings could potentially contribute to the development of personalized therapy for the management of PCa among African populations.

References

1. Ferlay J, Colombet M, Soerjomataram I, Parkin DM, Piñeros M, Znaor A, et al. Cancer statistics for the year 2020: An overview. Int J Cancer. 2021;149(4):778–89.

2. Rebbeck TR, Devesa SS, Chang B-L, Bunker CH, Cheng I, Cooney K, et al. Global Patterns of Prostate Cancer Incidence, Aggressiveness, and Mortality in Men of African Descent. Prostate Cancer. 2013;2013:1–12.

3. Sung H, Ferlay J, Siegel RL, Laversanne M, Soerjomataram I, Jemal A, et al. Global Cancer Statistics 2020: GLOBOCAN Estimates of Incidence and Mortality Worldwide for 36 Cancers in 185 Countries. CA Cancer J Clin. 2021 May 1;71(3):209–49.

4. Roth GA, Abate D, Abate KH, Abay SM, Abbafati C, Abbasi N, et al. Global, regional, and national age-sex-specific mortality for 282 causes of death in 195 countries and territories, 1980–2017: a systematic analysis for the Global Burden of Disease Study 2017. Lancet. 2018;392(10159):1736–88.

5. United Nations. World Population Prospects 2019: Methodology of the United Nations population estimates and projections. Departmenr Econ Soc Aff Popul Div. 2019;61.

6. Parkin DM, Bray F, Ferlay J, Jemal A. Cancer in Africa 2012. Cancer Epidemiol Biomarkers Prev. 2014;23(6):953–66.

7. Chen Z, Xu L, Shi W, Zeng F, Zhuo R, Hao X, et al. Trends of female and male breast cancer incidence at the global, regional, and national levels, 1990–2017. Breast Cancer Res Treat. 2020;180(2):481–90.

8. Hamdi Y, Abdeljaoued-Tej I, Zatchi AA, Abdelhak S, Boubaker S, Brown JS, et al. Cancer in Africa: The Untold Story. Front Oncol. 2021;11:650117.

9. Pisu M, Henrikson NB, Banegas MP, Yabroff KR. Costs of cancer along the care continuum: What we can expect based on recent literature. Vol. 124, Cancer. 2018. p. 4181–91.

10. Mariotto AB, Robin Yabroff K, Shao Y, Feuer EJ, Brown ML. Projections of the cost of cancer care in the United States: 2010-2020. J Natl Cancer Inst. 2011;103(2):117–28.

11. Sartorius K, Sartorius B, Govender PS, Sharma V, Sheriff A. The future cost of cancer in South Africa: An interdisciplinary cost management strategy. Vol. 106, South African

Medical Journal. 2016. p. 949–50.

12. Cassell A, Yunusa B, Jalloh M, Ndoye M, Mbodji MM, Diallo A, et al. Management of Advanced and Metastatic Prostate Cancer: A Need for a Sub-Saharan Guideline. Vol. 2019, Journal of Oncology. 2019. p. 1785428.

13. Adeloye D, David RA, Aderemi AV, Iseolorunkanmi A, Oyedokun A, Iweala EEJ, et al. An estimate of the incidence of prostate cancer in Africa: A systematic review and meta-analysis. PLoS One. 2016 Apr 1;11(4).

14. Sonnenschein C, Soto AM. Theories of carcinogenesis: An emerging perspective. Vol. 18, Seminars in Cancer Biology. 2008. p. 372–7.

15. Kwasniewski W, Stupak A, Kotarski J, Gozdzicak-Jozefiak A. Chaos and cancers. Theories concerning carcinogenesis. Ginekol Pol. 2021;92(4):318–21.

16. Hodgson S. Mechanisms of inherited cancer susceptibility. Vol. 9, Journal of Zhejiang University: Science B. 2008. p. 1–4.

17. Hanahan D, Weinberg RA. The hallmarks of cancer. Vol. 100, Cell. 2000. p. 57–70.

18. Hanahan D, Weinberg RA. Hallmarks of cancer: The next generation. Vol. 144, Cell. 2011. p. 646–74.

19. Hanahan D. Hallmarks of Cancer: New Dimensions. Vol. 12, Cancer Discovery. 2022. p. 31–46.

20. Wogan GN, Hecht SS, Felton JS, Conney AH, Loeb LA. Environmental and chemical carcinogenesis. Semin Cancer Biol. 2004;14(6):473–86.

21. Baan R, Grosse Y, Straif K, Secretan B, El Ghissassi F, Bouvard V, et al. A review of human carcinogens--Part F: chemical agents and related occupations. Vol. 10, The lancet oncology. 2009. p. 1143–4.

22. Haughian JM, Reno EM, Thorne AM, Bradford AP. Protein kinase C alpha-dependent signaling mediates endometrial cancer cell growth and tumorigenesis. Int J Cancer. 2009 Dec 1;125(11):2556–64.

23. Marker PC, Donjacour AA, Dahiya R, Cunha GR. Hormonal, cellular, and molecular control of prostatic development. Vol. 253, Developmental Biology. 2003. p. 165–74.

24. Cunha GR, Ricke W, Thomson A, Marker PC, Risbridger G, Hayward SW, et al. Hormonal, cellular, and molecular regulation of normal and neoplastic prostatic development. J Steroid Biochem Mol Biol. 2004;92(4):221–36.

25. Vickman RE, Franco OE, Moline DC, Vander Griend DJ, Thumbikat P, Hayward SW. The role of the androgen receptor in prostate development and benign prostatic hyperplasia: A review. Vol. 7, Asian Journal of Urology. 2020. p. 191–202.

26. McLaughlin PW, Troyer S, Berri S, Narayana V, Meirowitz A, Roberson PL, et al. Functional anatomy of the prostate: Implications for treatment planning. Int J Radiat Oncol Biol Phys. 2005;63(2):479–91.

27. McNeal JE. The zonal anatomy of the prostate. Prostate. 1981;2(1):35–49.

28. Selman SH. The McNeal prostate: A review. Vol. 78, Urology. 2011. p. 1224–8.

29. McNeal JE. Anatomy of the prostate and morphogenesis of BPH. Vol. 145, Progress in clinical and biological research. 1984. p. 27–53.

30. Adler D, Lindstrot A, Ellinger J, Rogenhofer S, Buettner R, Perner S, et al. The peripheral zone of the prostate is more prone to tumor development than the transitional zone: Is the ETS family the key? Mol Med Rep. 2012;5(2):313–6.

31. Van Der Heul-Nieuwenhuijsen L, Hendriksen PJM, Van Der Kwast TH, Jenster G. Gene expression profiling of the human prostate zones. BJU Int. 2006;98(4):886–97.

32. Chughtai B, Forde JC, Thomas DDM, Laor L, Hossack T, Woo HH, et al. Benign prostatic hyperplasia. Nat Rev Dis Prim. 2016 May 5;2(1):1–15.

33. Ronquist G, Brody I, Gottfries A, Stegmayr B. An Mg2+ and Ca2+-Stimulated Adenosine Triphosphatase in Human Prostatic Fluid - Part II. Andrologia. 1978;10(6):427–33.

34. Ronquist G, Brody I, Gottfries A, Stegmayr B. An Mg2+ and Ca2+-Stimulated Adenosine Triphosphatase in Human Prostatic Fluid: Part I. Andrologia. 1978;10(4):261–72.

35. De Marzo AM, Platz EA, Sutcliffe S, Xu J, Grönberg H, Drake CG, et al. Inflammation in prostate carcinogenesis. Vol. 7, Nature Reviews Cancer. 2007. p. 256–69.

36.   Sciarra A, Mariotti G, Salciccia S, Gomez AA, Monti S, Toscano V, et al. Prostate growth and inflammation. Vol. 108, Journal of Steroid Biochemistry and Molecular Biology. 2008. p. 254–60.

37.   Vasto S, Carruba G, Candore G, Italiano E, Di Bona D, Caruso C. Inflammation and prostate cancer. Vol. 4, Future Oncology. 2008. p. 637–45.

38.   Krieger JN, Ross SO, Deutsch L, Riley DE. The NIH consensus concept of chronic prostatitis/chronic pelvic pain syndrome compared with traditional concepts of nonbacterial prostatitis and prostatodynia. Curr Urol Rep. 2002;3(4):301–6.

39.   Homma Y, Gotoh M, Yokoyama O, Masumori N, Kawauchi A, Yamanishi T, et al. Outline of JUA clinical guidelines for benign prostatic hyperplasia. Int J Urol. 2011 Nov;18(11):741–56.

40.   Kapoor A. Benign prostatic hyperplasia (BPH) management in the primary care setting. Can J Urol. 2012;19:10–7.

41.   Ho CKM, Habib FK. Estrogen and androgen signaling in the pathogenesis of BPH. Vol. 8, Nature Reviews Urology. 2011. p. 29–41.

42.   Kim EH, Andriole GL. Prostate Cancer Review. Mo Med. 2018;115(2):131.

43.   Litwin MS, Tan HJ. The diagnosis and treatment of prostate cancer: A review. Vol. 317, JAMA - Journal of the American Medical Association. 2017. p. 2532–42.

44.   WHO. Cancer Today. Vol. 418, Cancer Today. 1984. 1–2 p.

45.   Stefan DC. Cancer Care in Africa: An Overview of Resources. J Glob Oncol. 2015 Oct 23;1(1):30–6.

46.   Gann PH. Risk Factors for Prostate Cancer. Rev Urol. 2002;4(Suppl 5):S3.

47.   Mahal BA, Gerke T, Awasthi S, Soule HR, Simons JW, Miyahira A, et al. Prostate Cancer Racial Disparities: A Systematic Review by the Prostate Cancer Foundation Panel. Vol. 5, European urology oncology. 2022. p. 18–29.

48.   Sighoko D, Oluwole O, Zheng Y, Olopade OI. Opportunities in Genetic Epidemiology in Developing Countries. In: Cancer Epidemiology. 2014. p. 57–77.

49.   Odedina FT, Akinremi TO, Chinegwundoh F, Roberts R, Yu D, Reams RR, et al.

Prostate cancer disparities in Black men of African descent: A comparative literature review of prostate cancer burden among Black men in the United States, Caribbean, United Kingdom, and West Africa. In: Infectious Agents and Cancer. 2009. p. 1–8.

50. Powell IJ. Epidemiology and Pathophysiology of Prostate Cancer in African-American Men. Vol. 177, Journal of Urology. J Urol; 2007. p. 444–9.

51. Underwood W, DeMonner S, Ubel P, Fagerlin A, Sanda MG, Wei JT. Racial/ethnic disparities in the treatment of localized/regional prostate cancer. J Urol. 2004;171(4):1504–7.

52. Schwartz K, Powell IJ, Underwood W, George J, Yee C, Banerjee M. Interplay of Race, Socioeconomic Status, and Treatment on Survival of Patients With Prostate Cancer. Urology. 2009 Dec;74(6):1296–302.

53. Blackburn J, Vecchiarelli S, Heyer EE, Patrick SM, Lyons RJ, Jaratlerdsiri W, et al. TMPRSS2-ERG fusions linked to prostate cancer racial health disparities: A focus on Africa. Prostate. 2019 May 15;79(10):1191–6.

54. Jaratlerdsiri W, Chan EKF, Gong T, Petersen DC, Kalsbeek AMF, Venter PA, et al. Whole-genome sequencing reveals elevated tumor mutational burden and initiating driver mutations in African men with treatment-naïve, high-risk prostate cancer. Cancer Res. 2018 Dec 15;78(24):6736–46.

55. Johns LE, Houlston RS. A systematic review and meta-analysis of familial prostate cancer risk. Vol. 91, BJU International. 2003. p. 789–94.

56. Kiciński M, Vangronsveld J, Nawrot TS. An epidemiological reappraisal of the familial aggregation of prostate cancer: A meta-analysis. PLoS One. 2011 Nov 4;6(10).

57. Bruner DW, Moore D, Parlanti A, Dorgan J, Engstrom P. Relative risk of prostate cancer for men with affected relatives: Systematic review and meta-analysis. Int J Cancer. 2003 Dec 10;107(5):797–803.

58. Zeegers MPA, Jellema A, Ostrer H. Empiric risk of prostate carcinoma for relatives of patients with prostate carcinoma: A meta-analysis. Cancer. 2003 Apr 15;97(8):1894–903.

59. Kral M, Rosinska V, Student V, Grepl M, Hrabec M, Bouchal J. Genetic determinants

of prostate cancer: A review. Biomed Pap. 2011;155(1):3–10.

60. Prasad S, K Srivastava S. Mutations in Cancer Driver Genes: An Insight into Prostate Cancer Progression. Ann Urol Oncol. 2019;2(2):1–7.

61. Willis MS, Wians FH. The role of nutrition in preventing prostate cancer: A review of the proposed mechanism of action of various dietary substances. Vol. 330, Clinica Chimica Acta. 2003. p. 57–83.

62. Chandler PD, Scott JB, Drake BF, Ng K, Manson JAE, Rifai N, et al. Impact of vitamin D supplementation on inflammatory markers in African Americans: Results of a four-arm, randomized, placebo-controlled trial. Cancer Prev Res. 2014;7(2):218–25.

63. Gann PH, Ma J, Giovannucci E, Willett W, Sacks FM, Hennekens CH, et al. Lower prostate cancer risk in men with elevated plasma lycopene levels: Results of a prospective analysis. Cancer Res. 1999;59(6):1225–30.

64. Cohen JH, Kristal AR, Stanford JL. Fruit and vegetable intakes and prostate cancer risk. J Natl Cancer Inst. 2000;92(1):61–8.

65. Yan L, Spitznagel EL. Soy consumption and prostate cancer risk in men: A revisit of a meta-analysis. Am J Clin Nutr. 2009;89(4):1155–63.

66. Huncharek M, Sue Haddock K, Reid R, Kupelnick B. Smoking as a risk factor for prostate cancer: A meta-analysis of 24 prospective cohort studies. Am J Public Health. 2010 Apr 1;100(4):693–701.

67. Rohrmann S, Linseisen J, Key TJ, Jensen MK, Overvad K, Johnsen NF, et al. Alcohol consumption and the risk for prostate cancer in the european prospective investigation into cancer and nutrition. Cancer Epidemiol Biomarkers Prev. 2008;17(5):1282–7.

68. Hayes RB, Brown LM, Schoenberg JB, Greenberg RS, Silverman DT, Schwartz AG, et al. Alcohol use and prostate cancer risk in US blacks and whites. Am J Epidemiol. 1996 Apr 1;143(7):692–7.

69. De Stefani E, Fierro L, Barrios E, Ronco A. Tobacco, alcohol, diet and risk of prostate cancer. Tumori. 1995 Apr 23;81(5):315–20.

70. Böcking A, Kiehn J, Heinzel-Wach M. Combined histologic grading of prostatic carcinoma. Cancer. 1982;50(2):288–94.

71.   Gleason DF. Classification of prostatic carcinomas. Cancer Chemother Rep. 1966;50(3):125–8.

72.   Gleason DF, Mellinger GT, Ardving LJ. Prediction of prognosis for prostatic adenocarcinoma by combined histological grading and clinical staging. J Urol. 1974;111(1):58–64.

73.   Epstein JI, Egevad L, Amin MB, Delahunt B, Srigley JR, Humphrey PA, et al. The 2014 international society of urological pathology (ISUP) consensus conference on gleason grading of prostatic carcinoma definition of grading patterns and proposal for a new grading system. Am J Surg Pathol. 2016;40(2):244–52.

74.   Kryvenko ON, Epstein JI. Prostate cancer grading: A decade after the 2005 modified gleason grading system. In: Archives of Pathology and Laboratory Medicine. 2016. p. 1153–6.

75.   Gobbi H, Simpson JE, Jensen RA, Coogan AC, Page DL, Pacelli A, et al. Prostatic adenocarcinoma with glomeruloid features [3] (multiple letters). Vol. 30, Human Pathology. 1999. p. 111–2.

76.   Epstein JI. Prostatic ductal adenocarcinoma: A mini review. Vol. 19, Medical Principles and Practice. 2009. p. 82–5.

77.   Gleason DF. Histologic grading of prostate cancer: A perspective. Hum Pathol. 1992;23(3):273–9.

78.   WHO Classification of Tumours of the Central Nervous System 4th Edition. World Health Organization Classification of Tumours, 4th Edition. Vol. 10, Pathology and Genetics. Tumours of the Urinary System and Male Genital Organs. IARC Press; 2007. 2005 177–9.

79.   Moch H, Humphrey PA, Ulbright TM. WHO Classification of Tumours of the Urinary System and Male Genital Organs. Fourth edition. International Agency for Research on Cancer (IARC). 2016. 2;77-133.

80.   Inamura K. Prostatic cancers: Understanding their molecular pathology and the 2016 WHO classification. Vol. 9, Oncotarget. 2018. p. 14723–37.

81.   Jewett HJ. The present status of radical prostatectomy for stages A and B prostatic

cancer. Urol Clin North Am. 1975;2(1):105–24.

82. Whitmore WF. Hormone therapy in prostatic cancer. Am J Med. 1956;21(5):697–713.

83. Chandler JR, Guillamondegui OM, Sisson GA, Strong EW, Baker HW. Clinical staging of cancer of the head and neck: A new "new" system. Am J Surg. 1976;132(4):525–8.

84. Colditz GA. American Joint Committee on Cancer. In: The SAGE Encyclopedia of Cancer and Society. 2015.

85. Oesterling JE, Rice DC, Glenski WJ, Bergstralh EJ. Effect of cystoscopy, prostate biopsy, and transurethral resection of prostate on serum prostate-specific antigen concentration. Urology. 1993;42(3):276–82.

86. Nadler RB, Humphrey PA, Smith DS, Catalona WJ, Ratliff TL. Effect of Inflammation and Benign Prostatic Hyperplasia on Elevated Serum Prostate Specific Antigen Levels. J Urol. 1995;154(2):407–13.

87. Underwood DJ, Zhang J, Denton BT, Shah ND, Inman BA. Simulation optimization of PSA-threshold based prostate cancer screening policies. Health Care Manag Sci. 2012 Dec 1;15(4):293–309.

88. Oesterling JE, Jacobsen SJ, Chute CG, Guess HA, Girman CJ, Panser LA, et al. Serum Prostate-Specific Antigen in a Community-Based Population of Healthy Men: Establishment of Age-Specific Reference Ranges. JAMA J Am Med Assoc. 1993;270(7):860–4.

89. Deantoni EP, Crawford ED, Oesterling JE, Ross CA, Berger ER, McLeod DG, et al. Age- and race-specific reference ranges for prostate-specific antigen from a large community-based study. Urology. 1996;48(2):234–9.

90. Ikuerowo S, Ajala M, Abolarinwa A, Omisanjo O. Age-specific serum prostate specific antigen ranges among apparently healthy Nigerian men without clinical evidence of prostate cancer. Niger J Surg. 2016;22(1):5.

91. Hodge KK, McNeal JE, Terris MK, Stamey TA. Random systematic versus directed ultrasound guided transrectal core biopsies of the prostate. J Urol. 1989;142(1):71–4.

92. Gestaut MM, Cai W, Vyas S, Patel BJ, Hasan SA, MunozMaldonado Y, et al. Low-Dose-Rate Brachytherapy Versus Cryotherapy in Low- and Intermediate-Risk Prostate

Cancer. Int J Radiat Oncol Biol Phys. 2017;98(1):101–7.

93. Bulut S, Aktas BK, Gokkaya CS, Akdemir AO, Erkmen AE, Karabakan M, et al. Association between pre–biopsy white blood cell count and prostate biopsy – related sepsis. Cent Eur J Urol. 2015;68(1):86–90.

94. National Comprehensive Cancer Network. NCCN clinical practice guidelines in oncology. prostate cancer: version 1.2018. www.nccn.org/professionals/physician_gls/pdf/prostate.pdf. Accessed February 17, 2018 - Bing [Internet]. [cited 2021 Feb 19]. Available from: https://www.bing.com/search?q=National+Comprehensive+Cancer+Network.+NCCN +clinical+practice+guidelines+in+oncology.+prostate+cancer%3A+version+1.2018.+ www.nccn.org%2Fprofessionals%2Fphysician_gls%2Fpdf%2Fprostate.pdf.+Accessed +February+17%2C+2018&cvid=7eb12087befe45b28e6297f417890806&pglt=547&F ORM=ANNAB1&PC=LCTS

95. Iczkowski KA, Van Leenders GJLH, Van Der Kwast TH. The 2019 International Society of Urological Pathology (ISUP) Consensus Conference on Grading of Prostatic Carcinoma. Vol. 45, American Journal of Surgical Pathology. 2021. p. 1005–7.

96. Filson CP, Marks LS, Litwin MS. Expectant management for men with early stage prostate cancer. CA Cancer J Clin. 2015 Jul 1;65(4):264–82.

97. Donnelly BJ, Saliken JC, Brasher PMA, Ernst SD, Rewcastle JC, Lau H, et al. A randomized trial of external beam radiotherapy versus cryoablation in patients with localized prostate cancer. Cancer. 2010 Jan 15;116(2):323–30.

98. Koupparis A, Gleave ME. Multimodal approaches to high-risk prostate cancer. Curr Oncol. 2010 Sep 1;17(SUPPL. 2):33–7.

99. Klein EA. Radical prostatectomy versus watchful waiting for early prostate cancer: Finally, an answer. Vol. 2, Nature Clinical Practice Urology. Nature Publishing Group; 2005. p. 412–3.

100. Bill-Axelson A, Holmberg L, Ruutu M, Garmo H, Stark JR, Busch C, et al. Re: Radical prostatectomy versus watchful waiting in early prostate cancer. Vol. 186, Journal of Urology. 2011. p. 1875.

101. Hayden AJ, Catton C, Pickles T. Radiation therapy in prostate cancer: A risk-adapted strategy. Curr Oncol. 2010;17(SUPPL. 2):18–24.

102. Law AB, McLaren DB. Non-surgical treatment for early prostate cancer. J R Coll Physicians Edinb. 2010;40(4):340–2.

103. Kaarbø M, Klokk TI, Saatcioglu F. Androgen signaling and its interactions with other signaling pathways in prostate cancer. Vol. 29, BioEssays. 2007. p. 1227–38.

104. Ramsay AK, Leung HY. Signalling pathways in prostate carcinogenesis: Potentials for molecular-targeted therapy. Vol. 117, Clinical Science. 2009. p. 209–28.

105. Morgentaler A. Testosterone and Prostate Cancer: An Historical Perspective on a Modern Myth. Vol. 50, European Urology. Elsevier; 2006. p. 935–9.

106. Aragon-Ching JB, Dahut WL. Novel androgen deprivation therapy (ADT) in the treatment of advanced prostate cancer. Vol. 7, Drug Discovery Today: Therapeutic Strategies. 2010. p. 31–5.

107. Morgentaler A. Testosterone and Prostate Cancer: An Historical Perspective on a Modern Myth. Vol. 50, European Urology. 2006. p. 935–9.

108. Saad F, Shore ND. Relugolix: a novel androgen deprivation therapy for management of patients with advanced prostate cancer. Vol. 13, Therapeutic Advances in Medical Oncology. 2021. p. 1758835921998586.

109. D'Amico A V., Chen MH, Renshaw AA, Loffredo M, Kantoff PW. Androgen suppression and radiation vs radiation alone for prostate cancer: A randomized trial. JAMA - J Am Med Assoc. 2008;299(3):289–95.

110. Jones CU, Hunt D, McGowan DG, Amin MB, Chetner MP, Bruner DW, et al. Radiotherapy and Short-Term Androgen Deprivation for Localized Prostate Cancer. N Engl J Med. 2011 Jul 14;365(2):107–18.

111. Horwitz EM, Bae K, Hanks GE, Porter A, Grignon DJ, Brereton HD, et al. Ten-year follow-up of radiation therapy oncology group protocol 92-02: A phase III trial of the duration of elective androgen deprivation in locally advanced prostate cancer. J Clin Oncol. 2008;26(15):2497–504.

112. Saad F. Re: Combined androgen deprivation therapy and radiation therapy for locally

advanced prostate cancer: A Randomised, Phase 3 Trial. Vol. 62, European Urology. 2012. p. 932–3.

113. Virgo KS, Basch E, Andrew Loblaw D, Oliver TK, Rumble RB, Carducci MA, et al. Second-line hormonal therapy for men with chemotherapy-naive, castration-resistant prostate cancer: American society of clinical oncology provisional clinical opinion. J Clin Oncol. 2017 Jun 10;35(17):1952–64.

114. Kantoff PW, Higano CS, Shore ND, Berger ER, Small EJ, Penson DF, et al. Sipuleucel-T Immunotherapy for Castration-Resistant Prostate Cancer. N Engl J Med. 2010 Jul 29;363(5):411–22.

115. Rocco B, Sighinolfi MC, Sandri M, Spandri V, Cimadamore A, Volavsek M, et al. Digital Biopsy with Fluorescence Confocal Microscope for Effective Real-time Diagnosis of Prostate Cancer: A Prospective, Comparative Study. Eur Urol Oncol. 2021 Sep 18;4(5):784–91.

116. Khan T, Altamimi MA, Hussain A, Ramzan M, Ashique S, Alhuzani MR, et al. Understanding of PSA biology, factors affecting PSA detection, challenges, various biomarkers, methods, and future perspective of prostate cancer detection and diagnosis. Adv Cancer Biol - Metastasis. 2022;5(July):100059.

117. Di Meo A, Bartlett J, Cheng Y, Pasic MD, Yousef GM. Liquid biopsy: A step forward towards precision medicine in urologic malignancies. Vol. 16, Molecular Cancer. BioMed Central Ltd.; 2017. p. 1–4.

118. Mandel P, Metais P. Les acides nucléiques du plasma sanguin chez l'homme. C R Seances Soc Biol Fil. 1948;142(3–4):241–3.

119. Leon SA, Shapiro B, Sklaroff DM, Yaros MJ. Free DNA in the Serum of Cancer Patients and the Effect of Therapy. Cancer Res. 1977;37(3):646–50.

120. Czeiger D, Shaked G, Eini H, Vered I, Belochitski O, Avriel A, et al. Measurement of circulating cell-free DNA levels by a new simple fluorescent test in patients with primary colorectal cancer. Am J Clin Pathol. 2011;135(2):264–70.

121. Umetani N, Giuliano AE, Hiramatsu SH, Amersi F, Nakagawa T, Martino S, et al. Prediction of breast tumor progression by integrity of free circulating DNA in serum. J

Clin Oncol. 2006 Sep 10;24(26):4270–6.

122. Giacona MB, Ruben GC, Iczkowski KA, Roos TB, Porter DM, Sorenson GD. Cell-free DNA in human blood plasma: Length measurements in patients with pancreatic cancer and healthy controls. Pancreas. 1998;17(1):89–97.

123. Jiang P, Chan CWM, Chan KCA, Cheng SH, Wong J, Wong VWS, et al. Lengthening and shortening of plasma DNA in hepatocellular carcinoma patients. Proc Natl Acad Sci U S A. 2015;112(11):E1317–25.

124. Snyder MW, Kircher M, Hill AJ, Daza RM, Shendure J. Cell-free DNA comprises an in vivo nucleosome footprint that informs its tissues-of-origin. Vol. 100, Transplantation. 2016. p. 698.

125. Jahr S, Hentze H, Englisch S, Hardt D, Fackelmayer FO, Hesch RD, et al. DNA fragments in the blood plasma of cancer patients: Quantitations and evidence for their origin from apoptotic and necrotic cells. Cancer Res. 2001;61(4):1659–65.

126. Stroun M, Maurice P, Vasioukhin V, Lyautey J, Lederrey C, Lefort F, et al. The origin and mechanism of circulating DNA. In: Annals of the New York Academy of Sciences. 2000. p. 161–8.

127. Stroun M, Lyautey J, Lederrey C, Olson-Sand A, Anker P. About the possible origin and mechanism of circulating DNA: Apoptosis and active DNA release. In: Clinica Chimica Acta. 2001. p. 139–42.

128. Canzoniero JVL, Park BH. Use of cell free DNA in breast oncology. Vol. 1865, Biochimica et Biophysica Acta - Reviews on Cancer. 2016. p. 266–74.

129. Stötzer OJ, Lehner J, Fersching-Gierlich D, Nagel D, Holdenrieder S. Diagnostic relevance of plasma DNA and DNA integrity for breast cancer. Tumor Biol. 2014;35(2):1183–91.

130. Lui YYN, Chik KW, Chiu RWK, Ho CY, Lam CWK, Lo YMD. Predominant hematopoietic origin of cell-free dna in plasma and serum after sex-mismatched bone marrow transplantation. Clin Chem. 2002;48(3):421–7.

131. Schwarzenbach H, Hoon DSB, Pantel K. Cell-free nucleic acids as biomarkers in cancer patients. Vol. 11, Nature Reviews Cancer. 2011. p. 426–37.

132. Wang BG, Huang HY, Chen YC, Bristow RE, Kassauei K, Cheng CC, et al. Increased plasma DNA integrity in cancer patients. Cancer Res. 2003;63(14):3966–8.

133. Cheng F, Su L, Qian C. Circulating tumor DNA: A promising biomarker in the liquid biopsy of cancer. Vol. 7, Oncotarget. 2016. p. 48832–41.

134. Husain H, Nykin D, Bui N, Quan D, Gomez G, Woodward B, et al. Cell-free DNA from ascites and pleural effusions: Molecular insights into genomic aberrations and disease biology. Mol Cancer Ther. 2017;16(5):948–55.

135. Wang JY, Hsieh JS, Chang MY, Huang TJ, Chen FM, Cheng TL, et al. Molecular detection of APC, K-ras, and p53 mutations in the serum of colorectal cancer patients as circulating biomarkers. World J Surg. 2004;28(7):721–6.

136. Stroun M, Anker P, Maurice P, Lyautey J, Lederrey C, Beljanski M. Neoplastic characteristics of the DNA found in the plasma of cancer patients. Oncology. 1989;46(5):318–22.

137. Zhang H, Liu R, Yan C, Liu L, Tong Z, Jiang W, et al. Advantage of Next-Generation Sequencing in Dynamic Monitoring of Circulating Tumor DNA over Droplet Digital PCR in Cetuximab Treated Colorectal Cancer Patients. Transl Oncol. 2019 Mar 1;12(3):426–31.

138. Wyatt AW, Annala M, Aggarwal R, Beja K, Feng F, Youngren J, et al. Concordance of Circulating Tumor DNA and Matched Metastatic Tissue Biopsy in Prostate Cancer. J Natl Cancer Inst. 2017;109(12):djx118.

139. Hennigan ST, Trostel SY, Terrigino NT, Voznesensky OS, Schaefer RJ, Whitlock NC, et al. Low Abundance of Circulating Tumor DNA in Localized Prostate Cancer. JCO Precis Oncol. 2019;(3):1–13.

140. Snyder MW, Kircher M, Hill AJ, Daza RM, Shendure J. Cell-free DNA Comprises an in Vivo Nucleosome Footprint that Informs Its Tissues-Of-Origin. Cell. 2016 Jan 14;164(1–2):57–68.

141. Ulz P, Perakis S, Zhou Q, Moser T, Belic J, Lazzeri I, et al. Inference of transcription factor binding from cell-free DNA enables tumor subtype prediction and early detection. Nat Commun. 2019;10(1):1–11.

142. Chen G, Jia G, Chao F, Xie F, Zhang Y, Hou C, et al. Urine- and Blood-Based Molecular Profiling of Human Prostate Cancer. Front Oncol. 2022;12:759791.

143. Mayrhofer M, De Laere B, Whitington T, Van Oyen P, Ghysel C, Ampe J, et al. Cell-free DNA profiling of metastatic prostate cancer reveals microsatellite instability, structural rearrangements and clonal hematopoiesis. Genome Med. 2018;10(1):85.

144. Malapelle U, Sirera R, Jantus-Lewintre E, Reclusa P, Calabuig-Fariñas S, Blasco A, et al. Profile of the Roche cobas® EGFR mutation test v2 for non-small cell lung cancer. Expert Rev Mol Diagn. 2017 Mar 4;17(3):209–15.

145. Potter NT, Hurban P, White MN, Whitlock KD, Lofton-Day CE, Tetzner R, et al. Validation of a real-time PCR-based qualitative assay for the detection of methylated SEPT9 DNA in human plasma. Clin Chem. 2014;60(9):1183–91.

146. Ou S-HI, Nagasaka M, Zhu VW. Liquid Biopsy to Identify Actionable Genomic Alterations. Am Soc Clin Oncol Educ B. 2018 May;(38):978–97.

147. Fernando MR, Jiang C, Krzyzanowski GD, Ryan WL. New evidence that a large proportion of human blood plasma cell-free DNA is localized in exosomes. PLoS One. 2017 Aug 1;12(8):e0183915.

148. Zaborowski MP, Balaj L, Breakefield XO, Lai CP. Extracellular Vesicles: Composition, Biological Relevance, and Methods of Study. Vol. 65, BioScience. Bioscience; 2015. p. 783–97.

149. Borges FT, Reis LA, Schor N. Extracellular vesicles: Structure, function, and potential clinical uses in renal diseases. Vol. 46, Brazilian Journal of Medical and Biological Research. Braz J Med Biol Res; 2013. p. 824–30.

150. Raposo G, Stoorvogel W. Extracellular vesicles: Exosomes, microvesicles, and friends. Vol. 200, Journal of Cell Biology. 2013. p. 373–83.

151. Johnstone RM, Adam M, Hammond JR, Orr L, Turbide C. Vesicle formation during reticulocyte maturation. Association of plasma membrane activities with released vesicles (exosomes). J Biol Chem. 1987;262(19):9412–20.

152. Kalluri R, LeBleu VS. The biology, function, and biomedical applications of exosomes. Vol. 367, Science. NIH Public Access; 2020. p. eaau6977.

153. Harding C V., Heuser JE, Stahl PD. Exosomes: Looking back three decades and into the future. Vol. 201, Journal of Cell Biology. 2013. p. 485.

154. Xu R, Rai A, Chen M, Suwakulsiri W, Greening DW, Simpson RJ. Extracellular vesicles in cancer — implications for future improvements in cancer care. Vol. 15, Nature Reviews Clinical Oncology. Nature Publishing Group; 2018. p. 617–38.

155. Qin J, Xu Q. Functions and applications of exosomes. Vol. 71, Acta Poloniae Pharmaceutica - Drug Research. 2014. p. 537–43.

156. Sheridan C. Exosome cancer diagnostic reaches market. Vol. 34, Nature biotechnology. 2016. p. 359–60.

157. Vanni I, Alama A, Grossi F, Dal Bello MG, Coco S. Exosomes: a new horizon in lung cancer. Vol. 22, Drug Discovery Today. 2017. p. 927–36.

158. Witwer KW, Buzás EI, Bemis LT, Bora A, Lässer C, Lötvall J, et al. Standardization of sample collection, isolation and analysis methods in extracellular vesicle research. J Extracell Vesicles. 2013;2(1):20360.

159. Beccard IJ, Hofmann L, Schroeder JC, Ludwig S, Laban S, Brunner C, et al. Immune suppressive effects of plasma-derived exosome populations in head and neck cancer. Cancers (Basel). 2020 Jul 1;12(7):1–15.

160. Whiteside TL. Tumor-Derived Exosomes and Their Role in Cancer Progression. In: Advances in Clinical Chemistry. NIH Public Access; 2016. p. 103–41.

161. Xu R, Greening DW, Zhu HJ, Takahashi N, Simpson RJ. Extracellular vesicle isolation and characterization: Toward clinical application. Vol. 126, Journal of Clinical Investigation. American Society for Clinical Investigation; 2016. p. 1152–62.

162. Minciacchi VR, Freeman MR, Di Vizio D. Extracellular Vesicles in Cancer: Exosomes, Microvesicles and the Emerging Role of Large Oncosomes. Vol. 40, Seminars in Cell and Developmental Biology. NIH Public Access; 2015. p. 41–51.

163. Sahu R, Kaushik S, Clement CC, Cannizzo ES, Scharf B, Follenzi A, et al. Microautophagy of Cytosolic Proteins by Late Endosomes. Dev Cell. 2011 Jan 18;20(1):131–9.

164. Record M. Intercellular communication by exosomes in placenta: A possible role in cell

fusion? Placenta. 2014 May 1;35(5):297–302.

165. Dai J, Su Y, Zhong S, Cong L, Liu B, Yang J, et al. Exosomes: key players in cancer and potential therapeutic strategy. Vol. 5, Signal Transduction and Targeted Therapy. Nature Publishing Group; 2020. p. 1–10.

166. Hessvik NP, Llorente A. Current knowledge on exosome biogenesis and release. Vol. 75, Cellular and Molecular Life Sciences. Cell Mol Life Sci; 2018. p. 193–208.

167. Colombo M, Moita C, Van Niel G, Kowal J, Vigneron J, Benaroch P, et al. Analysis of ESCRT functions in exosome biogenesis, composition and secretion highlights the heterogeneity of extracellular vesicles. J Cell Sci. 2013 Dec 15;126(24):5553–65.

168. Schöneberg J, Lee IH, Iwasa JH, Hurley JH. Reverse-topology membrane scission by the ESCRT proteins. Vol. 18, Nature Reviews Molecular Cell Biology. NIH Public Access; 2016. p. 5–17.

169. Hurley JH, Hanson PI. Membrane budding and scission by the ESCRT machinery: It's all in the neck. Vol. 11, Nature Reviews Molecular Cell Biology. NIH Public Access; 2010. p. 556–66.

170. Choezom D, Gross JC. Neutral sphingomyelinase 2 controls exosome secretion by counteracting V-ATPase-mediated endosome acidification. J Cell Sci. 2022 Mar 1;135(5):jcs259324.

171. Tian X, Shen H, Li Z, Wang T, Wang S. Tumor-derived exosomes, myeloid-derived suppressor cells, and tumor microenvironment. Vol. 12, Journal of Hematology and Oncology. BioMed Central; 2019. p. 1–18.

172. Bellingham SA, Coleman BM, Hill AF. Small RNA deep sequencing reveals a distinct miRNA signature released in exosomes from prion-infected neuronal cells. Nucleic Acids Res. 2012 Nov 1;40(21):10937–49.

173. Huang X, Yuan T, Tschannen M, Sun Z, Jacob H, Du M, et al. Characterization of human plasma-derived exosomal RNAs by deep sequencing. BMC Genomics. 2013 May 10;14(1):1–14.

174. Xiao D, Ohlendorf J, Chen Y, Taylor DD, Rai SN, Waigel S, et al. Identifying mRNA, MicroRNA and Protein Profiles of Melanoma Exosomes. PLoS One. 2012 Oct

9;7(10):e46874.

175. Kosaka N, Iguchi H, Yoshioka Y, Takeshita F, Matsuki Y, Ochiya T. Secretory mechanisms and intercellular transfer of microRNAs in living cells. J Biol Chem. 2010 Jun 4;285(23):17442–52.

176. Dreux M, Garaigorta U, Boyd B, Décembre E, Chung J, Whitten-Bauer C, et al. Short-range exosomal transfer of viral RNA from infected cells to plasmacytoid dendritic cells triggers innate immunity. Cell Host Microbe. 2012 Oct 18;12(4):558–70.

177. H V, K E, A B, M S, JJ L, JO L. Exosome-mediated transfer of mRNAs and microRNAs is a novel mechanism of genetic exchange between cells. Nat Cell Biol. 2007 Jun;9(6):654–9.

178. Villarroya-Beltri C, Gutiérrez-Vázquez C, Sánchez-Cabo F, Pérez-Hernández D, Vázquez J, Martin-Cofreces N, et al. Sumoylated hnRNPA2B1 controls the sorting of miRNAs into exosomes through binding to specific motifs. Nat Commun. 2013;4(1):1–10.

179. Groot M, Lee H. Sorting Mechanisms for MicroRNAs into Extracellular Vesicles and Their Associated Diseases. Vol. 9, Cells. Cells; 2020. p. 1044.

180. Goldie BJ, Dun MD, Lin M, Smith ND, Verrills NM, Dayas C V., et al. Activity-associated miRNA are packaged in Map1b-enriched exosomes released from depolarized neurons. Nucleic Acids Res. 2014 Aug 18;42(14):9195–208.

181. Guduric-Fuchs J, O'Connor A, Camp B, O'Neill CL, Medina RJ, Simpson DA. Selective extracellular vesicle-mediated export of an overlapping set of microRNAs from multiple cell types. BMC Genomics. 2012 Aug 1;13(1):1–14.

182. Wei J xing, Lv L hong, Wan Y le, Cao Y, Li G lin, Lin H ming, et al. Vps4A functions as a tumor suppressor by regulating the secretion and uptake of exosomal microRNAs in human hepatoma cells. Hepatology. 2015 Apr 1;61(4):1284–94.

183. Cha DJ, Franklin JL, Dou Y, Liu Q, Higginbotham JN, Beckler MD, et al. KRAS-dependent sorting of miRNA to exosomes. Elife. 2015 Jul 1;4(JULY 2015):e07197.

184. Gibbings DJ, Ciaudo C, Erhardt M, Voinnet O. Multivesicular bodies associate with components of miRNA effector complexes and modulate miRNA activity. Nat Cell

Biol. 2009;11(9):1143–9.

185. Koppers-Lalic D, Hackenberg M, Bijnsdorp I V., van Eijndhoven MAJ, Sadek P, Sie D, et al. Nontemplated nucleotide additions distinguish the small RNA composition in cells from exosomes. Cell Rep. 2014 Sep 25;8(6):1649–58.

186. Rahbarghazi R, Jabbari N, Sani NA, Asghari R, Salimi L, Kalashani SA, et al. Tumor-derived extracellular vesicles: Reliable tools for Cancer diagnosis and clinical applications. Vol. 17, Cell Communication and Signaling. Cell Commun Signal; 2019. p. 1–17.

187. Liu Y, Luo F, Wang B, Li H, Xu Y, Liu X, et al. STAT3-regulated exosomal miR-21 promotes angiogenesis and is involved in neoplastic processes of transformed human bronchial epithelial cells. Cancer Lett. 2016 Jan 1;370(1):125–35.

188. Fang JH, Zhang ZJ, Shang LR, Luo YW, Lin YF, Yuan Y, et al. Hepatoma cell-secreted exosomal microRNA-103 increases vascular permeability and promotes metastasis by targeting junction proteins. Hepatology. 2018 Oct 1;68(4):1459–75.

189. Hsu YL, Hung JY, Chang WA, Lin YS, Pan YC, Tsai PH, et al. Hypoxic lung cancer-secreted exosomal MIR-23a increased angiogenesis and vascular permeability by targeting prolyl hydroxylase and tight junction protein ZO-1. Oncogene. 2017 Aug 24;36(34):4929–42.

190. Le MTN, Hamar P, Guo C, Basar E, Perdigão-Henriques R, Balaj L, et al. MiR-200-containing extracellular vesicles promote breast cancer cell metastasis. J Clin Invest. 2014 Dec 1;124(12):5109–28.

191. Xu Y, Qin S, An T, Tang Y, Huang Y, Zheng L. MiR-145 detection in urinary extracellular vesicles increase diagnostic efficiency of prostate cancer based on hydrostatic filtration dialysis method. Prostate. 2017;77(10):1167–75.

192. Foj L, Ferrer F, Serra M, Arévalo A, Gavagnach M, Giménez N, et al. Exosomal and Non-Exosomal Urinary miRNAs in Prostate Cancer Detection and Prognosis. Prostate. 2017;77(6):573–83.

193. Suer I, Guzel E, Karatas OF, Creighton CJ, Ittmann M, Ozen M. MicroRNAs as prognostic markers in prostate cancer. Prostate. 2019 Feb 1;79(3):265–71.

194. Dallavalle C, Albino D, Civenni G, Merulla J, Ostano P, Mello-Grand M, et al. MicroRNA-424 impairs ubiquitination to activate STAT3 and promote prostate tumor progression. J Clin Invest. 2016 Dec 1;126(12):4585–602.

195. Albino D, Falcione M, Uboldi V, Temilola DO, Sandrini G, Merulla J, et al. Circulating extracellular vesicles release oncogenic miR-424 in experimental models and patients with aggressive prostate cancer. Commun Biol. 2021 Jan 26;4(1):1–13.

196. Huang X, Yuan T, Liang M, Du M, Xia S, Dittmar R, et al. Exosomal miR-1290 and miR-375 as prognostic markers in castration-resistant prostate cancer. Eur Urol. 2015;67(1):33–41.

197. Che Y, Shi X, Shi Y, Jiang X, Ai Q, Shi Y, et al. Exosomes Derived from miR-143-Overexpressing MSCs Inhibit Cell Migration and Invasion in Human Prostate Cancer by Downregulating TFF3. Mol Ther - Nucleic Acids. 2019;18:232–44.

198. Milane L, Singh A, Mattheolabakis G, Suresh M, Amiji MM. Exosome mediated communication within the tumor microenvironment. Vol. 219, Journal of Controlled Release. 2015. p. 278–94.

199. Kossinova OA, Gopanenko A V., Tamkovich SN, Krasheninina OA, Tupikin AE, Kiseleva E, et al. Cytosolic YB-1 and NSUN2 are the only proteins recognizing specific motifs present in mRNAs enriched in exosomes. Biochim Biophys Acta - Proteins Proteomics. 2017;1865(6):664–73.

200. Wei Z, Batagov AO, Schinelli S, Wang J, Wang Y, El Fatimy R, et al. Coding and noncoding landscape of extracellular RNA released by human glioma stem cells. Nat Commun. 2017;8(1):1–15.

201. Rodríguez M, Bajo-Santos C, Hessvik NP, Lorenz S, Fromm B, Berge V, et al. Identification of non-invasive miRNAs biomarkers for prostate cancer by deep sequencing analysis of urinary exosomes. Vol. 16, Molecular Cancer. 2017. p. 1–6.

202. Hendriks RJ, Dijkstra S, Jannink SA, Steffens MG, Van Oort IM, Mulders PFA, et al. Comparative analysis of prostate cancer specific biomarkers PCA3 and ERG in whole urine, urinary sediments and exosomes. Clin Chem Lab Med. 2016;54(3):483–92.

203. Xu H, Dong X, Chen Y, Wang X. Serum exosomal hnRNPH1 mRNA as a novel marker

for hepatocellular carcinoma. Clin Chem Lab Med. 2018;56(3):479–84.

204. Goldvaser H, Gutkin A, Beery E, Edel Y, Nordenberg J, Wolach O, et al. Characterisation of blood-derived exosomal hTERT mRNA secretion in cancer patients: A potential pan-cancer marker. Br J Cancer. 2017;117(3):353–7.

205. Ji J, Chen R, Zhao L, Xu Y, Cao Z, Xu H, et al. Circulating exosomal mRNA profiling identifies novel signatures for the detection of prostate cancer. Vol. 20, Molecular Cancer. 2021. p. 1–6.

206. McKiernan J, Donovan MJ, O'Neill V, Bentink S, Noerholm M, Belzer S, et al. A novel urine exosome gene expression assay to predict high-grade prostate cancer at initial biopsy. JAMA Oncol. 2016;2(7):882–9.

207. Gan J, Zeng X, Wang X, Wu Y, Lei P, Wang Z, et al. Effective Diagnosis of Prostate Cancer Based on mRNAs From Urinary Exosomes. Front Med. 2022;9:736110.

208. Zhou B, Xu K, Zheng X, Chen T, Wang J, Song Y, et al. Application of exosomes as liquid biopsy in clinical diagnosis. Vol. 5, Signal Transduction and Targeted Therapy. 2020. p. 1–14.

209. Li W, Li C, Zhou T, Liu X, Liu X, Li X, et al. Role of exosomal proteins in cancer diagnosis. Vol. 16, Molecular Cancer. 2017. p. 1–12.

210. Jeppesen DK, Fenix AM, Franklin JL, Higginbotham JN, Zhang Q, Zimmerman LJ, et al. Reassessment of Exosome Composition. Cell. 2019;177(2):428-445.e18.

211. Lötvall J, Hill AF, Hochberg F, Buzás EI, Vizio D Di, Gardiner C, et al. Minimal experimental requirements for definition of extracellular vesicles and their functions: A position statement from the International Society for Extracellular Vesicles. Vol. 3, Journal of Extracellular Vesicles. 2014. p. 26913.

212. Dhondt B, Geeurickx E, Tulkens J, Van Deun J, Vergauwen G, Lippens L, et al. Unravelling the proteomic landscape of extracellular vesicles in prostate cancer by density-based fractionation of urine. J Extracell Vesicles. 2020;9(1):1736935.

213. Panigrahi GK, Praharaj PP, Kittaka H, Mridha AR, Black OM, Singh R, et al. Exosome proteomic analyses identify inflammatory phenotype and novel biomarkers in African American prostate cancer patients. Cancer Med. 2019;8(3):1110–23.

214. Fujita K, Kume H, Matsuzaki K, Kawashima A, Ujike T, Nagahara A, et al. Proteomic analysis of urinary extracellular vesicles from high Gleason score prostate cancer. Sci Rep. 2017;7(1):1–9.

215. Kharaziha P, Chioureas D, Rutishauser D, Baltatzis G, Lennartsson L, Fonseca P, et al. Molecular profiling of prostate cancer derived exosomes may reveal a predictive signature for response to docetaxel. Oncotarget. 2015;6(25):21740–54.

216. Nilsson J, Skog J, Nordstrand A, Baranov V, Mincheva-Nilsson L, Breakefield XO, et al. Prostate cancer-derived urine exosomes: A novel approach to biomarkers for prostate cancer. Br J Cancer. 2009;100(10):1603–7.

217. Sequeiros T, Rigau M, Chiva C, Montes M, Garcia-Grau I, Garcia M, et al. Targeted proteomics in urinary extracellular vesicles identifies biomarkers for diagnosis and prognosis of prostate cancer. Oncotarget. 2017;8(3):4960–76.

218. Khan S, Simpson J, Lynch JC, Turay D, Mirshahidi S, Gonda A, et al. Racial differences in the expression of inhibitors of apoptosis (IAP) proteins in extracellular vesicles (EV) from prostate cancer patients. PLoS One. 2017;12(10):e0183122.

219. Khan S, Jutzy JMS, Valenzuela MMA, Turay D, Aspe JR, Ashok A, et al. Plasma-Derived Exosomal Survivin, a Plausible Biomarker for Early Detection of Prostate Cancer. PLoS One. 2012;7(10):e46737.

220. Mucci LA, Wilson KM, Giovannucci EL. Epidemiology of prostate cancer. In: Pathology and Epidemiology of Cancer. 2016. p. 107–25.

221. Filella X, Foj L. Emerging biomarkers in the detection and prognosis of prostate cancer. Vol. 53, Clinical Chemistry and Laboratory Medicine. 2015. p. 963–73.

222. Liong ML, Lim CR, Yang H, Chao S, Bong CW, Leong WS, et al. Blood-Based Biomarkers of Aggressive Prostate Cancer. PLoS One. 2012 Sep 28;7(9):e45802.

223. Carlson R V, Boyd KM, Webb DJ. The revision of the Declaration of Helsinki: Past, present and future. Vol. 57, British Journal of Clinical Pharmacology. 2004. p. 695–713.

224. Williams JR. The Declaration of Helsinki and public health. Vol. 86, Bulletin of the World Health Organization. 2008. p. 650–2.

225. World Medical Association declaration of Helsinki: Ethical principles for medical

research involving human subjects. Vol. 310, JAMA - Journal of the American Medical Association. 2013. p. 2191–4.

226. Sumrin A, Moazzam S, Khan AA, Ramzan I, Batool Z, Kaleem S, et al. Exosomes as biomarker of cancer. Brazilian Arch Biol Technol. 2018;61.

227. Taylor DD, Shah S. Methods of isolating extracellular vesicles impact down-stream analyses of their cargoes. Vol. 87, Methods. 2015. p. 3–10.

228. Chen J, Li P, Zhang T, Xu Z, Huang X, Wang R, et al. Review on Strategies and Technologies for Exosome Isolation and Purification. Vol. 9, Frontiers in Bioengineering and Biotechnology. 2022. p. 811971.

229. Helwa I, Cai J, Drewry MD, Zimmerman A, Dinkins MB, Khaled ML, et al. A comparative study of serum exosome isolation using differential ultracentrifugation and three commercial reagents. PLoS One. 2017;12(1):e0170628.

230. Martins TS, Catita J, Rosa IM, Da Cruz e Silva OAB, Henriques AG. Exosome isolation from distinct biofluids using precipitation and column-based approaches. PLoS One. 2018;13(6):e0198820.

231. Bronkhorst AJ, Ungerer V, Holdenrieder S. Comparison of methods for the isolation of cell-free DNA from cell culture supernatant. Tumor Biol. 2020 Apr 1;42(4):1010428320916314.

232. Diefenbach RJ, Lee JH, Kefford RF, Rizos H. Evaluation of commercial kits for purification of circulating free DNA. Cancer Genet. 2018 Dec 1;228–229:21–7.

233. Markus H, Contente-Cuomo T, Farooq M, Liang WS, Borad MJ, Sivakumar S, et al. Evaluation of pre-analytical factors affecting plasma DNA analysis. Sci Rep. 2018 Dec 1;8(1):1–10.

234. Sorber L, Zwaenepoel K, Deschoolmeester V, Roeyen G, Lardon F, Rolfo C, et al. A Comparison of Cell-Free DNA Isolation Kits: Isolation and Quantification of Cell-Free DNA in Plasma. J Mol Diagnostics. 2017 Jan 1;19(1):162–8.

235. van der Leest P, Boonstra PA, Elst A Ter, van Kempen LC, Tibbesma M, Koopmans J, et al. Comparison of circulating cell-free dna extraction methods for downstream analysis in cancer patients. Cancers (Basel). 2020 May 1;12(5):1222.

236. Lee EY, Lee EJ, Yoon H, Lee DH, Kim KH. Comparison of four commercial kits for isolation of urinary cell-free DNA and sample storage conditions. Diagnostics. 2020 Apr 1;10(4):234.

237. Mullis KB. The unusual origin of the polymerase chain reaction. Sci Am. 1990;262(4):56–65.

238. Saiki RK, Gelfand DH, Stoffel S, Scharf SJ, Higuchi R, Horn GT, et al. Primer-directed enzymatic amplification of DNA with a thermostable DNA polymerase. Science (80-). 1988;239(4839):487–91.

239. Holland PM, Abramson RD, Watson R, Gelfand DH. Detection of specific polymerase chain reaction product by utilizing the $5' \rightarrow 3'$ exonuclease activity of Thermus aquaticus DNA polymerase. Proc Natl Acad Sci U S A. 1991;88(16):7276–80.

240. Higuchi R, Dollinger G, Sean Walsh P, Griffith R. Simultaneous amplification and detection of specific DNA sequences. Bio/Technology. 1992;10(4):413–7.

241. Pedini P, Graiet H, Laget L, Filosa L, Chatron J, Cherouat N, et al. Qualitative and quantitative comparison of cell-free DNA and cell-free fetal DNA isolation by four (semi-)automated extraction methods: impact in two clinical applications: chimerism quantification and noninvasive prenatal diagnosis. J Transl Med. 2021;19(1):1–11.

242. Hwu HR, Roberts JW, Davidson EH, Britten RJ. Insertion and/or deletion of many repeated DNA sequences in human and higher ape evolution. Proc Natl Acad Sci U S A. 1986;83(11):3875–9.

243. Gu Z, Wang H, Nekrutenko A, Li WH. Densities, length proportions, and other distributional features of repetitive sequences in the human genome estimated from 430 megabases of genomic sequence. Gene. 2000;259(1–2):81–8.

244. Fertig EJ, Ding J, Favorov A V., Parmigiani G, Ochs MF. CoGAPS: An R/C++ package to identify patterns and biological process activity in transcriptomic data. Bioinformatics. 2010;26(21):2792–3.

245. Greene KL, Albertsen PC, Babaian RJ, Carter HB, Gann PH, Han M, et al. Prostate specific antigen best practice statement: 2009 update. J Urol. 2013;189(1 SUPPL):S2–11.

246. Spugnini EP, Logozzi M, Di Raimo R, Mizzoni D, Fais S. A role of tumor-released exosomes in paracrine dissemination and metastasis. Vol. 19, International Journal of Molecular Sciences. 2018. p. 3968.

247. Yáñez-Mó M, Siljander PRM, Andreu Z, Zavec AB, Borràs FE, Buzas EI, et al. Biological properties of extracellular vesicles and their physiological functions. Vol. 4, Journal of Extracellular Vesicles. 2015. p. 1–60.

248. Fais S, O'Driscoll L, Borras FE, Buzas E, Camussi G, Cappello F, et al. Evidence-Based Clinical Use of Nanoscale Extracellular Vesicles in Nanomedicine. Vol. 10, ACS Nano. 2016. p. 3886–99.

249. Camussi G, Deregibus MC, Bruno S, Cantaluppi V, Biancone L. Exosomes/microvesicles as a mechanism of cell-to-cell communication. Vol. 78, Kidney International. 2010. p. 838–48.

250. Barry OP, Praticò D, Savani RC, FitzGerald GA. Modulation of monocyte-endothelial cell interactions by platelet microparticles. J Clin Invest. 1998;102(1):136–44.

251. Logozzi M, Spugnini E, Mizzoni D, Di Raimo R, Fais S. Extracellular acidity and increased exosome release as key phenotypes of malignant tumors. Vol. 38, Cancer and Metastasis Reviews. 2019. p. 93–101.

252. Lee AH, Koh IL, Dawson MR. The role of exosome heterogeneity in epithelial ovarian cancer. Adv Cancer Biol - Metastasis. 2022;4(March):100040.

253. Lucci A, Hall CS, Lodhi AK, Bhattacharyya A, Anderson AE, Xiao L, et al. Circulating tumour cells in non-metastatic breast cancer: A prospective study. Lancet Oncol. 2012;13(7):688–95.

254. Arbelaiz A, Azkargorta M, Krawczyk M, Santos-Laso A, Lapitz A, Perugorria MJ, et al. Serum extracellular vesicles contain protein biomarkers for primary sclerosing cholangitis and cholangiocarcinoma. Hepatology. 2017;66(4):1125–43.

255. Tavoosidana G, Ronquist G, Darmanis S, Yan J, Carlsson L, Wu D, et al. Multiple recognition assay reveals prostasomes as promising plasma biomarkers for prostate cancer. Proc Natl Acad Sci U S A. 2011;108(21):8809–14.

256. Overbye A, Skotland T, Koehler CJ, Thiede B, Seierstad T, Berge V, et al. Identification

of prostate cancer biomarkers in urinary exosomes. Oncotarget. 2015;6(30):30357–76.

257. Huang X, Yuan T, Liang M, Du M, Xia S, Dittmar R, et al. Exosomal miR-1290 and miR-375 as prognostic markers in castration-resistant prostate cancer. Eur Urol. 2015;67(1):33–41.

258. Otsu N. THRESHOLD SELECTION METHOD FROM GRAY-LEVEL HISTOGRAMS. IEEE Trans Syst Man Cybern. 1979;SMC-9(1):62–6.

259. Licursi V, Conte F, Fiscon G, Paci P. MIENTURNET: An interactive web tool for microRNA-target enrichment and network-based analysis. BMC Bioinformatics. 2019;20(1):1–10.

260. Kanehisa M, Sato Y, Kawashima M, Furumichi M, Tanabe M. KEGG as a reference resource for gene and protein annotation. Nucleic Acids Res. 2016;44(D1):D457–62.

261. Robinson MD, McCarthy DJ, Smyth GK. edgeR: A Bioconductor package for differential expression analysis of digital gene expression data. Bioinformatics. 2009;26(1):139–40.

262. Vlaeminck-Guillem V. Extracellular vesicles in prostate cancer carcinogenesis, diagnosis, and management. Vol. 8, Frontiers in Oncology. 2018. p. 222.

263. Amankwah EK, Anegbe E, Park H, Pow-Sang J, Hakam A, Park JY. MiR-21, miR-221 and miR-222 expression and prostate cancer recurrence among obese and non-obese cases. Asian J Androl. 2013 Mar;15(2):226–30.

264. Li Z, Li LX, Diao YJ, Wang J, Ye Y, Hao XK. Identification of urinary exosomal mirnas for the non-invasive diagnosis of prostate cancer. Cancer Manag Res. 2021;13:25–35.

265. Logozzi M, Angelini DF, Giuliani A, Mizzoni D, Raimo R Di, Maggi M, et al. Increased plasmatic levels of psa-expressing exosomes distinguish prostate cancer patients from benign prostatic hyperplasia: A prospective study. Cancers (Basel). 2019;11(10):1449.

266. Zlotogorski-Hurvitz A, Dayan D, Chaushu G, Salo T, Vered M. Morphological and molecular features of oral fluid-derived exosomes: oral cancer patients versus healthy individuals. J Cancer Res Clin Oncol. 2016;142(1):101–10.

267. Yuana Y, Koning RI, Kuil ME, Rensen PCN, Koster AJ, Bertina RM, et al. Cryo-electron microscopy of extracellular vesicles in fresh plasma. J Extracell Vesicles.

2013;2(1):21494.

268. Gercel-Taylor C, Atay S, Tullis RH, Kesimer M, Taylor DD. Nanoparticle analysis of circulating cell-derived vesicles in ovarian cancer patients. Anal Biochem. 2012;428(1):44–53.

269. Lyu TS, Ahn Y, Im YJ, Kim SS, Lee KH, Kim J, et al. The characterization of exosomes from fibrosarcoma cell and the useful usage of Dynamic Light Scattering (DLS) for their evaluation. PLoS One. 2021;16(1 1):e0231994.

270. Cao Z, Xu Y, Guo F, Chen X, Ji J, Xu H, et al. FASN Protein Overexpression Indicates Poor Biochemical Recurrence-Free Survival in Prostate Cancer. Dis Markers. 2020;2020:3904947.

271. Moossavi M, Parsamanesh N, Bahrami A, Atkin SL, Sahebkar A. Role of the NLRP3 inflammasome in cancer. Vol. 17, Molecular Cancer. 2018. p. 1–13.

272. Chen J, Wang J, Cui X, Liu Y, Yin L, Li Y, et al. Positive nin one binding protein expression predicts poor outcome in prostate cancer. Mol Med Rep. 2015;11(4):2671–6.

273. Zhang Y, Ni J, Zhou G, Yuan J, Ren W, Shan Y, et al. Cloning, expression and characterization of the human NOB1 gene. Mol Biol Rep. 2005;32(3):185–9.

274. Lin Y, Peng S, Yu H, Teng H, Cui M. RNAi-mediated downregulation of NOB1 suppresses the growth and colony-formation ability of human ovarian cancer cells. Med Oncol. 2012;29(1):311–7.

275. Wang H, Li P, Zhao B. Knockdown of NOB1 expression by RNAi inhibits cellular proliferation and migration in human gliomas. Gene. 2013;528(2):146–53.

276. Che JP, Li W, Yan Y, Liu M, Wang GC, Li QY, et al. Expression and clinical significance of the nin one binding protein and p38 MAPK in prostate carcinoma. Int J Clin Exp Pathol. 2013;6(11):2300–11.

277. Zhang X, Zhang D, Qu F, Hong Y, Cao J, Pan X, et al. Knockdown of NOB1 expression inhibits the malignant transformation of human prostate cancer cells. Mol Cell Biochem. 2014;396(1–2):1–8.

278. Liu K, Chen HL, Gu MM, You QS. Relationship between NOB1 expression and

prognosis of resected non-small cell lung cancer. Int J Biol Markers. 2015;30(1):e43–8.

279. Liu G, Shen D, Jiao L, Sun Y. Nin one binding protein expression as a prognostic marker in prostate carcinoma. Clin Transl Oncol. 2014;16(9):843–7.

280. Kusakabe T, Maeda M, Hoshi N, Sugino T, Watanabe K, Fukuda T, et al. Fatty acid synthase is expressed mainly in adult hormone-sensitive cells or cells with high lipid metabolism and in proliferating fetal cells. J Histochem Cytochem. 2000;48(5):613–22.

281. Shurbaji MS, Kalbfleisch JH, Thurmond TS. Immunohistochemical detection of a fatty acid synthase (OA-519) as a predictor of progression of prostate cancer. Hum Pathol. 1996;27(9):917–21.

282. Rossi S, Graner E, Febbo P, Weinstein L, Bhattacharya N, Onody T, et al. Fatty acid synthase expression defines distinct molecular signatures in prostate cancer. Mol Cancer Res. 2003;1(10):707–15.

283. Carvalho MA, Zecchin KG, Seguin F, Bastos DC, Agostini M, Rangel ALCA, et al. Fatty acid synthase inhibition with Orlistat promotes apoptosis and reduces cell growth and lymph node metastasis in a mouse melanoma model. Int J Cancer. 2008;123(11):2557–65.

284. Loda M, Migita T, Ruiz S, Fornari A, Fiorentino M, Priolo C, et al. Fatty acid synthase: A metabolic enzyme and candidate oncogene in prostate cancer. J Natl Cancer Inst. 2009;101(7):519–32.

285. Shah US, Dhir R, Gollin SM, Chandran UR, Lewis D, Acquafondata M, et al. Fatty acid synthase gene overexpression and copy number gain in prostate adenocarcinoma. Hum Pathol. 2006;37(4):401–9.

286. Ashida S, Nakagawa H, Katagiri T, Furihata M, Iiizumi M, Anazawa Y, et al. Molecular features of the transition from prostatic intraepithelial neoplasia (PIN) to prostate cancer: Genome-wide gene-expression profiles of prostate cancers and PINs. Cancer Res. 2004;64(17):5963–72.

287. Razmara M, Srinivasula SM, Wang L, Poyet JL, Geddes BJ, Distefano PS, et al. CARD-8 protein, a new CARD family member that regulates caspase-1 activation and apoptosis. J Biol Chem. 2002;277(16):13952–8.

288. da Silva WC, Oshiro TM, de Sá DC, Franco DDGS, Festa Neto C, Pontillo A. Genotyping and differential expression analysis of inflammasome genes in sporadic malignant melanoma reveal novel contribution of CARD8, IL1B and IL18 in melanoma susceptibility and progression. Cancer Genet. 2016;209(10):474–80.

289. Lavender NA, Rogers EN, Yeyeodu S, Rudd J, Hu T, Zhang J, et al. Interaction among apoptosis-associated sequence variants and joint effects on aggressive prostate cancer. BMC Med Genomics. 2012;5(1):1–10.

290. Mercer WE, Avignolo C, Baserga R. Role of the p53 protein in cell proliferation as studied by microinjection of monoclonal antibodies. Mol Cell Biol. 1984;4(2):276–81.

291. Oren M. p53: the ultimate tumor suppressor gene? FASEB J. 1992;6(13):3169–76.

292. Donehower LA, Soussi T, Korkut A, Liu Y, Schultz A, Cardenas M, et al. Integrated Analysis of TP53 Gene and Pathway Alterations in The Cancer Genome Atlas. Cell Rep. 2019;28(5):1370-1384.

293. Efeyan A, Serrano M. p53: Guardian of the genome and policeman of the oncogenes. Vol. 6, Cell Cycle. 2007. p. 1006–10.

294. Lane DP. p53, guardian of the genome. Vol. 358, Nature. 1992. p. 15–6.

295. Alimirah F, Panchanathany R, Cheny J, Zhang X, Ho SM, Choubey D. Expression of androgen receptor is negatively regulated by p531. Neoplasia. 2007;9(12):1152–9.

296. Shenk JL, Fisher CJ, Chen SY, Zhou XF, Tillman K, Shemshedini L. p53 Represses Androgen-induced Transactivation of Prostate-specific Antigen by Disrupting hAR Amino- to Carboxyl-terminal Interaction. J Biol Chem. 2001;276(42):38472–9.

297. Cronauer M V., Schulz WA, Burchardt T, Ackermann R, Burchardt M. Inhibition of p53 function diminishes androgen receptor-mediated signaling in prostate cancer cell lines. Oncogene. 2004;23(20):3541–9.

298. Grignon DJ, Caplan R, Sarkar FH, Lawton CA, Hammond EH, Pilepich M V., et al. p53 status and prognosis of locally advanced prostatic adenocarcinoma: A study based on RTOG 8610. J Natl Cancer Inst. 1997;89(2):158–65.

299. Wan J, Zhang JUN, Zhang J. Expression of p53 and its mechanism in prostate cancer. Oncol Lett. 2018;16(1):378–82.

300. Toren P, Zoubeidi A. Targeting the PI3K/Akt pathway in prostate cancer: Challenges and opportunities (Review). Vol. 45, International Journal of Oncology. 2014. p. 1793–801.

301. Dubrovska A, Kim S, Salamone RJ, Walker JR, Maira SM, García-Echeverría C, et al. The role of PTEN/Akt/PI3K signaling in the maintenance and viability of prostate cancer stem-like cell populations. Proc Natl Acad Sci U S A. 2009;106(1):268–73.

302. Xin L, Teitell MA, Lawson DA, Kwon A, Mellinghoff IK, Witte ON. Progression of prostate cancer by synergy of AKT with genotropic and nongenotropic actions of the androgen receptor. Proc Natl Acad Sci U S A. 2006;103(20):7789–94.

303. Carver BS, Chapinski C, Wongvipat J, Hieronymus H, Chen Y, Chandarlapaty S, et al. Reciprocal Feedback Regulation of PI3K and Androgen Receptor Signaling in PTEN-Deficient Prostate Cancer. Cancer Cell. 2011;19(5):575–86.

304. Kaarbø M, Mikkelsen ØL, Malerød L, Qu S, Lobert VH, Akgul G, et al. PI3K-AKT-mTOR pathway is dominant over androgen receptor signaling in prostate cancer cells. Cell Oncol. 2010;32(1–2):11–27.

305. Wang Y, Kreisberg J, Ghosh P. Cross-Talk Between the Androgen Receptor and the Phosphatidylinositol 3-Kinase/Akt Pathway in Prostate Cancer. Curr Cancer Drug Targets. 2007;7(6):591–604.

306. Mulholland DJ, Tran LM, Li Y, Cai H, Morim A, Wang S, et al. Cell autonomous role of PTEN in regulating castration-resistant prostate cancer growth. Cancer Cell. 2011;19(6):792–804.

307. Wang GL, Jiang BH, Rue EA, Semenza GL. Hypoxia-inducible factor 1 is a basic-helix-loop-helix-PAS heterodimer regulated by cellular O2 tension. Proc Natl Acad Sci U S A. 1995;92(12):5510–4.

308. Semenza GL. HIF-1 and mechanisms of hypoxia sensing. Vol. 13, Current Opinion in Cell Biology. 2001. p. 167–71.

309. Tong D, Liu Q, Liu G, Yuan W, Wang L, Guo Y, et al. The hif/phf8/ar axis promotes prostate cancer progression. Oncogenesis. 2016;5(12):e283–e283.

310. Lunardi P, Beauval JB, Roumiguié M, Soulié M, Cuvillier O, Malavaud B. Mécanismes

de résistance à la castration : L'hypoxie intratumorale stimule l'expression du récepteur aux androgènes. Prog en Urol. 2016;26(3):159–67.

311. Vergis R, Corbishley CM, Norman AR, Bartlett J, Jhavar S, Borre M, et al. Intrinsic markers of tumour hypoxia and angiogenesis in localised prostate cancer and outcome of radical treatment: a retrospective analysis of two randomised radiotherapy trials and one surgical cohort study. Lancet Oncol. 2008;9(4):342–51.

312. Huang M, Du H, Zhang L, Che H, Liang C. The association of HIF-1α expression with clinicopathological significance in prostate cancer: A meta-analysis. Cancer Manag Res. 2018;10:2809–16.

313. Fernandes RC, Toubia J, Townley S, Hanson AR, Dredge BK, Pillman KA, et al. Post-transcriptional Gene Regulation by MicroRNA-194 Promotes Neuroendocrine Transdifferentiation in Prostate Cancer. Cell Rep. 2021;34(1):108585.

314. Das R, Gregory PA, Fernandes RC, Denis I, Wang Q, Townley SL, et al. MicroRNA-194 promotes prostate cancer metastasis by inhibiting SOCS2. Cancer Res. 2017;77(4):1021–34.

315. Wang F, Wang W, Lu L, Xie Y, Yan J, Chen Y, et al. MicroRNA-16-5p regulates cell survival, cell cycle and apoptosis by targeting AKT3 in prostate cancer cells. Oncol Rep. 2020;44(3):1282–92.

316. Selth LA, Townley SL, Bert AG, Stricker PD, Sutherland PD, Horvath LG, et al. Circulating microRNAs predict biochemical recurrence in prostate cancer patients. Br J Cancer. 2013;109(3):641–50.

317. Alshalalfa M, Bader GD, Bismar TA, Alhajj R. Coordinate MicroRNA-mediated regulation of protein complexes in prostate cancer. PLoS One. 2013;8(12):e84261.

318. Logozzi M, Mizzoni D, Di Raimo R, Giuliani A, Maggi M, Sciarra A, et al. Plasmatic Exosome Number and Size Distinguish Prostate Cancer Patients From Healthy Individuals: A Prospective Clinical Study. Front Oncol. 2021;11:4258.

319. Seyedolmohadessin SM, Akbari MT, Nourmohammadi Z, Basiri A, Pourmand G. Assessing the diagnostic value of plasma-free DNA in prostate cancer screening. Iran Biomed J. 2015;22(5):331–7.

320. Tavoosidana G, Ronquist G, Darmanis S, Yan J, Carlsson L, Wu D, et al. Multiple recognition assay reveals prostasomes as promising plasma biomarkers for prostate cancer. Proc Natl Acad Sci U S A [Internet]. 2011;108(21):8809–14. Available from: www.pnas.org/cgi/doi/10.1073/pnas.1019330108

321. Nair N, Camacho-Vanegas O, Rykunov D, Dashkoff M, Camacho SC, Schumacher CA, et al. Genomic Analysis of Uterine Lavage Fluid Detects Early Endometrial Cancers and Reveals a Prevalent Landscape of Driver Mutations in Women without Histopathologic Evidence of Cancer: A Prospective Cross-Sectional Study. PLoS Med. 2016;13(12):e1002206.

322. Botezatu I, Serdyuk O, Potapova G, Shelepov V, Alechina R, Molyaka Y, et al. Genetic analysis of DNA excreted in urine: A new approach for detecting specific genomic DNA sequences from cells dying in an organism. Clin Chem. 2000;46(8 I):1078–84.

323. Krimmel JD, Schmitt MW, Harrell MI, Agnew KJ, Kennedy SR, Emond MJ, et al. Ultra-deep sequencing detects ovarian cancer cells in peritoneal fluid and reveals somatic TP53 mutations in noncancerous tissues. Proc Natl Acad Sci U S A. 2016;113(21):6005–10.

324. Mithani SK, Smith IM, Zhou S, Gray A, Koch WM, Maitra A, et al. Mitochondrial resequencing arrays detect tumor-specific mutations in salivary rinses of patients with head and neck cancer. Clin Cancer Res. 2007;13(24):7335–40.

325. Breitbach S, Tug S, Helmig S, Zahn D, Kubiak T, Michal M, et al. Direct quantification of cell-free, circulating DNA from unpurified plasma. PLoS One. 2014;9(3):e87838.

326. Volik S, Alcaide M, Morin RD, Collins C. Cell-free DNA (cfDNA): Clinical significance and utility in cancer shaped by emerging technologies. Vol. 14, Molecular Cancer Research. 2016. p. 898–908.

327. Fujiwara K, Fujimoto N, Tabata M, Nishii K, Matsuo K, Hotta K, et al. Identification of epigenetic aberrant promoter methylation in serum DNA is useful for early detection of lung cancer. Clin Cancer Res. 2005;11(3):1219–25.

328. Shaw JA, Smith BM, Walsh T, Johnson S, Primrose L, Slade MJ, et al. Microsatellite alterations in plasma DNA of primary breast cancer patients. Clin Cancer Res. 2000;6(3):1119–24.

329. Chen E, Cario CL, Leong L, Lopez K, Márquez CP, Li PS, et al. Cell-Free DNA Detection of Tumor Mutations in Heterogeneous, Localized Prostate Cancer Via Targeted, Multiregion Sequencing. JCO Precis Oncol. 2021;(5):710–25.

330. Carreira S, Romanel A, Goodall J, Grist E, Ferraldeschi R, Miranda S, et al. Tumor clone dynamics in lethal prostate cancer. Sci Transl Med. 2014;6(254):254ra125-254ra125.

331. Joseph JD, Lu N, Qian J, Sensintaffar J, Shao G, Brigham D, et al. A clinically relevant androgen receptor mutation confers resistance to second-generation antiandrogens enzalutamide and ARN-509. Cancer Discov. 2013;3(9):1020–9.

332. Heitzer E, Ulz P, Belic J, Gutschi S, Quehenberger F, Fischereder K, et al. Tumor-associated copy number changes in the circulation of patients with prostate cancer identified through whole-genome sequencing. Genome Med. 2013;5(4):1–16.

333. Azad AA, Volik S V., Wyatt AW, Haegert A, Le Bihan S, Bell RH, et al. Androgen receptor gene aberrations in circulating cell-free DNA: Biomarkers of therapeutic resistance in castration-resistant prostate cancer. Clin Cancer Res. 2015;21(10):2315–24.

334. Barata PC, Reisinger R, Bilen MA, Heath EI, Nandagopal L, Swami U, et al. Differences in the tumor genomic landscape between African Americans (AA) and Caucasians (CA) advanced prostate cancer (aPC) patients (pts) by comprehensive genomic profiling (CGP) of cell-free DNA (cfDNA). J Clin Oncol. 2021;39(15_suppl):5058–5058.

335. Zimmerman R, Bilen MA, Heath EI, Nandagopal L, Swami U, Kessel A, et al. Comprehensive Genomic Profiling of Cell-Free DNA in Men With Advanced Prostate Cancer: Differences in Genomic Landscape Based on Race. Oncologist. 2022 Oct 1;27:e815–8.

336. Chen S, Huang T, Zhou Y, Han Y, Xu M, Gu J. AfterQC: Automatic filtering, trimming, error removing and quality control for fastq data. BMC Bioinformatics. 2017;18(3):91–100.

337. Li H, Durbin R. Fast and accurate long-read alignment with Burrows-Wheeler transform. Bioinformatics. 2010;26(5):589–95.

338. Koboldt DC, Zhang Q, Larson DE, Shen D, McLellan MD, Lin L, et al. VarScan 2:

Somatic mutation and copy number alteration discovery in cancer by exome sequencing. Genome Res. 2012;22(3):568–76.

339. E. C, F. DN, F. L, A. B. Liquid biopsy: Monitoring cancer-genetics in the blood. Nat Rev Clin Oncol. 2013;10(8):472–84.

340. Umetani N, Kim J, Hiramatsu S, Reber HA, Hines OJ, Bilchik AJ, et al. Increased integrity of free circulating DNA in sera of patients with colorectal or periampullary cancer: Direct quantitative PCR for ALU repeats. Clin Chem. 2006;52(6):1062–9.

341. Chudasama DY, Aladag Z, Felicien MI, Hall M, Beeson J, Asadi N, et al. Prognostic value of the DNA integrity index in patients with malignant lung tumors. Oncotarget. 2018;9(30):21281–8.

342. Pu WY, Zhang R, Xiao L, Wu YY, Gong W, Lv XD, et al. Prediction of cancer progression in a group of 73 gastric cancer patients by circulating cell-free DNA. Vol. 16, BMC Cancer. 2016. p. 1–5.

343. Umetani N, Giuliano AE, Hiramatsu SH, Amersi F, Nakagawa T, Martino S, et al. Prediction of breast tumor progression by integrity of free circulating DNA in serum. J Clin Oncol. 2006 Sep 10;24(26):4270–6.

344. Sozzi G, Conte D, Leon ME, Cirincione R, Roz L, Ratcliffe C, et al. Quantification of free circulating DNA as a diagnostic marker in lung cancer. J Clin Oncol. 2003;21(21):3902–8.

345. Yi Z, Liu B, Guan X, Ma F. Plasma cell-free DNA and survival in non-small-cell lung cancer: A meta-analysis. Mol Clin Oncol. 2017;7(2):167–72.

346. Yoon KA, Park S, Sang HL, Jin HK, Jin SL. Comparison of circulating plasma DNA levels between lung cancer patients and healthy controls. J Mol Diagnostics. 2009;11(3):182–5.

347. Liu H, Gao Y, Vafaei S, Gu X, Zhong X. The Prognostic Value of Plasma Cell-Free DNA Concentration in the Prostate Cancer: A Systematic Review and Meta-Analysis. Vol. 11, Frontiers in Oncology. 2021. p. 599602.

348. Gordian E, Ramachandran K, Reis IM, Manoharan M, Soloway MS, Singal R. Serum free circulating DNA is a useful biomarker to distinguish benign versus malignant

prostate disease. Cancer Epidemiol Biomarkers Prev. 2010;19(8):1984–91.

349. Torquato S, Pallavajjala A, Goldstein A, Valda Toro P, Silberstein JL, Lee J, et al. Genetic Alterations Detected in Cell-Free DNA Are Associated With Enzalutamide and Abiraterone Resistance in Castration-Resistant Prostate Cancer. JCO Precis Oncol. 2019;(3):1–14.

350. Woodhouse R, Li M, Hughes J, Delfosse D, Skoletsky J, Ma P, et al. Clinical and analytical validation of foundation one liquid CDx, a novel 324-Gene cfDNA-based comprehensive genomic profiling assay for cancers of solid tumor origin. PLoS One. 2020;15(9 September):e0237802.

351. Abida W, Patnaik A, Campbell D, Shapiro J, Bryce AH, McDermott R, et al. Rucaparib in Men with Metastatic Castration-Resistant Prostate Cancer Harboring a BRCA1 or BRCA2 Gene Alteration. In: Journal of Clinical Oncology. 2020. p. 3763–72.

352. Yadav S, Anbalagan M, Baddoo M, Chellamuthu VK, Mukhopadhyay S, Woods C, et al. Somatic mutations in the DNA repairome in prostate cancers in African Americans and Caucasians. Oncogene. 2020;39(21):4299–311.

353. White JA, Kaninjing E, Adeniji KA, Jibrin P, Obafunwa JO, Ogo CN, et al. Abstract 1507: Tumor only analysis of whole exome sequencing from a multi-institutional Nigerian prostate cancer cohort reveals DNA repair genes associated with African ancestry. Cancer Res. 2022;82(12_Supplement):1507–1507.

354. Xu Y, Tsai CW, Chang WS, Han Y, Huang M, Pettaway CA, et al. Epigenome-wide association study of prostate cancer in African americans identifies DNA methylation biomarkers for aggressive disease. Biomolecules. 2021;11(12):1826.

355. Tulinius H, Egilsson V, Olafsdottir G, Sigvaldason H. Risk of prostate, ovarian, and endometrial cancer among relatives of women with breast cancer. Br Med J. 1992;305(6858):855–7.

356. Castro E, Goh C, Olmos D, Saunders E, Leongamornlert D, Tymrakiewicz M, et al. Germline BRCA mutations are associated with higher risk of nodal involvement, distant metastasis, and poor survival outcomes in prostate cancer. J Clin Oncol. 2013;31(14):1748–57.

357. Castro E, Eeles R. The role of BRCA1 and BRCA2 in prostate cancer. Vol. 14, Asian Journal of Andrology. 2012. p. 409–14.

358. Boulton SJ. Cellular functions of the BRCA tumour-suppressor proteins. Vol. 34, Biochemical Society Transactions. 2006. p. 633–45.

359. Gudmundsdottir K, Ashworth A. The roles of BRCA1 and BRCA2 and associated proteins in the maintenance of genomic stability. Vol. 25, Oncogene. 2006. p. 5864–74.

360. Urbanucci A, Waltering KK, Suikki HE, Helenius MA, Visakorpi T. Androgen regulation of the androgen receptor coregulators. BMC Cancer. 2008;8(1):1–10.

361. Park JJ, Irvine RA, Buchanan G, Koh SS, Park JM, Tilley WD, et al. Breast cancer susceptibility gene 1 (BRCA1) is a coactivator of the androgen receptor. Cancer Res. 2000;60(21):5946–9.

362. Carter HB, Helfand B, Mamawala M, Wu Y, Landis P, Yu H, et al. Germline Mutations in ATM and BRCA1/2 Are Associated with Grade Reclassification in Men on Active Surveillance for Prostate Cancer(Figure presented.). Eur Urol. 2019;75(5):743–9.

363. Na R, Zheng SL, Han M, Yu H, Jiang D, Shah S, et al. Germline Mutations in ATM and BRCA1/2 Distinguish Risk for Lethal and Indolent Prostate Cancer and are Associated with Early Age at Death [figure presented]. Eur Urol. 2017;71(5):740–7.

364. Ledet EM, Burgess EF, Sokolova AO, Jaeger EB, Hatton W, Moses M, et al. Comparison of germline mutations in African American and Caucasian men with metastatic prostate cancer. Prostate. 2021;81(7):433–9.

365. Mahal BA, Alshalalfa M, Kensler KH, Chowdhury-Paulino I, Kantoff P, Mucci LA, et al. Racial Differences in Genomic Profiling of Prostate Cancer. N Engl J Med. 2020;383(11):1083–5.

366. Hanawalt PC. The bases for Cockayne syndrome. Vol. 405, Nature. 2000. p. 415–6.

367. Tuo J, Chen C, Zeng X, Christiansen M, Bohr VA. Functional crosstalk between hOgg1 and the helicase domain of Cockayne syndrome group B protein. DNA Repair (Amst). 2002;1(11):913–27.

368. Spivak G. Nucleotide excision repair in humans. Vol. 36, DNA Repair. 2015. p. 13–8.

369. Borges L, Bigarella CL, Baratti MO, Crosara-Alberto DP, Joazeiro PP, Franchini KG, et al. ARHGAP21 associates with FAK and PKCζ and is redistributed after cardiac pressure overload. Biochem Biophys Res Commun. 2008;374(4):641–6.

370. Sanchez Bassères D, Vedelago Tizzei E, Duarte AAS, Ferreira Costa F, Olalla Saad ST. ARHGAP10, a novel human gene coding for a potentially cytoskeletal Rho-GTPase activating protein. Biochem Biophys Res Commun. 2002;294(3):579–85.

371. Vega FM, Ridley AJ. Rho GTPases in cancer cell biology. Vol. 582, FEBS Letters. 2008. p. 2093–101.

372. Dubois T, Chavrier P. ARHGAP10, a novel RhoGAP at the cross-road between ARF1 and Cdc42 pathways, regulates Arp2/3 complex and actin dynamics on Golgi membranes. Vol. 21, Medecine/Sciences. 2005. p. 692–4.

373. Sousa S, Cabanes D, Archambaud C, Colland F, Lemichez E, Popoff M, et al. ARHGAP10 is necessary for α-catenin recruitment at adherens junctions and for Listeria invasion. Nat Cell Biol. 2005;7(10):954–60.

374. Barcellos KSA, Bigarella CL, Wagner M V., Vieira KP, Lazarini M, Langford PR, et al. ARHGAP21 protein, a new partner of α-tubulin involved in cell-cell adhesion formation and essential for epithelial-mesenchymal transition. J Biol Chem. 2013;288(4):2179–89.

375. Bigarella CL, Borges L, Costa FF, Saad STO. ARHGAP21 modulates FAK activity and impairs glioblastoma cell migration. Biochim Biophys Acta - Mol Cell Res. 2009;1793(5):806–16.

376. Luo N, Guo J, Chen L, Yang W, Qu X, Cheng Z. ARHGAP10, downregulated in ovarian cancer, suppresses tumorigenicity of ovarian cancer cells. Cell Death Dis. 2016;7(3):e2157-e2157.

377. Gong H, Chen XY, Jin YC, Lu JS, Cai YJ, Wei O, et al. Expression of ARHGAP10 correlates with prognosis of prostate cancer. Int J Clin Exp Pathol. 2019;12(10):3839–46.

378. Liu L, Xie D, Xie H, Huang W, Zhang J, Jin W, et al. ARHGAP10 inhibits the proliferation and metastasis of CRC cells via blocking the activity of RhoA/AKT

signaling pathway. Onco Targets Ther. 2019;12:11507–16.

379. Teng JP, Yang ZY, Zhu YM, Ni D, Zhu ZJ, Li XQ. The roles of ARHGAP10 in the proliferation, migration and invasion of lung cancer cells. Oncol Lett. 2017;14(4):4613–8.

380. Dubail J, Apte SS. Insights on ADAMTS proteases and ADAMTS-like proteins from mammalian genetics. Vols. 44–46, Matrix Biology. 2015. p. 24–37.

381. Mead TJ, Apte SS. ADAMTS proteins in human disorders. Vols. 71–72, Matrix Biology. 2018. p. 225–39.

382. Rienks M, Barallobre-Barreiro J, Mayr M. The emerging role of the ADAMTS family in vascular diseases. Vol. 123, Circulation Research. 2018. p. 1279–81.

383. Fontanil T, Mohamedi Y, Cobo T, Cal S, Obaya ÁJ. Novel associations within the tumor microenvironment: Fibulins meet ADAMTSs. Vol. 9, Frontiers in Oncology. 2019. p. 796.

384. Hubmacher D, Apte SS. ADAMTS proteins as modulators of microfibril formation and function. Vol. 47, Matrix Biology. 2015. p. 34–43.

385. Tsutsui K, Manabe RI, Yamada T, Nakano I, Oguri Y, Keene DR, et al. ADAMTSL-6 is a novel extracellular matrix protein that binds to fibrillin-1 and promotes fibrillin-1 fibril formation. J Biol Chem. 2010;285(7):4870–82.

386. Liu M, Xu Y, Zhou Y, Lang R, Shi Z, Zhao J, et al. Integrated Analyses Reveal the Multi-Omics and Prognostic Characteristics of ATP5B in Breast Cancer. Front Genet. 2021;12:652474.

387. Zhou X, Li R, Jing R, Zuo B, Zheng Q. Genome-wide CRISPR knockout screens identify ADAMTSL3 and PTEN genes as suppressors of HCC proliferation and metastasis, respectively. J Cancer Res Clin Oncol. 2020;146(6):1509–21.

388. Koo BH, Hurskainen T, Mielke K, Phyu PA, Casey G, Autio-Harmainen H, et al. ADAMTSL3/punctin-2, a gene frequently mutated in colorectal tumors, is widely expressed in normal and malignant epithelial cells, vascular endothelial cells and other cell types, and its mRNA is reduced in colon cancer. Int J Cancer. 2007;121(8):1710–6.

389. Mcginley KF, Tay KJ, Moul JW. Prostate cancer in men of African origin. Vol. 13,

Nature Reviews Urology. 2016. p. 99–107.

390. Chornokur G, Dalton K, Borysova ME, Kumar NB. Disparities at presentation, diagnosis, treatment, and survival in African American men, affected by prostate cancer. Prostate. 2011;71(9):985–97.

391. Heidenreich A. Management of prostate cancer: EAU guidelines on screening, diagnosis and treatment. In: Management of Prostate Cancer: A Multidisciplinary Approach. Springer Berlin Heidelberg; 2012. p. 299–326.

392. Efesoy O, Bozlu M, Çayan S, Akbay E. Complications of transrectal ultrasound-guided 12-core prostate biopsy: A single center experience with 2049 patients. Turk Urol Derg. 2013;39(1):6–11.

393. Temilola DO, Wium M, Coulidiati TH, Adeola HA, Carbone GM, Catapano CV, et al. The Prospect and Challenges to the Flow of Liquid Biopsy in Africa. Vol. 8, Cells. 2019. p. 862.

394. Peter BM, Petkova D, Novembre J. Genetic landscapes reveal how human genetic diversity aligns with geography. Mol Biol Evol. 2020;37(4):943–51.

Supplementary data 1: Differential expressed TCGA and exosomal miRNAs.

Differentially expressed TCGA miRNA				Differentially expressed exosomal miRNA			
	logFC	P Value	FDR		logFC	P Value	FDR
hsa-mir-483	4.43	1.14E-54	1.20E-51	hsa-miR-4485-5p	-10.78	4.85E-16	1.42E-13
hsa-mir-508	-3.44	7.42E-34	3.88E-31	hsa-miR-4485-3p	-9.37	2.53E-12	3.71E-10
hsa-mir-592	1.88	1.28E-30	4.45E-28	hsa-miR-4284	-6.98	1.18E-10	1.16E-08
hsa-mir-210	1.45	6.24E-28	1.63E-25	hsa-miR-3123	-12.21	3.72E-10	2.73E-08
hsa-mir-372	-2.94	2.77E-19	5.80E-17	hsa-miR-4484	-10.14	1.06E-09	6.21E-08
hsa-mir-514-1	-2.52	3.68E-18	6.29E-16	hsa-miR-1282	-9.6	6.58E-09	3.22E-07
hsa-mir-425	0.57	4.21E-18	6.29E-16	p-hsa-miR-146	-7.75	1.86E-08	7.45E-07
hsa-mir-1274b	-1.43	6.30E-18	7.46E-16	hsa-miR-1973	-8.87	2.03E-08	7.45E-07
hsa-mir-708	0.55	6.42E-18	7.46E-16	hsa-miR-4461	-10.42	4.70E-08	1.54E-06
hsa-mir-514-3	-2.52	9.26E-18	9.69E-16	hsa-miR-6880-3p	-8.68	1.40E-07	4.13E-06
hsa-mir-3676	-1.25	1.09E-17	1.04E-15	hsa-miR-6723-5p	-10.78	9.84E-07	2.46E-05
hsa-mir-514-2	-2.5	1.82E-17	1.59E-15	p-hsa-miR-249	-8.06	1.01E-06	2.46E-05
hsa-mir-21	0.43	3.79E-17	3.05E-15	hsa-miR-6873-3p	-5.52	1.67E-06	3.78E-05
hsa-mir-519a-1	-3.04	6.09E-17	4.55E-15	p-hsa-miR-102-1__p-hsa-miR-102-2__p-hsa-miR-102-3	-5.44	3.42E-06	7.17E-05
hsa-mir-509-2	-2.52	4.28E-16	2.99E-14	hsa-miR-5096	-4.47	4.12E-06	7.81E-05
hsa-mir-509-3	-2.55	7.67E-16	5.02E-14	hsa-miR-6830-3p	-4.63	4.25E-06	7.81E-05
hsa-mir-217	0.82	8.54E-16	5.25E-14	hsa-miR-1273g-3p	-4.14	4.52E-06	7.81E-05
hsa-mir-133b	-0.95	1.15E-15	6.69E-14	hsa-miR-6739-5p	-6.19	6.39E-06	1.04E-04
hsa-mir-222	-0.56	3.51E-15	1.87E-13	hsa-miR-4668-5p	-3.53	7.21E-06	1.12E-04
hsa-mir-506	-3.04	3.58E-15	1.87E-13	hsa-miR-4644	-5.33	9.37E-06	1.38E-04
hsa-mir-509-1	-2.41	1.26E-14	6.27E-13	hsa-miR-4454	3.5	2.35E-05	3.29E-04
hsa-mir-133a-2	-0.95	2.62E-14	1.25E-12	hsa-miR-451a	3.27	5.50E-05	7.35E-04
hsa-mir-133a-1	-0.76	2.82E-14	1.28E-12	p-hsa-miR-121	-7.93	1.12E-04	1.43E-03
hsa-mir-221	-0.55	1.55E-12	6.77E-11	hsa-miR-6510-5p	-4.47	1.21E-04	1.43E-03
hsa-mir-30e	-0.23	9.43E-12	3.94E-10	hsa-miR-877-3p	-5.88	1.22E-04	1.43E-03
hsa-mir-519a-2	-2.41	1.25E-11	5.02E-10	hsa-miR-6832-3p	-4.33	1.74E-04	1.97E-03

hsa-mir-1-2	-0.59	2.98E-11	1.16E-09	hsa-miR-33a-5p	-3.7	2.20E-04	2.40E-03
hsa-mir-30a	-0.39	6.00E-11	2.24E-09	hsa-miR-10a-5p	9.21	2.78E-04	2.92E-03
hsa-mir-522	-2.46	6.79E-11	2.45E-09	p-hsa-miR-6	-3.6	3.63E-04	3.68E-03
hsa-mir-582	-0.57	1.24E-10	4.32E-09	hsa-miR-3195	9.08	4.60E-04	4.51E-03
hsa-mir-197	0.27	1.63E-10	5.50E-09	hsa-miR-7107-5p	-4.14	6.16E-04	5.84E-03
hsa-let-7d	0.19	2.47E-10	8.07E-09	p-hsa-miR-135	-4.3	6.58E-04	5.96E-03
hsa-mir-137	1.74	2.55E-10	8.10E-09	hsa-miR-6741-3p	-6.5	6.69E-04	5.96E-03
hsa-mir-378	-0.45	5.56E-10	1.71E-08	hsa-miR-6809-3p	-4.48	7.06E-04	6.11E-03
hsa-mir-653	0.54	1.18E-09	3.54E-08	hsa-miR-6809-5p	-4.03	1.12E-03	9.44E-03
hsa-mir-516a-1	-2.18	1.51E-09	4.39E-08	p-hsa-miR-208	-3.51	1.37E-03	1.12E-02
hsa-mir-516a-2	-2.17	1.64E-09	4.64E-08	hsa-miR-20a-5p	2.64	1.43E-03	1.14E-02
hsa-mir-129-2	0.94	2.96E-09	8.16E-08	hsa-miR-139-5p	3.45	2.76E-03	2.13E-02
hsa-mir-126	0.34	7.42E-09	1.99E-07	hsa-miR-4326	-6.56	3.18E-03	2.40E-02
hsa-mir-93	0.35	9.74E-09	2.55E-07	hsa-miR-556-3p	-5.31	3.39E-03	2.49E-02
hsa-mir-301a	0.37	1.43E-08	3.64E-07	hsa-miR-483-5p	-3.82	3.58E-03	2.57E-02
hsa-mir-129-1	0.85	4.02E-08	1.00E-06	hsa-miR-4488	3.97	4.71E-03	3.29E-02
hsa-mir-589	0.25	5.18E-08	1.26E-06	p-hsa-miR-103	-2.47	4.85E-03	3.31E-02
hsa-mir-181a-1	0.25	5.39E-08	1.26E-06	hsa-miR-194-5p	3.45	5.11E-03	3.34E-02
hsa-mir-574	-0.24	5.43E-08	1.26E-06	hsa-miR-877-5p	-3.11	5.12E-03	3.34E-02
hsa-mir-139	-0.35	5.62E-08	1.28E-06	hsa-miR-144-5p	2.3	5.72E-03	3.56E-02
hsa-mir-23c	-0.9	6.69E-08	1.49E-06	hsa-miR-6126	-4.21	5.77E-03	3.56E-02
hsa-mir-216a	0.78	1.06E-07	2.30E-06	hsa-let-7i-5p	1.95	5.81E-03	3.56E-02
hsa-mir-891a	-0.67	2.28E-07	4.86E-06	hsa-miR-130a-3p	-2.08	6.77E-03	4.06E-02
hsa-mir-2115	0.95	3.12E-07	6.52E-06	hsa-miR-4668-3p	-3.77	7.09E-03	4.17E-02
hsa-mir-378c	-0.36	3.49E-07	7.15E-06	hsa-miR-107	-3.42	7.40E-03	4.26E-02
hsa-mir-503	0.56	8.25E-07	1.66E-05	p-hsa-miR-336	3.1	8.42E-03	4.72E-02
hsa-mir-125b-1	-0.24	1.05E-06	2.07E-05	hsa-miR-1273a	-3.08	8.50E-03	4.72E-02
hsa-mir-371	-1.36	1.08E-06	2.10E-05	hsa-miR-7111-3p	-3.55	9.12E-03	4.97E-02
hsa-mir-192	0.31	1.21E-06	2.30E-05	hsa-miR-450a-5p	7.94	1.08E-02	5.80E-02
hsa-mir-1301	0.35	1.60E-06	2.98E-05	hsa-miR-92a-3p	2.05	1.23E-02	6.42E-02
hsa-mir-493	0.34	1.78E-06	3.27E-05	hsa-miR-7150	8.02	1.24E-02	6.42E-02
hsa-mir-96	0.34	2.29E-06	4.12E-05	hsa-miR-424-5p	2.21	1.32E-02	6.69E-02
hsa-mir-194-2	0.24	3.31E-06	5.87E-05	hsa-miR-6865-3p	-4.91	1.46E-02	7.30E-02
hsa-mir-194-1	0.25	3.41E-06	5.95E-05	hsa-miR-532-5p	2.52	1.64E-02	8.05E-02
hsa-mir-513c	-1.22	3.61E-06	6.19E-05	hsa-miR-16-5p	1.89	1.67E-02	8.05E-02
hsa-mir-30c-2	-0.22	3.93E-06	6.63E-05	hsa-miR-221-3p	-2.08	1.83E-02	8.51E-02

hsa-mir-16-1	0.19	4.42E-06	7.34E-05	hsa-miR-326	-2.15	1.84E-02	8.51E-02
hsa-mir-3065	0.41	5.12E-06	8.36E-05	hsa-miR-93-5p	1.67	1.85E-02	8.51E-02
hsa-mir-145	-0.3	5.48E-06	8.82E-05	hsa-miR-3613-5p	-1.87	2.19E-02	9.89E-02
hsa-mir-106b	0.19	7.41E-06	1.17E-04				
hsa-mir-449a	1.06	9.37E-06	1.44E-04				
hsa-mir-18b	0.52	9.37E-06	1.44E-04				
hsa-mir-128-1	0.19	1.08E-05	1.64E-04				
hsa-mir-23b	-0.22	1.21E-05	1.81E-04				
hsa-mir-374b	-0.22	1.30E-05	1.92E-04				
hsa-mir-1258	-0.56	1.35E-05	1.96E-04				
hsa-mir-212	-0.3	1.37E-05	1.96E-04				
hsa-mir-1911	0.86	1.42E-05	1.98E-04				
hsa-mir-484	0.2	1.42E-05	1.98E-04				
hsa-mir-625	0.23	1.69E-05	2.32E-04				
hsa-mir-143	-0.36	1.83E-05	2.49E-04				
hsa-mir-339	0.23	1.95E-05	2.61E-04				
hsa-mir-29c	-0.2	2.76E-05	3.66E-04				
hsa-mir-16-2	0.35	2.83E-05	3.70E-04				
hsa-mir-1298	0.83	3.43E-05	4.43E-04				
hsa-mir-206	-1.68	3.94E-05	5.03E-04				
hsa-mir-1-1	-0.68	4.37E-05	5.51E-04				
hsa-mir-18a	0.31	5.20E-05	6.47E-04				
hsa-mir-15a	0.2	5.38E-05	6.62E-04				
hsa-mir-30d	0.2	5.89E-05	7.16E-04				
hsa-mir-576	0.26	6.32E-05	7.60E-04				
hsa-mir-345	0.29	6.47E-05	7.69E-04				
hsa-mir-191	0.21	7.10E-05	8.34E-04				
hsa-mir-10a	0.3	9.52E-05	1.11E-03				
hsa-mir-103-1	0.18	1.06E-04	1.22E-03				
hsa-mir-373	-0.93	1.16E-04	1.32E-03				
hsa-mir-1247	-0.38	1.27E-04	1.42E-03				
hsa-mir-337	0.23	1.39E-04	1.54E-03				
hsa-mir-1283-2	-1.12	1.54E-04	1.70E-03				
hsa-mir-490	-0.96	1.71E-04	1.87E-03				
hsa-mir-29a	-0.17	1.87E-04	2.02E-03				
hsa-mir-32	0.27	1.97E-04	2.10E-03				

hsa-mir-132	-0.17	2.21E-04	2.34E-03				
hsa-mir-135a-2	-0.37	2.27E-04	2.35E-03				
hsa-mir-449b	0.75	2.27E-04	2.35E-03				
hsa-mir-454	0.22	2.29E-04	2.35E-03				
hsa-mir-409	0.22	2.72E-04	2.76E-03				
hsa-mir-1224	0.7	3.15E-04	3.16E-03				
hsa-mir-516b-1	0.62	3.24E-04	3.23E-03				
hsa-mir-1283-1	-1	3.45E-04	3.41E-03				
hsa-mir-184	-0.71	3.51E-04	3.43E-03				
hsa-mir-98	0.16	3.54E-04	3.43E-03				
hsa-mir-651	0.32	3.81E-04	3.66E-03				
hsa-mir-449c	0.72	3.92E-04	3.73E-03				
hsa-mir-3200	0.44	4.12E-04	3.88E-03				
hsa-mir-125a	-0.16	4.30E-04	4.01E-03				
hsa-mir-1296	0.25	4.79E-04	4.43E-03				
hsa-mir-326	-0.33	5.26E-04	4.83E-03				
hsa-mir-28	-0.15	5.45E-04	4.96E-03				
hsa-mir-590	0.18	5.93E-04	5.32E-03				
hsa-mir-190	-0.28	5.95E-04	5.32E-03				
hsa-mir-3615	0.36	7.65E-04	6.78E-03				
hsa-mir-142	0.33	8.42E-04	7.40E-03				
hsa-mir-507	-0.72	9.69E-04	8.45E-03				
hsa-mir-940	0.48	1.00E-03	8.68E-03				
hsa-mir-199a-1	0.16	1.47E-03	1.25E-02				
hsa-mir-3614	0.47	1.47E-03	1.25E-02				
hsa-mir-3152	-0.66	1.48E-03	1.25E-02				
hsa-mir-1307	0.17	1.56E-03	1.31E-02				
hsa-mir-577	0.59	1.68E-03	1.40E-02				
hsa-mir-20b	0.29	1.81E-03	1.49E-02				
hsa-mir-296	-0.42	1.87E-03	1.53E-02				
hsa-mir-125b-2	-0.17	2.07E-03	1.67E-02				
hsa-mir-335	0.2	2.29E-03	1.84E-02				
hsa-mir-30b	0.2	2.33E-03	1.86E-02				
hsa-mir-877	0.52	2.49E-03	1.98E-02				
hsa-mir-185	0.13	2.64E-03	2.07E-02				
hsa-mir-514b	-0.57	2.85E-03	2.22E-02				

hsa-mir-1248	-0.4	2.94E-03	2.28E-02				
hsa-mir-7-3	0.54	3.05E-03	2.35E-02				
hsa-mir-505	-0.13	3.10E-03	2.37E-02				
hsa-mir-512-1	0.55	3.13E-03	2.37E-02				
hsa-mir-513a-2	-0.49	3.20E-03	2.41E-02				
hsa-mir-3648	-0.39	3.40E-03	2.54E-02				
hsa-mir-495	0.18	3.62E-03	2.67E-02				
hsa-mir-942	0.31	3.63E-03	2.67E-02				
hsa-mir-520g	0.46	3.65E-03	2.67E-02				
hsa-mir-3074	0.26	3.80E-03	2.76E-02				
hsa-mir-513a-1	-0.51	4.02E-03	2.88E-02				
hsa-mir-15b	0.16	4.02E-03	2.88E-02				
hsa-mir-202	-0.44	4.14E-03	2.94E-02				
hsa-mir-501	0.17	4.89E-03	3.46E-02				
hsa-mir-520a	0.55	4.95E-03	3.48E-02				
hsa-let-7c	-0.17	5.09E-03	3.53E-02				
hsa-mir-615	0.38	5.10E-03	3.53E-02				
hsa-mir-518e	-0.79	5.48E-03	3.77E-02				
hsa-mir-153-1	-0.29	5.57E-03	3.81E-02				
hsa-mir-616	0.32	5.78E-03	3.92E-02				
hsa-mir-106a	0.24	5.81E-03	3.92E-02				
hsa-mir-660	0.16	5.95E-03	3.99E-02				
hsa-mir-331	-0.24	6.04E-03	4.02E-02				
hsa-mir-513b	-0.41	6.52E-03	4.32E-02				
hsa-mir-628	-0.17	6.92E-03	4.55E-02				
hsa-mir-9-1	0.37	7.07E-03	4.57E-02				
hsa-mir-937	0.43	7.10E-03	4.57E-02				
hsa-mir-3926-1	0.34	7.11E-03	4.57E-02				
hsa-mir-9-2	0.37	7.12E-03	4.57E-02				
hsa-mir-144	0.27	7.70E-03	4.91E-02				
hsa-mir-183	0.22	7.82E-03	4.96E-02				
hsa-mir-379	-0.19	8.16E-03	5.14E-02				
hsa-mir-663	-0.53	9.19E-03	5.74E-02				
hsa-mir-4326	0.25	9.21E-03	5.74E-02				
hsa-mir-520b	-0.65	9.50E-03	5.88E-02				
hsa-mir-3943	0.49	1.10E-02	6.75E-02				

hsa-mir-103-2	0.17	1.11E-02	6.75E-02				
hsa-mir-1264	0.49	1.12E-02	6.75E-02				
hsa-mir-1275	-0.43	1.12E-02	6.75E-02				
hsa-mir-451	0.27	1.12E-02	6.75E-02				
hsa-mir-26a-2	-0.12	1.13E-02	6.75E-02				
hsa-mir-525	0.44	1.15E-02	6.86E-02				
hsa-mir-1255a	0.36	1.20E-02	7.06E-02				
hsa-mir-618	0.42	1.24E-02	7.31E-02				
hsa-mir-204	-0.22	1.30E-02	7.59E-02				
hsa-mir-122	-0.79	1.32E-02	7.69E-02				
hsa-mir-556	0.47	1.42E-02	8.20E-02				
hsa-mir-381	-0.16	1.49E-02	8.55E-02				
hsa-mir-199a-2	0.12	1.70E-02	9.74E-02				
hsa-mir-128-2	0.12	1.75E-02	9.92E-02				
hsa-mir-504	-0.17	1.76E-02	9.92E-02				